CIVIL ENGINEERING STUDIES
STRUCTURAL RESEARCH SERIES NO. 207

ANCHORAGE ZONE STRESSES IN PRESTRESSED CONCRETE BEAMS

By
N. M. HAWKINS
V. SRINIVASAGOPALAN
and
M. A. SOZEN

Issued as a Part
of the
NINTH PROGRESS REPORT
of the
INVESTIGATION OF PRESTRESSED REINFORCED
CONCRETE FOR HIGHWAY BRIDGES

UNIVERSITY OF ILLINOIS
URBANA, ILLINOIS
NOVEMBER 1960

ANCHORAGE ZONE STRESSES
IN PRESTRESSED CONCRETE BEAMS

by

N. M. HAWKINS

V. SRINIVASAGOPALAN

and

M. A. SOZEN

Prepared as a Part of an Investigation

Conducted By

THE ENGINEERING EXPERIMENT STATION
UNIVERSITY OF ILLINOIS

In Cooperation with

THE DIVISION OF HIGHWAYS
STATE OF ILLINOIS

and

U. S. DEPARTMENT OF COMMERCE
BUREAU OF PUBLIC ROADS

Project IHR-10
INVESTIGATION OF PRESTRESSED CONCRETE
FOR HIGHWAY BRIDGES

URBANA, ILLINOIS
AUGUST 1960

TABLE OF CONTENTS

TABLE OF CONTENTS (Continued)

LIST OF FIGURES

Figure No.

LIST OF FIGURES (Continued)

1. INTRODUCTION

1.1 General Remarks

In the calculation of stresses in prestressed concrete beams, it is assumed that the distribution of stress caused by the prestressing force is linear, the stress gradient varying in accordance with the eccentricity of the centroid of the prestressing force. However, the prestressing force is applied on the beam at a point or at a series of points and not in ideal conformity with the desired distribution of stresses. It requires a certain distance from the end of the beam for these applied forces to "flow" into the desired stress distribution. The length of this distance, usually called the transfer length, depends primarily on the type of prestressing (pre-or post-tensioning) the number and distribution of points at which the load is applied, and the material and geometrical properties of the cross section.

As the prestressing force flows from the tensioning element into the concrete section, very high compressive (bearing) stresses may be produced immediately at the point of application of the force. Moreover, high tensile and shearing stresses may occur at other points within the transfer zone, owing to the action of these compressive forces flowing out over the cross section. Cracking of the beam or significant local deformations, caused by either one or both of these effects can lead to failure of the beam or to a significant loss in the prestressing force. In both cases, benefit may be derived from the use of transverse reinforcement. This study is concerned with the problems arising from the "flow" of the prestressing force from the tensioning element into the concrete and with the effect of transverse reinforcement in the "anchorage zone", of a prestressed concrete beam.

Before discussing the practical implications of the problem, it should be mentioned that it may be fundamentally incorrect to divide anchorage zone failures into bearing failures or failures due to longitudinal cracking. Both phenomena are failures of the same material under complex systems of stress and should relate to the same basic criteria. These criteria need not necessarily be expressed in terms of stresses. In the absence of a completely satisfactory theory of failure for concrete, the studies in this report are

related to the traditional concepts of failure of concrete in compression and tension. However, it is hoped that these assumptions will be questioned at every stage of progress of the future investigation, especially in the interpretation of the effect of transverse reinforcement.

One operational aspect of this problem merits mention. In pre-tensioned and post-tensioned bonded beams, each operation of releasing the reinforcement or post-stressing is a test in itself. If failure does not occur at the time of that operation, it is unlikely that it will occur later. Normally, the prestress level is expected to reduce and the concrete strength to increase with time. If the bond is reasonably good and the beam does not fail in "shear", the anchorage zone stresses should not increase appreciably under any circumstance. Consequently, the problem is not very critical in terms of public safety. The majority of the failures, if any, should occur in the yard or during construction. However, this is not true for unbonded beams or for bonded beams without satisfactory bond.

At present, there is no generally accepted method for the design of transverse reinforcement in the anchorage zone of prestressed concrete beams. The contribution of such reinforcement to bearing strength is often ignored. A common method for its design is to compute tensile stresses on the basis of an "elastic" theory, and to provide reinforcement to take all the tensile stress in excess of a nominal permissible stress. This is not a consistent method, since the concrete must be cracked before the reinforcement can be used efficiently; and once the concrete is cracked the computed tensile stresses cease to have any meaning.

The over-all object of this investigation is to seek through tests and studies an interpretation of the action of transverse reinforcement in the anchorage zone that will lead to an effective design procedure. An immediate practical object is to investigate the feasibility of not using end-blocks in pretensioned I-beams. Consequently, the early work is slanted toward the study of anchorage zone stresses in pretensioned beams.

1.2 Object and Scope

The object of this report is to present:

(a) A comprehensive review of the research on anchorage zone stresses in prestressed concrete beams.

(b) A review of research on bond characteristics of prestressing reinforcement.

(c) A quantitative comparison of anchorage zone stresses in pre-and post-tensioned beams according to "elastic" theories.

(d) A proposal for an exploratory program of tests.

The report summarizes the available information on anchorage zone stresses. Knowledge on bond characteristics of prestressing reinforcement is presented because it is related intimately to anchorage zone stresses in pretensioned beams. The anchorage zone stresses in particular cross sections were analyzed in detail primarily to obtain an approximate idea of the possible zones of distress, and also to compare the results of various theoretical methods.

1.3 Acknowledgments

This study was carried out as a part of the research under the Illinois Cooperative Highway Research Program Project IHR-10. "Investigation of Prestressed Reinforced Concrete for Highway Bridges". The work on the project was conducted by the Department of Civil Engineering of the University of Illinois in cooperation with the Division of Highways, State of Illinois, and the U. S. Department of Commerce, Bureau of Public Roads.

At the University, the work covered by this report was carried out under the general administrative supervision of W. L. Everitt, Dean of the College of Engineering, Ross J. Martin, Director of the Engineering Experiment Station, N. M. Newmark, Head of the Department of Civil Engineering, and Ellis Danner, Director of the Illinois Cooperative Highway Research Program and Professor of Highway Engineering.

At the Division of Highways of the State of Illinois, the work was under the administrative direction of R. R. Bartelsmeyer, Chief Highway Engineer, Theodore F. Morf, Engineer of Research and Planning, and W. E. Chastain, Sr., Engineer of Physical Research.

The program of investigation has been guided by a Project Advisory Committee consisting of the following:

Representing the Illinois Division of Highways

W. E. Chastain, Sr., Engineer of Physical Research
Illinois Division of Highways

W. J. Mackay, Bridge Section, Bureau of Design, Illinois Division of Highways

C. E. Thurman, Jr., Bridge Section, Bureau of Design, Illinois Division of Highways

Representing the Bureau of Public Roads

Harold Allen, Chief, Division of Physical Research, Bureau of Public Roads

E. L. Erickson, Chief, Bridge Division, Bureau of Public Roads

Representing the University of Illinois

C. E. Kesler, Professor of Theoretical and Applied Mechanics

Narbey Khachaturian, Professor of Civil Engineering

Fred Kellam, Bridge Engineer, Bureau of Public Roads, and G. S. Vincent, Chief, Bridge Research Branch, Bureau of Public Roads, also participated in the meetings of the Advisory Committee and contributed materially to the guidance of the program.

The investigation was directed by Dr. C. P. Siess, Professor of Civil Engineering, as Project Supervisor and as ex officio chairman of the Project Advisory Committee. Immediate supervision of the investigation was provided by Dr. M. A. Sozen, Associate Professor of Civil Engineering, as Project Investigator.

2. REVIEW OF STUDIES OF ANCHORAGE ZONE STRESSES IN PRESTRESSED CONCRETE BEAMS

2.1 General Remarks

Previous investigations of the anchorage zones stresses in prestressed concrete beams or investigations of other "concentrated load" problems related to this problem, have utilized a variety of methods. Although most of the investigations have been theoretical in nature, they have been supplemented to some degree by photoelastic investigations and in a few cases by actual tests. Most of the work has been two-dimensional in nature and has been confined to investigations of the stresses in post-tensioned beams. It is only within the past few years that three-dimensional investigations have been attempted and that the problems arising in pretensioned beams, have been considered.

The earliest investigation of problems which entailed conditions similar to those existing in the end-block of a prestressed concrete beam was reported by Ribière (1)* in 1889. This work was followed by a rigorous mathematical treatment of the subject of eccentric loads by Bleich (2) in 1923. Bleich was mainly concerned with problems arising in steel structures. It was not until 1956 that Sievers (3) simplified his solution and attempted to extend it to three-dimensional problems in prestressed concrete.

The problem of eccentrically loaded concrete blocks was first investigated by Mörsch (4) in 1923. However interest was not again aroused until the past decade when prestressed concrete came into its own as a structural entity and engineers began to realize the importance of this problem as applied to post-tensioned prestressed concrete beams. Several papers were published in quick succession. Magnel (5) in 1948 and Chaikes (6) in 1951 published similar solutions for the anchorage zone stresses in post-tensioned beams. The principal advantage of these methods was its simplicity, the principal disadvantage was that they in effect assumed the solution before they started. Magnel also reported two tests and maintained that his theoretical work was in essence supported by a photoelastic investigation by Bruggeling (7).

---

* Numbers in parentheses refer to corresponding entries in the list of references.

A more rigorous treatment of the subject was given by Guyon (8) in 1951 who considered the problems of both longitudinal and transverse loads, and also the transverse stresses in an axially symmetrical three-dimensional case. In order to facilitate the application of his results, he published his work in the form of tables. Guyon in his first book on prestressed concrete (9) extended his analysis for post-tensioned beams to cover the end-blocks of pretensioned prestressed concrete beams.

Christodoulides considered two particular problems: A mathematical and photoelastic investigation of symmetrically loaded two-dimensional post-tensioned end-blocks (10), and a three-dimensional photoelastic investigation of a model and strain measurements on an actual post-tensioned concrete beam (11).

At the World Conference on Prestressed Concrete held in San Franscisco in 1957, two papers on end-blocks were presented. The first was an experimental investigation by Ban, Maguruma and Ogaki (12) who reported tests on 41 concrete specimens. They compared measured concrete strains, with strains predicted in accordance with both Bleich's and Guyon's solutions. The second paper was a theoretical investigation employing a lattice analogy. This paper was presented by Ramaswamy and Goel (13). Their results were not in agreement with those obtained in previous investigations.

A further photoelastic investigation was reported by Mahajan (14) in 1958. Although the investigation was confined to post-tensioned beams, the results of two photoelastic tests for pretensioned beams were shown. The transverse stresses obtained did not agree with either Magnel's or Guyon's theoretical investigation.

Two further papers were published in 1960. The first was a theoretical and experimental treatment of an axially symmetrical three-dimensional problem investigated by Douglas and Trahair (15). They found extremely large discrepancies between the measured and computed ultimate capacities of their test specimens. The second paper was a further note on a lattice analogy approach by Ross (16). The results obtained did not agree with those of Ramaswamy and Goel, who also used the lattice analogy.

Two studies applicable to anchorage zone stresses in pretensioned beams have been made in addition to the extrapolation from the post-tensioned case by Guyon. The first was measurements of strains in the end-blocks of pretensioned factory units by Base (17) and the second a laboratory investigation by Marshall (18). The results of this latter investigation are not as yet available.

In the following chapter, a review of a selected number of these investigations has been made. It has been attempted to confine this review to those investigations which made tangible theoretical or experimental advances or which gave different results to those reported by other investigators. Each review outlines the object, scope and principal results of the investigation.

The investigations can be divided roughly into five parts. Since much more attention has been devoted to analyses of post-tensioned than pretensioned beams, previous analyses of the former subject can be subdivided into four parts, while analyses of the latter subject are sufficient for one part only. The parts into which the post-tensioned analyses can be subdivided appear in this chapter in the following order: (i) two-dimensional elastic analyses and other investigations related directly to these analyses (ii) photoelastic analyses (iii) lattice analogy analyses (iv) three-dimensional analyses. The fifth part contains analyses of pretensioned beams. The chapter concludes with a critical summary of the results obtained in these investigations.

2.2 Analysis by F. Bleich (2)

A solution was developed by F. Bleich for the longitudinal, transverse, and shear stresses in a plate of depth 2b and width 2a, subjected to external forces P_o and P_u on two parallel edges as shown in Fig. 1a. Two loading conditions were considered. In the first loading condition, the plate was subjected to two loads equidistant from the longitudinal axis (Fig. 1a) and in the second loading condition, the plate was subjected to two equal and opposite forces at the same locations on either side of the longitudinal axis (Fig. 1b). The first condition (symmetrical loading) and the second condition (anti-symmetrical loading) can be combined to obtain a solution for an eccentric load.

The solution was based on Lagrange's equation

$$\frac{\partial^4 F}{\partial x^4} + 2\frac{\partial^4 F}{\partial x^2 \partial y^2} + \frac{\partial^4 F}{\partial y^4} = 0$$

where F was Airy's stress function. The external loads were expressed in terms of a Fourier Series. Four boundary conditions were used as follows:

$$\text{For } y = -b;\ \sigma_y = P_o(x)$$
$$\tau = 0$$
$$\text{For } y = +b;\ \sigma_y = P_u(x)$$
$$\tau = 0$$

The symbols x and y are defined in Fig. 1a. However, the solution based on these boundary conditions was not final since the boundary conditions at $x = \pm a$ (Fig. 1a) were not satisfied. The solution resulted in normal stresses on the longitudinal boundary in the case of the symmetrical loading and shear stresses on the same free boundary in the case of the anti-symmetrical loading. Bleich recommended correcting the normal stresses on the free boundary in the case of symmetrical loading by superimposing equal and opposite stresses for plates in which b is large compared to a. He did not correct for the shear stresses on the free boundary in the case of antisymmetrical loading.

The derivation of the exact mathematical solutions for the longitudinal, transverse, and shear stresses for a generalized system of loading, is presented in Appendix A.1. Mathematical approximations are presented in this appendix, that allow the conversion of these exact expressions into usable approximate expressions. These approximate expressions are used for the numerical evaluation of the stresses in the particular cases given in Chapter 4.

2.3 Approximate Analysis by H. Sievers (3)

H. Sievers developed an approximate method to determine the transverse stresses along the longitudinal axis only, in the anchorage zone of a "two-dimensional" post-tensioned beam. He also recommended an approximate method by which a three-dimensional problem could be reduced to a two-dimensional one. The development of his approximate method was based on the assumption that Bleich's solution was correct.

The case of a plate with two symmetrical loads at the top and a uniformly distributed load on the lower side (Fig. 2) was considered. There were no shear and no transverse stresses at the top and bottom sides. A reasonable shape for the resultant stress trajectory was assumed. The stress trajectory started and ended with vertical tangents as shown in Fig. 2. The equation for the resultant stress trajectory was assumed as

$$r = m\,(1 + \alpha\eta)\,e^{-\alpha\eta}$$

where $m = (\ell - a/2)$

$\eta = y/a$

α = a constant

The transverse stress, σ_x, can be written as follows

$$\sigma_x = -\frac{P}{t} \cdot \frac{d^2 r}{dy^2}$$

or $$\sigma_x^* = \frac{P}{t} \frac{m}{a^2} \alpha^2 (1-\alpha\eta)$$

If α is assumed to be 2.5, the final expression for the transverse stress along the longitudinal axis is given by

$$\sigma_x = \frac{8\ P\ m}{t\ a^2} (1 - 2.5\ y/a)\ .e^{-0.8\ \pi \frac{y}{a}}$$

The following expression was proposed for an approximate evaluation of the shearing force along the longitudinal axis for anti-symmetrical loading:

$$V = \frac{P}{2}\ 0.5 - \frac{3(a-\ell)}{2a}$$

In order to reduce a three-dimensional problem into a two-dimensional one, the "effective width" t of the end-block was assumed to vary (Fig. 2) according to the following expression

$$t = t_u - (t_u - t_o)\ (1 + 2.5\ \frac{y}{a})\ e^{-0.8\pi\ \frac{y}{a}}$$

where

t_u = width of the end-block

t_o = width of the loading plate

2.4 Analysis by Y. Guyon (8)

The paper by Guyon is divided into two parts. The first part contains solutions for the longitudinal, transverse, and shear stresses in a plate of finite width and infinite length. The solutions obtained for the anchorage zone stresses are quite similar to those developed by Bleich. The loading system, first symmetrical and then anti-symmetrical loads, is the same as that used by Bleich. The major difference between the solutions by Bleich and Guyon is that Guyon corrects for the shear stresses along the longitudinal boundaries by applying equal and opposite tractions along these boundaries. These tractions

---

*The expression for σ_x according to F. Bleich being

$$\sigma_x = 2 \sum_1^{\infty} A_n\ (1-\alpha\eta) e^{-\alpha\eta}$$

$\alpha = n\ \pi$ and $n = 1, 3, 5\ \ldots$

create normal forces and shears at the upper free surface. These shear forces are again corrected by the application of further equal and opposite forces, in such a manner as to not create any further extraneous forces. The procedure used in the development of this final correction is quite complicated and Guyon applies this final correction only in the calculation of the transverse stress distribution. Tables of stresses for various cases of loading are given, the transverse stresses being "exact" (the final correction having been applied) and the longitudinal and shear stresses being approximate (the final correction having not been applied).

The second part of the paper contains a solution for the transverse stresses in the case of a prism subject to a symmetrical load. The particular case considered is that of a square concentrated load acting on a square end-block. The analysis showed that there is a rapid increase in the concentration factor (ratio of the maximum tensile stress for the three-dimensional analysis to that for the two-dimensional analysis) as the ratio of the width of the block "a" to the width of the loaded area "a'" increased. The results are summarized below.

Ratio a/a'	Concentration Factor
2	1.5
4	2.65
10	4.7
∞	∞

The analysis also showed that the position at which this maximum stress occurred altered from a depth $y = a/2$ for $a = a'$ to a depth of $y = a/6$ as a' approached zero.

The two-dimensional stress analysis is based on Lagrange's equation with loading and boundary conditions expressed in essentially the same manner as in Bleich's solution. The three-dimensional analysis is derived in a similar manner to the two-dimensional analysis using a double rather than a single Fourier series.

The expressions for the two-dimensional analysis are derived (in the case of longitudinal loadings) in Appendix A.2.

2.5 Tests on End-Blocks by Ban, Muguruma, and Ogaki (12)

Forty-one specimens simulating rectangular end-blocks in post-tensioned beams were tested by Ban, Muguruma, and Ogaki in order to investigate the effect of the size of the bearing plate and of the presence of spiral reinforcement on cracking and ultimate strength of the end-block. Five series of tests were carried out.

The first five specimens were designated as two-dimensional tests. The tests were carried out on mortar blocks measuring 4.75 by 7.1 by 20.8 in. They were subjected to axial line loads, 2.1 in. wide, applied on opposite faces (4.75 by 7.1 in.). Concrete strains were measured in the transverse direction at various points along the longitudinal axis of the surface of the specimen. The strains computed by Bleich's solution agreed with the measured strains, while the strains computed from Guyon's solution did not agree with the measured strains.

The next thirty-six specimens were designated as three-dimensional tests and divided into four series I, II, III, and IV. The specimens measured 4 by 8 by 20 in. and were loaded through 3/4-in. nuts bearing on plates embedded in the ends of the specimens. These plates were always smaller than the cross section of the specimen. Each specimen had a concentric longitudinal hole 0.9 in. in diameter. A general detail of the three-dimensional test specimens and the loading arrangement is shown in Fig. 3.

The major variables in the three-dimensional test series were (a) Size of the bearing plate (2 by 2 to 6 by 4 in.), (b) Amount of spiral reinforcement, (c) Concrete strength (3200 to 5900 psi) and (d) Thickness of the bearing plate (0.25 to 0.75 in.). Concrete strains were measured in the case of test series I only (6 specimens, all unreinforced).

The test results indicated that the size of the bearing plate had no effect on the (longitudinal) cracking or ultimate load. The use of transverse (spiral) reinforcement was found to be the most efficacious method of increasing both the cracking and ultimate loads. Both the cracking and ultimate loads were found to be linearly proportional to the concrete strength and the thickness of the bearing plate. The concrete strains measured in test series I agreed with those computed using Sievers' approximation for the effective width of the end-block as a modification of Bleich's solution.

2.6 Approximate Analysis by G. Magnel (5)

Magnel developed approximate expressions for the stresses in the end-block of a post-tensioned prestressed concrete beam from consideration

of a two-dimensional prism acted upon by concentrated loads on one side and a distributed load on the opposite side. He assumed that a bending moment and shear stresses existed at any horizontal section. The transverse stress diagram due to the moment was assumed as a cubical parabola.

$$\sigma_x = A + By + Cy^2 + Dy^3$$

The four constants were solved from the assumed boundary conditions. At the end of the transfer zone

$$\sigma_x = 0$$

$$\frac{\partial \sigma_x}{\partial y} = 0$$

and

$$\int_{-L_t/2}^{+L_t/2} \sigma_x . b . dy = 0$$

$$\int_{-L_t/2}^{+L_t/2} \sigma_x . y . b dy = M$$

where L_t = anchorage zone length.

b = breadth of the beam.

The following expressions for σ_x and τ were obtained

$$\sigma_x = K \frac{M}{b(L_t)^2}$$

where

$$K = 5 \left(-1 + \frac{12\, y^2}{(L_t)^2} + 16 \frac{y^3}{(L_t)^3}\right)$$

and

$$\tau = K_1 \frac{S}{bL_t}$$

where

$$K_1 = 5 \left(1/4 + \frac{y}{L_t} - \frac{4\, y^3}{L_t^3} - \frac{4\, y^4}{L_t^4}\right)$$

To determine the values of σ_y, it was assumed that the pressure under the anchorages of the cables dispersed at an angle of 45° in the end of the beam and that at each vertical plane the ordinary formulas for eccentric compression were applicable.

Magnel conducted a test on the end-block shown in Fig. 4. The 8-in. cube compressive strength of the concrete was 5660 psi. The tensile strength of the concrete as determined in bending was 775 psi. In the test, the first crack appeared at 1012 kips which produced a calculated tensile principal stress of 520 psi. The crack occurred at $y/2a = 0.2$. The end-block failed at a load of 1247 kips.

Magnel also reported an observation on a post-tensioned beam the dimensions of which are shown in Fig. 5. While this beam was being prestressed with a cable having 24 wires of 5mm diameter, a longitudinal crack was observed near the end of the beam. The principal tensile stress calculated according to Magnel's method was 465 psi while the tensile strength of the concrete in the beam as determined in bending after four weeks was 555 psi. The compressive strength of the concrete was 4835 psi (8-in. cube).

2.7 Two-Dimensional Photoelasticity Investigation by S. P. Christodoulides (10)

Christodoulides made a comparison of the stresses in an end-block determined on the basis of mathematical analysis and photoelasticity investigation. A particular end-block subjected to symmetrical loading (Fig. 6) was considered. The photoelastic model measured 1.5 by 1.5 by 0.25 in.

The photoelastic analysis indicated that the maximum shear stresses and the absolute maximum principal stresses occurred immediately under and on the center line of the "anchorages". The maximum principal tensile stress occurred near the surface of the loaded end between the applied load and the center line of the end-block (Fig. 7). Maximum values of the principal tensile stress, the principal compressive stress, and the shear stress were 0.6, 4.0, and 2.0 times the average compressive stress.

In order to compare the results of the photoelastic method with the theoretical solution, the position of the isotropic point (the point where the difference between the principal stresses is zero) was determined theoretically and compared with that indicated by the photoelastic method. The theoretical determination of this point was obtained from stresses calculated by superposing a number of solutions developed from Airy's Function for simple loading conditions with the longitudinal boundary conditions ignored. The distance

from the loaded surface to the isotropic point was 0.2 in. for the photoelastic method as compared to 0.35 in. for the theoretical method. The author ascribed the discrepancy to the presence of boundaries at a finite distance in the actual model.

2.8 Three-Dimensional Photoelasticity Investigation and a Test on an End-Block by S. P. Christodoulides (11)

Christodoulides investigated the stresses in the end-block of a prestressed Gantry beam by a three-dimensional photoelasticity method. He verified the stresses by embedding strain gages inside the end of an actual beam.

The three-dimensional photoelastic analysis was carried out by the "frozen stress" technique. The model material used was "Araldite B." Models were made true to the shape of prototypes and approximately 1/25 full size. The prestressing cables were represented by brass wires and anchorages by washers. Contours of the transverse stresses were obtained and compared with those given by Guyon and Magnel.

The stress distribution in the end-block of the full size beam was determined by using internal electric gages within the beam and by using electrical and mechanical strain gages on the surface of the beam. Strains were measured in two directions on the surface and in four directions at an interior point. Strains were measured due to dead load and prestressing.

According to Christodoulides, the use of photoelastic models to represent concrete end-blocks was justified because the results of the three-dimensional photoelastic method compared favorably with the actual strain measurements. The transverse tensile stresses around the anchorages of the three-dimensional model were found to be considerably greater than the stresses indicated by Guyon's results. The maximum transverse tensile stress in the longitudinal plane was 2.25 times mean compression. Generally Guyon's results are different in distribution and considerably smaller than those obtained in the three-dimensional model. The maximum transverse stress in the third principal plane was 1.25 times the mean compressive stress.

2.9 Photoelastic Analysis by K. D. Mahajan (14)

Photoelastic tests were made to determine the maximum principal stresses, the general stress distribution and the anchorage zone length in a rectangular end-block of a prestressed concrete beam.

The models were made of Araladite resin B. They were loaded eccentrically at about 3/4 of the depth of the model by tensioning piano wires passing through a duct in the model and attached to its surfaces. The prestressing load was designed so as to give a maximum bending stress of 200 psi (tension) on the normal section. Stresses were determined from slices using a "frozen" stress technique.

Close agreement was obtained between the measured maximum principal compressive stresses and the value of these stresses as predicted by Guyon and Magnel. No such agreement was obtained for the maximum principal tensile stresses. The maximum tensile stress by Guyon's method was 399 psi and occurred under the anchorage on the axis of the force. For Magnel's method the value was 110 psi at 0.13 times the depth of the beam from the end of the beam and on the plane of maximum shear. The photoelastic value was 165 psi and it occurred at 0.0875 times the depth of the beam from the beam end and on the axis of the force. Fig. 8a shows a comparison of the measured principal compressive stresses and those computed by Guyon. Fig. 8b is a similar comparison for principal tensile stresses.

Transverse photoelastic slices, showed that stresses in the third principal plane were small and occurred only near the anchorages. The length of the anchorage zone was found by determining the distance at which the stress distribution became normal. This distance was found to be at 0.6 times the depth of the beam from the anchorage.

2.10 Lattice Analogy Solution by G. S. Ramaswamy and H. Goel (13)

Ramaswamy and Goel have investigated the stresses in the end-block of a post-tensioned beam by Lattice Analogy.

A two-dimensional plate acted upon by a central concentrated load was considered. The problem was solved by treating the end-block as a deep beam and using a 64-square lattice. To arrive at a preliminary solution, the solid block was replaced by a 16-square coarse lattice frame, supported on 5 rollers (Fig. 9a). Since it was easier to deal with a displacement at the boundary than with a load, an arbitrary displacement of -100 was applied instead of a load and the resulting displacements using the 16-square lattice, calculated; then the displacements in the 64-square lattice were worked out.

The maximum tensile stress was found to be 0.6 times the average compressive stress. It occurred at a point situated at more than half the depth of the end-block, at a level where other analyses indicate almost no transverse stress. Fig. 9b shows the transverse stress distribution obtained.

2.11 Lattice Analogy Solution by A. D. Ross (16)

Ross reports a Lattice Analogy solution for the stresses in the end-block of a post-tensioned beam. An end-block 12-in. deep loaded axially by an end plate 4-in. deep was considered. (Fig. 10a).

Longitudinal stresses became effectively uniform, and the transverse and shear stresses became zero at a distance of 0.8d from the free end. Zero and maximum tensile stresses were found at 0.18d and 0.35d from the end, respectively, Guyon's figures being 0.17d and 0.38d. Fig. 10b shows the transverse tensile stress distribution along the horizontal axis. The magnitudes of the tensile stresses were only one half of those predicted by Guyon's theory. They were also much smaller than by Magnel's approximate method.

According to Ross, the reason for the discrepancy is not obvious. The relaxation approach to this single problem is quite different from the general solution of Guyon using a Fourier Series. Although problems of this kind are not generally sensitive to changes in Poisson's ratio, the differences in transverse stresses may not be wholly unconnected with the assumed value of Poisson's Ratio, namely 1/3.

2.12 Three-Dimensional Analysis and Tests by D. J. Douglas and N. S. Trahair (15)

Douglas and Trahair developed expressions for the stresses in a three-dimensional end-block by idealizing it as a cylinder having a concentric hole and subjected to an axial load. The computed strains were compared with those measured in tests. One limitation of the theoretical analysis was that the boundary conditions for the radial stress on the free inner and outer cylindrical surfaces were not satisfied. Fig. 11 shows a comparison of transverse stress distributions for analyses by Magnel, Guyon, Guyon three-dimensional, and Douglas and Trahair.

Three series of tests on concrete cylinders were carried out. The first series consisted of 18 cylinders and was purely exploratory in nature. The object of this test series was to determine the effect of the central hole and of variations in the diameter of the loaded area. The second series consisted of 24 cylinders, the diameter of the loaded area being maintained constant at the value used in the original theoretical analysis.

The third test series consisted of 11 cylinders. Strain measurements were made to verify the theoretical stress distribution. One-inch or half-inch electrical strain gages were attached at varying points both on the inner and

outer cylindrical surfaces in order to measure both circumferential tensile and longitudinal compressive strains. Gages were also placed on the upper (unloaded portion) surface to measure spalling strains.

The comparison of results of the three series showed that the load at failure depended on the tensile strength of concrete. The presence of the concentric hole caused a reduction in the ultimate load of nine percent.

Good agreement was observed between measured and predicted circumferential strains on the inner surface of the cylinder (Fig. 12a). Hoop strains on the outside of the cylinder did not agree well with theory, tending to be about 30 percent higher than predicted. (Fig. 12b)

The ultimate load of the test specimens varied from 3.6 to 4.6 times the predicted load, calculated on the basis that the failure would occur when the circumferential stress reached the tensile strength of the concrete as measured by horizontal splitting tests on cylinders. This large discrepancy between the predicted ultimate loads and test results suggested the inadequacy of the theory of failure used. The strains measured on the unloaded portion of the upper surface showed no evidence of the high spalling stresses predicted by Guyon.

2.13 Analysis of Anchorage Zone Stresses in Pretensioned Beams by Y. Guyon (9)

Guyon made a theoretical analysis of the anchorage zone stresses in a pretensioned beam. Essentially, his analysis involved the superposition of the effect of a series of individual loads acting along the cable. The effects of the individual loads were obtained from the solutions for external loads acting on the "free end" of a rectangular plate (8). The distribution of the individual loads along the anchorage length of the cable was based on an assumed bond stress versus distance from "free end" relationship.

Naturally, the results of the analysis indicated that the better the bond, the closer were the stresses to those in a post-tensioned beam.

2.14 Strain Measurements in the Anchorage Zone of Pretensioned Beams by G. D. Base (27)

In connection with his field investigations of transfer length Base measured longitudinal strains on the surface of the concrete in the anchorage zone of several pretensioned prestressed concrete beams. Transverse strains were also measured in two of these beams (one rectangular and one inverted T-beam). The strain distributions for these latter two beams are reproduced in Fig. 13 and 14 respectively. Average strains were determined over an 8-in. gage length using a "Demec" gage. Measurements were taken at intervals of 1 in. in the longitudinal direction.

Figure 13a shows the dimensions, arrangement of reinforcement and gage lines for the rectangular beam. This beam was prestressed with closely grouped 0.08-in. diameter wires. Figure 13b shows the longitudinal strain distribution and Fig. 13c shows the transverse strain distribution. The numbers shown on the figures are typical values of the actual strains measured along the various gage lines for intervals of five inches in the longitudinal direction.

Figure 14a shows the dimensions, arrangement of reinforcement and gage lines for the inverted T-beam. This beam was prestressed with 0.2-in. diameter wires. The anchorage zone was reinforced with 10 vertical 3/8-in. square twisted bars in the end 9 in. Figure 14b shows the build-up in transverse strains in the web between gage lines 2 and 3. Figure 14c shows the longitudinal strain distribution. Since Base's principal interest was an investigation of anchorage length he did not make any comments on these strain distributions.

2.15 Summary and Discussion

Investigations of anchorage zone stresses have been largely confined to studies applicable to post-tensioned beams. Little information is available on the now common problem of the stresses in pretensioned beams. Both experimental and theoretical approaches to the determination of anchorage zone stresses have been made. In general, the basic theoretical analysis has been two-dimensional, extrapolated to give the solution in three-dimensions. The majority of the experimental work has been made to verify a proposed or existing theory. The experimental work has been extremely limited.

In this chapter, the object, scope and principal results of 13 investigations are summarized. Eleven of these investigations are directly applicable to the determination of anchorage zone stresses in post-tensioned beams and only two investigations are applicable to pretensioned beams. Eleven of the investigations were theoretical and only two experimental. Seven of the theoretical analyses were basically two-dimensional, one was an extrapolation from a two-dimensional solution, and three were three-dimensional.

In the remainder of the section, the investigations are discussed under two headings; Part I is devoted to theoretical work and Part II to experimental work.

I. Theoretical Work

Theoretical investigations of anchorage zone stresses in prestressed concrete beams can be best discussed according to the method of approach. These approaches have been (a) the theory of elasticity (b) photoelasticity and (c) lattice analogy.

For post-tensioned beams, the theory of elasticity has been used in five separate investigations, photoelasticity has been used in three investigations and lattice analogy in two. For pretensioned beams, there has been only one theoretical investigation based on the theory of elasticity.

The results obtained in the various investigations are discussed relative to Guyon's two-dimensional analysis since numerical solutions for it are readily available.

(a) Theory of Elasticity Solutions

For pretensioned beams, the only analysis has been suggested by Guyon. In this analysis the post-tensioned solution is extrapolated to give the pretensioned solution. The assumptions and limitations of this method will be discussed in detail in Chapter 4.

For post-tensioned beams, investigations have been carried out by Guyon, Bleich, Sievers, Magnel, and Douglas and Trahair.

Both Bleich's and Guyon's analyses are two-dimensional. Although the analyses are quite similar, Guyon has attempted a more refined solution than Bleich. The assumptions and limitations of their methods are discussed in detail in Chapter 4. The original analyses are summarized in the Appendix.

Guyon has simplified the use of his solution by publishing it in tabular form. However, these values should not be used indiscriminately. They represent stresses at specific points only and these points are not necessarily the points of maximum stress. Furthermore, the values for the transverse tensile stresses close to the loaded surface of the block are approximate. In this region, a major part of the transverse stress coefficient was obtained by the summation of the first 10 terms of an infinite series. The terms of this series alternate in sign and the convergence is extremely slow. For an exact solution, the summation of a much larger number of terms would have been necessary. For example, for a point in a similar position in Bleich's solution, it was necessary to sum the first 30 terms of a series in order to obtain a number significant to three digits, and the summation of the first 10 terms was appreciably different from the final result for 30 terms.

Bleich's solution is available in the form of a general expression. It can be used as a check on the effect of the further refinements developed by Guyon. In the regions in which the stress distributions for the two solutions are similar, it can be used to locate more closely the theoretical magnitude and position of the maximum stresses.

Both Bleich's and Guyon's two-dimensional solutions have been extrapolated to give solutions in three-dimensions for particular conditions only. Guyon developed expressions for the three-dimensional transverse stresses in an axially-loaded square block. Stress concentrations factors based on these stresses are quite high, and if correct inelastic action would occur at an early stage of loading. Sievers extended Bleich's analysis to give the solution for the three-dimensional problem of a block subject to symmetrical loads. The approach used is quite reasonable but its applications are limited.

Magnel's method gives maximum transverse tensile stresses of approximately the same magnitude as those determined by Guyon's analysis. The distribution of these transverse stresses and the magnitude and distribution of both the longitudinal and shear stresses are completely different from Guyon's analysis. The distribution of these stresses becomes important when the two-dimensional solution is transformed to enable the solution of a three-dimensional problem. The method is approximate since there is no a priori basis for assuming the transverse stresses to be distributed in the shape of a cubic parabola or the pressure under the anchorages to disperse at an angle of 45°.

Douglas and Trahair's analysis is the only strictly three-dimensional solution. The hoop stresses obtained by this analysis are similar to the transverse stresses obtained in Guyon's three-dimensional analysis. The applicability of this solution is limited by the assumption of axial symmetry and by the fact that the radial stress conditions on the inner and outer longitudinal boundaries are not satisfied.

(b) Photoelastic Solutions

Methods of photoelasticity were used for the analysis of post-tensioned beams. Two of these investigations were made by Christodoulides and one by Mahajan.

The particular advantage of the photoelastic method is that the "frozen stress" technique can be used to determine stresses in three-dimensions. The major disadvantage is that a new photoelastic model must be prepared and tested for each new prototype.

Both investigators found that the transverse stresses in the longitudinal direction were smaller than those predicted by Guyon and that the tensile stresses in the third principal plane were small and occurred only on the surface.

(c) Lattice Analogy Solutions

The lattice analogy approach has been applied to post-tensioned beams in two investigations; one by Ramaswamy and Goel, and one by Ross.

One difficulty with the lattice analogy approach is that some value must be assumed for the Poisson's Ratio of the concrete. This quantity is difficult to measure and can vary over a wide range. An alteration in its magnitude may have a significant effect on the magnitude of the derived stress.

Since this method is complicated and laborious, only simple cases have been attempted. Ramaswamy and Goel determined the stresses for an axially applied, concentrated load. Their solution gives maximum values at much greater depths than would be predicted by Guyon. Ross determined the stresses for an axially applied distributed load. The values of the maximum tensile stresses are about half those predicted by Guyon but they occur at approximately the same position in both cases.

II Experimental Work

Experimental work has been performed by five separate investigators. Four of these investigations pertained to post-tensioned beams and one to pretensioned beams. In all but one case, attempts were made to measure the actual strain distributions. The experimental work has been of such a limited nature that no one test series can be compared directly with another test series.

The only investigation for pretensioned beams was carried out by Base. He measured strains in the end-blocks of prestressed members made in the factory. Unfortunately, the conditions under which the measurements were made precluded the full documentation of the variables involved. However, the measured strain distributions showed that the build-up of strains is similar to the result predicted by applying Guyon's method for the determination of these anchorage zone stresses in pretensioned beams. Furthermore, the measurements showed that the maximum strains, and therefore the maximum stress, occurred very close to the end of the beam, and slightly above the center of gravity of the prestressing wires.

For post-tensioned beams experimental investigations have been carried out by Ban, Magnel, Christodoulides, and Douglas and Trahair.

Ban et al. carried out tests on axially loaded rectangular blocks. These tests represent the only comprehensive experimental investigation that has been undertaken. Cracking and ultimate loads were found to increase with increase in the amount of spiral reinforcement, in the concrete strength, or in the stiffness of the bearing plate. Electrical strain gages were used to measure tensile strains on the outside of some of the test specimens. These measured strains were comparable with strains computed in accordance with Bleich's solution for similar positions along the axis of loading. One difficulty encountered in assessing the true value of these tensile strains was that the high longitudinal compressive strains in combination with the transverse sensitivity of the gages gave values of comparable magnitude to the actual tensile strain that the gage was measuring.

Magnel reported two tests on full scale post-tensioned end-blocks. One test was a laboratory test and the other "test" was the failure in the field of an end-block. In both specimens, cracking occurred along the axis of loading. For the laboratory test, it initiated at a point about three tenths of the depth of the block away from the loaded surface at a position somewhat closer to the end of the beam than predicted. Computed principal tensile stresses at cracking were comparable for the two tests and were about twenty percent lower than the measured tensile strength of the concrete. The discrepancies between the observed and predicted positions of cracking and the stresses at cracking are not unreasonable in view of the approximate nature of the analysis.

Christodoulides measured concrete strains in the end-block of an actual post-tensioned beam. This end-block had been designed in accordance with a previous photoelastic investigation. Good agreement was obtained between the measured and predicted strains. The test showed that the photoelastic design procedure was safe but that the method did not give any idea of the factor of safety against failure.

Douglas and Trahair carried out several tests on axially loaded cylindrical test specimens. Tensile strains were measured on the inner and outer longitudinal surfaces and tensile strains on the loaded surface of the block. Reasonable agreement was obtained between the measured and computed strains on the longitudinal surfaces. The tensile stresses on the loaded surface were not significant. Measured ultimate capacities were several times greater than predicted. The specimens finally failed in

bearing. These results are not in agreement with those reported by Ban. In these tests, the tensile strains on the inner longitudinal surface of the specimen were much greater than those on the outside of the specimen. The failure loads were proportionately much higher than those reported by Ban.

3. REVIEW OF STUDIES OF BOND CHARACTERISTICS OF PRESTRESSING REINFORCEMENT

3.1 General Remarks

Various studies of the bond characteristics of prestressing reinforcement have been made within the past two decades. Most of these studies have been concerned with the length of reinforcement over which a certain prestress can be transferred to the concrete; anchorage bond rather than "flexural bond" has been the issue. Although the basic information available from tests on ordinary reinforcing bars has been of help in understanding bond in prestressed concrete, this information is not sufficient. First, because prestressing reinforcement has surface characteristics that are different from those for ordinary reinforcement. Second, because there are certain basic differences between the manner in which bond is developed in prestressed and ordinary reinforcement.

In the anchorage zone of a pretensioned beam, the maximum slip and the maximum diameter of the reinforcement occur at the point of zero stress (the end) and the minimum slip (zero) and the minimum diameter of the reinforcement occur at the point of maximum stress. In pull-out tests, from which most of the information on ordinary reinforcing bars is derived, this slip versus stress (or strain) and the reinforcement diameter versus slip relationships are reversed. Furthermore, for pretensioned beams this increase in diameter with slip, causes the reinforcement to exert a radial pressure on the surrounding concrete. The resultant wedging action improves the apparent bond strength of the reinforcement. In pull-out tests, this type of wedging action does not occur. Thus, it would have been necessary to make independent studies of the rate of stress transfer in anchorage zones of pretensioned beams, even if the different surface characteristics of the prestressing reinforcement had not required it.

In the following discussion, the term "anchorage length" is used to denote the length of reinforcement required to transmit completely the prestressing force from the reinforcement to the concrete. "Anchorage length" as used here should be distinguished from "transfer length" which is used to denote the length required to reach a linear stress distribution in the section. Thus, the transfer length is always greater than the anchorage length.

One of the earliest expressions for the anchorage length was derived by Hoyer (19) in 1939 on the supposition that bond was entirely due to the wedging action resulting from the lateral expansion of the wire. In 1949 Marshall (20) reported tests on wires of two different diameters. He proposed an equation for bond based on the experimental observation that the rate of change of the steel stress was linearly proportional to the rate of change in the bond stress.

In his book on prestressed concrete published in 1951 Guyon (9) reported several test results. He developed an expression for anchorage length in terms of the measured end-slip and the initial stress in the steel. In 1954 Janney (21) carried out several tests and developed expressions for the steel stress in smooth clean wires assuming that bond was frictional only.

Linzell (22) was one of the first to report on the bond characteristics of strand. In 1954, his measurements of the steel strain indicated that for 3/8-in. diameter strand the anchorage length was about seven inches.* In 1955 Lin (23) reported measured values of end-slip of 0.04 to 0.10 in. for 3/8-in. in diameter strand which he considered to be satisfactory. In 1956 Ozell (24) reported 12 to 20-in. anchorage lengths for 7/16-in. diameter strand and Ruble (25) reported 6-in. anchorage lengths for 1/2-in. diameter strand. In 1957 Monson (26) reported a 7-in. anchorage length for 3/8-in. diameter strand.

At the F.I.P. conference in Berlin in 1958, two papers were presented on bond. Ratz (27) reported numerous tests on several different types of wires. From these results he derived an expression for a single function that could be used to characterize the change in steel stress along the anchorage length for any given wire. Base (17) reported comparisons between field and laboratory measurements. For plain wires he recommended that the average anchorage length be taken as a simple multiple of the diameter of the wire.

Dinsmore (28) (1958) concluded that measured values of end-slip and anchorage length were not consistent and depended to a large degree on manufacturing techniques. Evans (29) (1958) summarized his work as of that date,

*Anchorage length for ordinary prestress level (about seventy percent of the reinforcement strength at release.

on bond in prestressed concrete. He attributed bond to a combination of factors but discounted the effect of adhesion and maintained that all bond stresses, no matter how small, were always associated with slip. Evans recommended expressions for anchorage lengths based on the measured end-slip and the steel strain before transfer. Faulkes (33) (1958) investigated the specific effects of concrete strength, time and depth under the reinforcement.

The references reviewed in the following chapter have been confined to those investigations for which the results were intended to have a relatively wide application or from which a general theoretical expression was derived. The object, scope, and principal results of the various investigations are outlined wherever possible.

3.2 Studies and Tests by G. Marshall (20)

In order to investigate the anchorage length of prestressing wire, Marshall conducted 20 tests on pretensioned concrete prisms, 4 by 4 in. in cross section and from 4 to 72 in. long. The cube strength of the concrete was 11,500 psi. The test program was divided into two series of 10 specimens. Each prism in the first series contained 52 wires of 0.08 in. diameter prestressed to 224,000 psi. Each prism in the second series contained 12 wires of 0.2 in. diameter prestressed to 156,800 psi. The surface condition of the wires at prestressing was not stated.

Concrete strains were measured on the surface of the test specimens using a travelling microscope. For the specimens with 0.08 in. diameter wires, the concrete strain at each end increased rapidly along the specimen until a constant strain was reached. For the specimens with 0.2 in. diameter wires, this constant strain region was never reached indicating that slip may have occurred over the full length of the specimen.

Marshall assumes that the anchorage length is the length required from the free end of the column to reduce the bond stress to zero. In every case this length was estimated from the concrete strain measurements.

Marshall observed that the anchorage length varied with time. For 0.08 in. diameter wires, this length varied from 60 at one day to 90 diameters at one year after release.

Since slip had occurred over the full length of the test specimens for 0.2 in. diameter wires, an extra specimen 10-ft. long was cast. Both steel and concrete strains were measured. The steel strains were measured with

mechanical strain gages using access holes in the concrete to reach the reinforcement. The anchorage length, estimated from concrete strains, was between 125 and 150 diameters. For this specimen Marshall found that the rate of change of steel stress was linearly proportional to the rate of change of bond stress (estimated from steel recovery strains) along the length of the wire.

This latter result formed the basis for Marshall's theoretical work. He expressed the bond stress (adhesion and friction) at a distance y from the free end as:

$$f_b = f_{bi} e^{-\frac{2a}{r} y}$$

where f_b = bond stress at a distance "y" from the free end

f_{bi} = initial bond stress

a = constant

r = radius of the wire

From the above expression the steel stress at any distance y from the free end was expressed as;

$$f_s = f_{se} \left[1 - e^{\frac{-2a}{r} y}\right]$$

where f_s = stress in the steel at a distance "y" from the end

f_{se} = effective prestress

For the 0.2 in. diameter wires the constants "a" and "f_{bi}" were evaluated from the test data and the following expression for bond stress obtained:

$$f_b = 1.060e^{-0.145y}$$

3.3 Investigation of Anchorage Length by Y. Guyon (9)

In his book "Prestressed Concrete, Vol. I" Guyon devotes a chapter to the problem of anchorage by bond. In the course of this chapter he indicates the results of three test series carried out to determine the effect of variations in the diameter of the wires on the anchorage lengths of plain wires. He also develops theoretical expressions for relationships between end-slip and anchorage length.

In the first test series conducted by Guyon end-slips were measured in numerous precast prestressed concrete beams. Plain 0.2-in. diameter wires were used at a prestress of 141 ksi. The concrete cube strength varied

between 5600 and 7000 psi. End-slips averaged between 0.04 and 0.08 in. with an upper bound of 0.14 in.

The second test series conducted by Guyon involved measurements of end-slips in 45 prestressed beams. Wires of 0.1-in. diameter were used at a prestress of 168 ksi. The concrete cube strength varied between 4,500 and 7,800 psi. The mean value of the end-slips was 0.17 in. with a standard deviation of 0.06 in. and a range of 0.08 to 0.35 in. The corresponding calculated anchorage lengths varied between 26 and 66 in. The concrete strength did not seem to have a consistent effect on the observed end-slips.

The third test series conducted by the British Railways involved careful measurements of end-slips in seven prestressed concrete railroad ties. Plain 0.2-in. diameter wires were used at a prestress of 141 ksi. The concrete cube strength was 6,000 psi. Measured end-slips varied between 0.024 and 0.063 in. corresponding to calculated anchorage lengths of 7 to 19 in.

From these results and those reported by Evans (29) and Marshall (20), Guyon concludes that the question of the relative merits of small or large diameter plain wires is meaningless. A slight variation in one of the properties of the concrete can vary the anchorage length between wide limits. If the anchorage length has to be reduced, some type of wire other than plain wire must be used.

Guyon developed theoretically an expression for the transfer length in a pretensioned beam in terms of the measured end-slip g_o

$$\frac{2 E_s g_o}{f_{si}} < l_t < \frac{3 E_s g_o}{f_{si}}$$

From these expressions he concluded that the total anchorage length was about 500 to 600 time the measured end-slip, for steel stresses of the order of 145 ksi.

3.4 Tests on Anchorage Bond in Pretensioned Prestressed Beams by J. R. Janney (21)

The object of this investigation was to determine the influence of the following variables on the anchorage bond in pretensioned concrete beams: (1) Wire diameter, (2) surface conditions of the wire, (3) concrete strength.

Tests were carried out on an unspecified number of prestressed concrete prisms 2 by 2 in. in cross section and 72 or 96 in. long. Each prism contained a single pretensioned wire or strand at the longitudinal axis. The

wire diameters and surface conditions used were: 0.100, 0.197, 0.276 in. diameter wires and 5/16 in. diameter strand, both clean and lubricated; 0.162 in. diameter wire, clean, lubricated and rusted. The concrete strength used was about 4500 psi. An additional specimen containing a 0.162 in. diameter clean wire and having a concrete strength of 6500 psi was tested. The reinforcement was prestressed to 120,000 psi. Each wire was fitted with two SR-4 electric strain gages and each strand with four SR-4 gages. The distribution of prestress was determined from strain measurements recorded on 26 SR-4 electrical strain gages attached to the concrete surface.

For smooth clean wires, Janney discounted the contributions of both mechanical resistance and adhesion and developed the following approximate expression for steel stresses based on friction bond only.

$$\log \frac{f_{se} - f_s}{fse} = - \frac{2\varphi \, \mu_s \, y}{r[1+(1+\mu_c) \frac{E_s}{E_c}]}$$

where φ = coefficient of friction between steel and concrete

μ_s = Poisson's ratio of wire

μ_c = Poisson's ratio of concrete

The general shape of the theoretical curves obtained from this equation was similar to the measured stress distributions.

From his tests, Janney found that the anchorage length increased slightly as the diameter of the wire increased. Rusted wire developed the prestress at a faster rate and in somewhat less distance than clean wire. The latter wire was in turn much better than lubricated wire. Typical stress transfer distributions obtained for different wire diameters and surface conditions are shown in Fig. 15. An increase in the concrete strength improved the bond only if this increase was accompanied by an improvement in concrete quality.

3.5 Tests by E. H. Ratz (27)

The object of this study was to determine experimentally the character of the relative movements of the concrete and steel in the anchorage zone of pretensioned beams on release of the prestress. In particular, the effects of concrete strength and surface conditions for 18 different types of wire commonly used in the USSR were investigated.

Two hundred rectangular specimens were made, varying in widths from 1.57 to 3.2 in. and in length from 52 to 280 in. The concrete cube strength was varied from 2900 to 7100 psi. The prestress was applied uniformly using from 1 to 15 wires stressed from 14,000 to 170,000 psi. Both plain and indented wires and two and seven wire strands were used. In all specimens end-slips were measured for transfer increments of 7 to 8 percent of the full prestress using a microscope attached to the concrete at 0.4 - 0.8 in. from the end. In some specimens displacements at several points within the anchorage zone were measured using microscopes attached to the concrete at these points.

Ratz found that the end-slip g_o expressed as a function of the change in steel stress of the projecting wire, was a reproducible characteristic for a given concrete strength and type of wire such that

$$g_o = A\left[e^{(\Delta f_o - \delta)/K} - 1\right]$$

where $\Delta f_o = \dfrac{\text{change in steel stress at the end}}{\dfrac{1+E_s}{E_c}\,p}$

p = reinforcement ratio

A and K are empirical factors dependent only on the concrete strength for any given wire and δ is the change in steel stress at which end-slip first becomes measurable.

Ratz extended this equation to cover the full length of the anchorage zone on the assumptions that plane sections remained plane and that relative movements did not depend on the distance from the free end. He showed theoretically that a single function could be used to characterize the change in steel stress along the length of the anchorage zone for any given wire. He also derived an expression for the tangential stress variation.

The experiments showed that the bond was strongly dependent on the strength of the concrete. For the indented wire, bond depended mainly on the depth of the indentations although it did tend to approach a limiting value as the depth of the indentations increased. Alterations in the pitch of indentations or placement of wires in pairs had little effect. For low concrete strengths the strand consisting of seven 0.063-in. diameter wires had a bond strength comparable to that of 0.12 and 0.16-in. diameter idented wires. For higher concrete strengths, the strand had lower bond strength than the indented wire.

Long-time observations showed that contrary to the results for plain wires the increase in length of the anchorage zone was small for indented wires; averaging only 8 to 10 percent.

3.6 Tests by G. D. Base (17)

The object of this investigation was to determine the variations in anchorage lengths that occur in practice and to compare these results with laboratory investigations. These laboratory investigations also included the effects of time, method of release, position of the wires, etc.

Field measurements were made of concrete strains in the anchorage zones of 150 units cast in five different factories. Strains were measured on several gage lengths over the depth of the beam using an 8 in. "Demec" gage. A wide variety of cross sections and wire types were encountered. The size of the units varied from small lintels to 12 by 40-in. beams and 45 by 13-in. slabs. The prestress at transfer varied from 800 to 2,500 psi. Wires used included 0.08, 0.2 and 0.276-in. diameter plain wires and 0.2-in. diameter indented and crimped wires.

For any particular factory there did not appear to be any significant difference in the average results or in the scatter. It was found that the anchorage lengths for various sizes of plain wires could be expressed as multiples of the wire diameter. The average anchorage length was 95 to 100 diameters and the range, with a few exceptions 60 to 160 diameters. No significant difference in anchorage lengths were found for indented and plain wires. Wires with large "crimps" were approximately 50 percent better than plain wires. The field measurements indicated that although concrete strength was an important factor in the rapid build-up of strain, the compaction of the concrete at the ends of the actual units seemed to be of even greater importance.

In the laboratory tests plain, indented and crimped wires were used similar to those used in the field tests. The range of wires was extended to include 5/8-in. diameter Macalloy bars and 5/16 and 3/4-in. diameter strand. The laboratory results were more consistent and gave shorter average anchorage lengths than the field tests. A comparison of the measured anchorage lengths under laboratory and factory conditions is made in the following table.

No.	Dia. of Wire	Anchorage Length	
		Factory Condition	Laboratory Condition
1	0.08 in. plain	6 to 13 in.	
2	0.2 in. plain and indented	30% were more than 20 in. 6 to 32 in.	All under 20 in. 70% under 12 in. 7 to 18 in.
3	0.276 in.	12 to 45 in.	12 to 23 in.

Anchorage lengths for the 3/4-in. strand varied between 12 and 17 in. and for the 5/16-in. strand between 9 and 19 in. It was also found that wires near the top of a specimen sometimes had greater anchorage lengths than wires near the bottom. No significant increase in anchorage lengths with time were found. Flame cutting of the wires increased anchorage lengths considerably. Early results from repeated loading tests showed no indication of increase in anchorage lengths.

3.7 Tests by G. A. Dinsmore (28)

The object of this investigation was to explore the problem of anchorage bond failures and in particular to determine experimentally the anchorage length and distribution of anchorage bond stress for 7/16-in. diameter strand.

The bond stresses in a prism centrally prestressed by a single plain wire (Fig. 16) were considered first. The anchorage length was hypothesized to consist of a friction zone AC and an elastic zone CF. In the friction zone the adhesion between the concrete and the steel is destroyed and relative movements occur. The bond transfer in this zone is dependent on the coefficient of friction between concrete and steel and the radial pressure at their interface. In the elastic zone adhesive bond is retained and the displacement of the concrete and the steel at their interface is the same. At the end of the elastic zone (plane F-F) there are no relative concrete displacements over the depth of the cross section since the "dishing effect" at the level of the wire no longer exists.

For strand the anchorage length is decreased owing to the added effect of mechanical resistance. In contrast to smooth wires, strand must rotate or screw in along predetermined grooves in the concrete. Release also causes a radial expansion and a decrease in pitch of the strand. Mechanical resistance is thus developed along the ridges in the concrete. The added effect of this mechanical resistance makes the anchorage length for strand more susceptible to creep in the concrete than for smooth wires.

In the experimental investigation 42 pull-out tests were carried out to determine (1) the slip-limit envelope and (2) the bond stress distribution. Clean 7/16-in. diameter strand and 6000-psi concrete were used. For seven of the specimens, the strand failed in the grips. The remaining specimens had 4 by 4-in. cross sections and bonded lengths varying from 1 to 12 ft. An unbonded length of between 0.5 and 1.5 ft. was provided near the bearing end to reduce stress concentrations at this surface during the pull-out test. All specimens had a single, centrally located, prestressing wire.

Dial gages were used to measure the end-slips on release. The bond distribution was analyzed from measurements of the concrete strain on the surface of the specimen at the level of the strand. Either SR-4 electrical gages or Huggenberger extensometers on an 8-in. gage length were used. Strand rotation was measured by protractors attached to the strand.

Measured values of end-slip were not consistent. No practical slip-limit envelope could be found from the pull-out tests. Concrete strength did not appear to be a major variable effecting bond strength. The degree of vibration and the resultant compaction of the concrete seemed to be more important variables. The manner of release (either sudden or gradual) did not appear to affect the bond strength.

For the maximum period investigated, namely 130 hours, the anchorage length was independent of time. The bond strength of the strand as measured in these pull-out tests did not appear to be significantly affected by the initial prestress.

3.8 Studies and Tests by R. H. Evans (29)

The object of this paper was to resolve such questions on bond in pretensioned members as (1) the effectiveness of the wedge or Poisson's ratio action at the ends of pretensioned wires, (2) the effect of surface conditions, (3) the use of strand, (4) time effects, (5) the mechanism of bond. The paper serves effectively as a summary of Evans' previous publications on bond in prestressed concrete.

Evans (30) estimated the possible wedge action in two ways (1) by calculating the normal pressure between the steel and concrete, and, knowing the rate of change of steel stress in the wires from laboratory observations and the coefficient of friction, determining the total bond stress (2) by using the standard thick-cylinder theory formulas considering the equilibrium of the mating surfaces of the steel and concrete and assuming values for Poisson's

ratio and the coefficient of friction. The former method gave a maximum bond stress at the end of 840 psi at a radial pressure of 5,600 psi, while the latter method gave a bond stress of 980 psi at a pressure of 6,900 psi. For comparison, tests on plain untensioned wires gave maximum bonds stresses of 650-750 psi and tests on mild steel bars (31) gave stresses of 550-750 psi. At the most the wedge action amounts to 200-300 psi and only very small radial strains would be necessary to reduce even this contribution significantly.

Evans (32) investigated the effect of surface conditions of the wire on bond by embedding marks with high X-Ray absorption coefficients in the prestressing wires before casting the specimen. Radiographs taken before and after release enabled the strain to be determined. Several test series were carried out.

In the first series four samples of wire were tested with grease films ranging in thickness from 0.8×10^{-6} up to 49×10^{-6} in. The calculated bond stresses ranged from 850 to 1,630 psi.

In the second series, specimens including wires of four different diameters, namely 0.08, 0.104, 0.2, and 0.276 in. and different surface conditions were tested. The initial prestress ranged from 143 to 182 ksi. The cube strength of the concrete varied between 6000 and 9000 psi. Anchorage lengths varied between 3.8 and 47 in. The variations in the observed anchorage lengths were greatest with the rusted wires. It appeared there was little difference between the anchorage lengths of plain, crimped or indented wires, when these wires were rusted.

In the third series, specimens prestressed with 5/16-in. diameter strand tensioned to 7,000 lb. were tested. The strand consisted of 49 wires, each of 0.036 in. diameter. The concrete cube strength was 11,000 psi. The initial anchorage length was 5.6 in. and this increased after one week to 5.8 in.

In relation to the question of the effect of time on anchorage length and "pull-in," Evans stated that the effect of creep could be substantially reduced if rusty wires were used in lieu of bright wires. Evans suggested the following formulas for relation between end-slip and anchorage length.

Bright wires $$L_t = 3.6 \frac{g_o}{\epsilon_{si}}$$

Rusted wires $L_t = 1.8 \frac{g_o}{\epsilon_{si}}$

Strand $L_t = 2.6 \frac{g_o}{\epsilon_{si}}$

where ϵ_{si} = steel strain before transfer.

With regard to the nature of bond, Evans maintained that the X-Ray method showed that all bond stresses, no matter how small, were always associated with slip. A slip of the order of 0.001 in. must occur before the maximum bond stress of 1,500 psi is developed for 0.08 in-diameter wires. After a slip of 0.004 in. however the bond stress decreases rapidly.

Evans attributed bond to a combination of factors including mechanical interlock of the concrete with surface indentations, normal friction between the concrete and steel, manufactured indentations, and wedge action.

3.9 Tests by K. A. Faulkes (33)

The object of this investigation was to determine the effects on the anchorage length of the following variables: (a) The concrete strength at transfer, (b) the time after transfer, and (c) the depth of concrete beneath the wire.

Fourteen specimens 4 by 3 in. in cross section and 10 ft long were cast. The reinforcement consisted of five 0.2-in. diameter wires distributed uniformly over the cross section. Wires were cleaned of all grease and rust. The initial prestress was 152 ksi. Eight specimens were prestressed using smooth wires and six using indented wires. Prestress was released slowly. End-slips were measured and the anchorage lengths determined by measuring concrete strains on the top surface of the beam using a direct-reading dial gage instrument. Strains were read at two hours after transfer (the time necessary for the readings to stabilize) and at various intervals up to several months.

The test results for these specimens showed that there was no significant decrease in the anchorage length as the concrete strength increased from 2100 through to 5800 psi. The measured lengths varied between 18 and 21 in. for indented wires. Over a period of several months, the anchorage lengths increased only about 6 in. for smooth wires and about 2 in. for indented wires. Most of this increase took place in the first two days after

transfer. For smooth wires the ratio of the anchorage length to end-slip was about 310. For indented wires this ratio decreased as the concrete strength increased.

The effect of a variation in the height of the wire in the beam was investigated in three different ways: (a) the end-slips were measured for the different wire heights (1 in. to 3 in.) used in the above series, (b) End-slips were measured for full scale specimens in which the wire height varied from 1 to 25 in., and (c) the ultimate capacity was determined for 110 pull out specimens in which the wire height was varied from 1 to 9 in. In the latter case, 0.276-in. diameter unstressed wires, both plain and indented, were used. The width of the specimens was 4 1/4 in., the embedment length was 10 in, and the over-all depth of the specimens was varied from 4 to 10 in. The concrete strength was 5840 psi.

End-slips increased in proportion to the height of the wire above the bottom of the beam. The pull-out tests gave bond strengths for smooth wires that varied simply with the height of the wires. This strength varied from 175 psi for a 1 in. height through a 25 psi for a 9-in. height. The bond strengths for indented wires depended on the ratio h/d of the height of the wires to the total depth of the specimen. The strength varied from 850 psi for h/d = 0.1 to 490 psi for h/d = 0.9.

Additional pull-out tests were carried out in which the embedment length for indented wires was varied from 3 in. up to a length sufficient to develop the full tensile strength of the wire. The average maximum bond stress was found to be independent of the length of embedment.

3.10 Summary and Discussion

Insofar as this investigation of anchorage zone stresses is concerned, the work on bond characteristics of prestressing reinforcement can be summarized in relation to how well the rate of stress transfer for given conditions can be predicted. It is evident from the foregoing that this cannot be done with any degree of precision. However, it is interesting to note the range of values for anchorage lengths that could be derived for a particular case from the results of some of the experimental studies. Suppose end-slips of 0.02 to 0.06 in. with an average of 0.033 in. were measured for

0.2-in. diameter rusted high strength single wire reinforcement prestressed to 135,000 psi*. The following table lists the "predicted" anchorage lengths in inches:

	Average	Lower Limit	Upper Limit
Marshall	25-30	-	-
Guyon	14-21	9-13.5	26-39
Janney	24	-	-
Base	7-18	-	-
Evans	13	8	23
Faulkes	10	7	20

The maximum and minimum values for the average anchorage length are 30 and 7 in. respectively. This is too large a range in opinion or even in interpretation of opinion to be of great help in studying stresses in anchorage zones.

The picture appears to be worse for strand. The following table lists the reported anchorages lengths for various sizes of strand. Wherever only the end-slip was reported, the anchorage length was computed on the basis of Evans' expression. The prestress level, where available is listed for each case.

	Strand Diameter in.	Initial Prestress ksi	%Ultimate	End-Slip in.	Anchorage Length in.
Base	5/16	190	-	-	9-19
Janney	5/16	120	-	-	20
Evans	5/16	190	70	-	6
Morson	3/8	170	70	-	7
Lin	3/8	175	70	0.04-0.10	18-48
Linzell	3/8				7
Dinsmore	7/16	160	60	0.02-0.05	9-24
Ozell	7/16				12-20
Ruble	1/2				6
Base	3/4	190	-		12-17

It appears disturbing that while the anchorage length was measured to be 6 in. for 1/2-in. diameter strand, it would be 20 in. for 5/16-in. diameter strand.

* These values are typical for measurements made on beams having such wires in the course of the project "Investigation of Prestressed Reinforced Concrete for Highway Bridges".

Obviously, methods of measurement, definition of the anchorage length, and other critical variables such as the concrete strength and the surface conditions of the reinforcement play an important part in determining the anchorage length.

These results point to the fact that an experimental investigation of anchorage zone stresses in pretensioned beams would be incomplete without a series of "control tests" to determine the bond characteristics of the particular reinforcement used under the particular conditions of the tests on the beams' anchorage zones.

The interpretations of the experimental results described in the preceding sections were not always in agreement. The conclusions concerning some of the effects studied by more than one investigator are compared below. Before this is done, however, it is pertinent to summarize the methods of measurement used by each investigator. The anchorage length was determined by measurements of steel strain, concrete strain, and end-slip as follows:

(a) The anchorage length was based on concrete strains measured on the surface of the specimen by Base, Dinsmore, Faulkes and Janney.

(b) The anchorage length was based on steel strains measured with a mechanical strain gage by Marshall and with a traveling microscope by Marshall and Ratz.

(c) The anchorage length was based on slip of the reinforcement determined with the use of X-ray equipment by Evans.

(d) Guyon based his estimate of the anchorage length on measurements of end-slip.

Surface Conditions of Reinforcement. The effect of the surface conditions of high strength single wire reinforcement was studied by Base, Evans, Faulkes, Janney, and Ratz. The surface condition varied from lubricated to rusted. Indented, crimped, and smooth wires were tested. All investigators agreed that rusted wires had better bond characteristics than lubricated or unrusted wires. However, opinions as to the relative merits of smooth and deformed wires varied considerably. Faulkes and Ratz found that indented wires had higher bond strength than smooth wires. Base found no difference between the bond strength of indented and smooth wires but reported that crimped wire had superior bond characteristics. On the other hand, Evans reported all three types of wire had comparable bond characteristics provided all wires were well rusted. As would be expected, tests on strand indicated greater bond strength than those on wire.

Concrete Strength. The effect of concrete strength was studied by Base, Dinsmore, Faulkes, Janney and Ratz. The concrete strength was varied from 2000 to 7000 psi. The consensus was that an increase in concrete strength improved the bond only if it was accompanied by better mixing and casting methods. Ratz was the only investigator to report that bond strength was directly dependent on concrete strength.

Size of Wire. The effect of the size of wire was studied by Base, Evans, Guyon, Janney and Marshall. The wires tested had diameters ranging from 0.08 to 0.276 in. Marshall and Base concluded that the anchorage length was almost linearly proportional to the diameter. Janney and Evans reported only a slight increase in anchorage length with wire diameter. Guyon stated that the effect of the diameter on bond was too small to be distinguishable from test data.

Manner of Release. The effect of the manner of release (gradual or sudden) was investigated by Base and Dinsmore. In contrast to Base's observation that the anchorage length was affected critically by the manner of release, Dinsmore reported very little effect.

Depth of Concrete Under Reinforcement. Both Base and Faulkes reported decrease in bond strength with increase in depth of concrete under the reinforcement (effect of settlement), this effect being very critical for smooth wires.

Time-Dependent Effects. An increase in anchorage length with time of as much as 50 percent was reported by Marshall for smooth wire. For strand, this effect seemed to be quite small.

4. ANALYSIS

4.1 Introduction

The object of this analysis is to determine the changes in the relative magnitudes of the anchorage zone stresses that will result from alterations in the point of application of the load and the anchorage length of the prestressing reinforcement. The results obtained from this analysis are used as a guide for the determination of the variables to be investigated in the proposed test series outlined in Chapter 5.

Although several methods of analysis have been outlined in Chapter 2, only two of these methods can be considered to be suitable for the more detailed analysis and comparisons undertaken in this chapter. The two methods that have been chosen are the methods of Bleich (2) and Guyon (8). These methods are essentially similar. Guyon's solution is a refinement of Bleich's original solution. In Guyon's solution however, the analysis becomes so involved that stresses are obtained for specific points only, and these points are not necessarily the points of maximum stress. On the other hand, Bleich's solution, although not as refined as Guyon's solution, can be expected to yield essentially the same results. The simpler nature of the solution does, however, allow more exact determination of the points of maximum stress. By a comparison of the two methods, a fairly accurate and complete over-all picture can be obtained. It must be emphasized that these stresses are based on an elastic analysis.

This chapter is set forth in the following manner. The basic assumptions used in the analysis are outlined first. Solutions are given for the stresses in a block resulting from (1) a single eccentric concentrated line load applied at the upper surface of the block and (2) a single eccentric line load distributed over some finite depth of the block. Case (1) is hypothesized to correspond to the stresses that would occur in the anchorage zone of a post-tensioned prestressed concrete beam. Case (2) is hypothesized to correspond to the anchorage zone stresses in a pretensioned prestressed concrete beam.

These analyses are two-dimensional only. The solutions ignore both the effects of stresses in the third principal plane and the effect of alterations in the shape of the cross section. Such problems are of importance but the difficulties involved in obtaining quantitative solutions have necessitated that these effects be discussed in qualitative terms only, at the end of the chapter.

4.2 Basic Assumptions

For the purposes of this analysis, the anchorage zone of the prestressed beam has been assumed to consist of a homogeneous, isotropic, elastic material. The assumptions of homogeneity and isotropy are probably more unrealistic in the end zone than in any other region of the concrete beam. Concrete placed in these regions, usually shows greater segregation of the aggregates, greater leaching of the cement paste, and the inclusion of a higher percentage of voids.

The assumption of a linear stress-strain relationship for concrete either in tension or compression is only approximately correct even at low stresses. However, in the actual anchorage zone, there are several points of high stress concentration both in tension and compression, which are associated with relatively high stress gradients. It appears reasonable that some inelastic response would exist well in advance of failure.

(a) Post-Tensioned Prestressed Concrete Beams

It is assumed that the anchorage zone stresses in a post-tensioned prestressed concrete can be obtained from a two-dimensional solution of the stress distribution due to the application of a single concentrated line load on the upper surface of a block of elastic material of finite dimensions.

This hypothesis ignores the following facts: (a) The stress distribution must be affected by alterations in the shape of the cross section (b) an applied load cannot be concentrated at a single point, but must be distributed over some finite width (c) there must be a hole underneath the load point for the passage of the prestressing cable (d) an actual anchorage zone may be subject to some additional external force, caused by reactions due to dead load, applied loads or prestressing, which would act at right angles to the prestress force.

If the shape of the cross section is to be considered, a three-dimensional rather than a two-dimensional analysis is necessary. For rectangular end-blocks subject to line loads, it is reasonable to assume that the presence of the free boundaries in the third principal plane (direction of the line load) will not affect materially the stress pattern in the center of the beam.

The high stress concentrations under the anchorages of the cables of post-tensioned beams necessitates the use of bearing plates in order that the bearing capacity of the concrete, at this point, is not exceeded. The prestressing force must thus be distributed over some finite width. Unless the bearing plate is infinitely stiff, the distribution of pressure beneath it cannot be uniform and is more likely to be parabolic in nature.

Goodier (34) has carried out a theoretical analysis of this problem by a consideration of a block of elastic material of depth "b" to width "a" with a b/a ratio of 2, subject to an axially symmetrical distributed compressive line force of width α. From a two-dimensional analysis he found that the average tensile stress per unit width was $\frac{P}{\pi b}$ and the maximum tensile stress when $\alpha = 0$ was $1.82 \frac{P}{\pi b}$. For $\frac{\alpha}{a} = \frac{1}{10}$, the maximum tensile stress decreased to 1.62 for a uniform distribution of load and to 1.70 for a parabolic distribution of load. For $\frac{\alpha}{a} = \frac{1}{5}$ the maximum tensile stress decreased to 1.24 for a uniform distribution and to 1.42 for a parabolic distribution. This conclusion is in accordance with the results obtained by Ban, Muguruma and Ogaki (12) who found that the cracking and ultimate loads for their specimens increased as the load bearing area was increased. The foregoing results clearly show the conservative nature of this second assumption in the hypothesis that the prestress force can be represented by a load concentrated at a point.

The third assumption that the effect of the hole underneath the load point can be ignored, may or may not be important. The rigid elastic solution for a circular plate with or without a hole gives that the maximum transverse stresses in the former case are always at least twice the stresses in the latter case. On the other hand, Douglas and Trahair found that the presence of the hole caused a reduction in strength of only nine percent. In an actual prestressed beam the duct is nearly always grouted and its effect could be reduced correspondingly.

Reactive forces due to dead load, applied live loads or prestressing would in general cause stresses in the opposite sense to those caused by the normal eccentric load. The neglection of the effect of these forces will generally give an added factor of safety to the solution.

(b) Pretensioned Prestressed Concrete Beams

It is assumed that the anchorage zone stresses in a pretensioned prestressed concrete beam, can be obtained by the superposition of stresses caused by a series of individual loads. A relationship is assumed for the

stress transfer between the concrete and the steel. The distance over which the transfer is assumed to be complete is divided into a finite number of equal increments and the total force transferred over each increment calculated. In the analysis, this force is assumed to act at the mid-depth of the increment and it is hypothesized that the stress at any point in the anchorage zone can be obtained by the addition of the stresses caused by the incremental forces at this point. The stress at any point due to an incremental force is taken to be the same as that which would be obtained at that point if this incremental force were acting at a free boundary at the level within the block at which it is applied.

Such a solution assumes that the distribution of bond stress in the anchorage zone is completely known. The solution ignores (a) the effect of the material behind the assumed point of application of each incremental force and (b) the possibility of relative movements of the cables affecting the stress distribution.

The exact distribution of the bond stress in the anchorage zone is difficult to determine. It will depend on the type and condition of the reinforcement, the properties and strength of the concrete, the method of release of the prestress, and the proximity of other prestressing cables. Previous investigations have shown that the stress transfer from the steel to the concrete can be fairly well approximated by a parabola of the algebraic form $y = Ax + Bx^2$. The evaluation of the constants A and B is presented in Section 4.4.

The assumption that the material behind the point of application of each incremental force does not affect the resultant stress distribution is probably quite reasonable. Since the total force on any section within the body must be in equilibrium, the assumed free surface must be acted upon by a small longitudinal tension. The intensity of the longitudinal tensile stress will be greatest away from the point of application of the load, and their effect on this critical region will be small. Furthermore, since the largest incremental force is assumed to occur in the interval which is the closest to the actual free surface, the effect of the material behind each other assumed free surface will be correspondingly smaller, and the net effect of this material on the over-all stress distribution will be small.

4.3 Solution for a Single Concentrated Load

Solutions are given in Figs. 18-25 for the transverse, shear, longitudinal, and maximum principal stress distributions in the end-block of a prestressed concrete beam subjected to a single concentrated eccentric load.

Two different values of eccentricity are used. In Figs. 18-21 the stresses are evaluated for an eccentricity equal to a quarter of the depth of the beam and in Figs. 22-25 the stresses are evaluated for an eccentricity equal to three eights of the depth of the beam. Solutions are given for both Bleich's and Guyon's methods.

The end-block is assumed to have a depth of 2a and to be subjected to a concentrated load P applied at a distance u from the axis of symmetry. The coordinate system chosen is shown in Fig. 17. Grid reference lines A through G are located at increments of $y = \frac{a}{6}$ along the longitudinal axis.

Any exact solution of the stresses must satisfy the following boundary conditions.

Condition I at $y = 0$; $x = -a$ to $x = u$ $\sigma_y = 0$

$x = u$ to $x = a$ $\sigma_y = 0$

Condition II at $y = 0$ $x = -a$ to $x = +a$ $\tau = 0$

Condition III at $x = -a$ or $x = +a$ $y = 0$ to $y = L_t$ $\sigma_x = 0$

Condition IV at $x = -a$ or $x = +a$ $y = 0$ to $y = L_t$ $\tau = 0$

Condition V at $y = L_t$; $\int_{-a}^{a} \sigma_y \, dx = P$

Condition VI at $y = L_t$; $\int_{-a}^{a} \sigma_y \, x \, dx = P.u.$

In interpreting the significance of the stress distributions shown in Figs. 18-25, it should be remembered that the original stress functions for both Bleich's and Guyon's solutions satisfy conditions I, II, and V. Guyon's expressions for the loading functions also satisfy condition VI whereas Bleich's do not. As a result the longitudinal stresses (as shown in Fig. 20a and 24a) according to Bleich's solution, do not approach the distribution for pure bending as they do in Guyon's solution (Fig 20b and 24b) but approach the condition of a uniform compression over the whole of the section. Furthermore, although both Bleich and Guyon consider it necessary to correct for condition III, only Guyon corrects for condition IV. Thus, although the transverse stresses for both Bleich's and Guyon's solutions vanish on the longitudinal boundaries (Fig. 18 and 22) the shear stresses on these boundaries are zero only in the case of Guyon's solution (Figs. 19 and 23). Since these corrective distributions do not necessarily satisfy the conditions of equilibrium and compatibility, their use may only introduce additional errors. Therefore, it

is appropriate to reproduce both Bleich's and Guyon's solutions. The discrepancies arising from the effect of these corrective distributions are most noticeable in the principal stress distributions.

The stresses for Bleich's solution in Figs. 18-25 are evaluated along the grid lines A to G at horizontal increments of $\frac{a}{3}$, except for positions close to the load point for which these increments are subdivided further. The stresses for Guyon's solution are reproduced directly from the tables published in Reference (9). In this reference the stresses have been evaluated along the grid lines A to G at horizontal increments of $\frac{a}{4}$.

In Figs. 18-25 the suffix "a" is applied to the figure representing Bleich's solution and the suffix "b" to the figure representing Guyon's solution. For any given figure the actual stress per unit width of the block, can be evaluated at any particular reference point, by multiplying the coefficient at the reference point by the average stress per unit width, namely $\frac{P}{2a}$. For all figures except those showing the longitudinal stresses, contour lines are drawn through positions of equal stress for coefficient increments of 0.2. Larger increments are used in the case of the longitudinal stresses. In all figures, zones of tension are hatched.

(a) Transverse Stresses

Figures 18 and 22 give the transverse stress distributions for both Bleich's and Guyon's solutions for the loads applied with eccentricities of $u = \frac{a}{2}$ and $u = \frac{3a}{4}$, respectively. An examination of these figures shows that the transverse stress distribution can be divided approximately into four zones. These zones are more readily distinguishable in Bleich's than in Guyon's solution owing to the symmetry of the stress function (Appendix A.1) giving a line of zero stress within the body. Tensile stresses occur in two of these zones, and compressive stresses in the other two zones.

One of the tension zones occurs directly under and along the axis of the applied load. The zones of "equal stress" are pear-shaped, the points of highest stress concentration being located close to the upper surface of the beam and directly beneath the load. These stresses are termed bursting stresses. The second tension zone is located on (Guyon) or immediately below (Bleich) the free surface of the beam. It occurs away from the axis of loading on one or, if there is sufficient room, both sides of the load point. These stresses are termed spalling stresses. The maximum spalling stresses occur on the surface in Guyon's solution because of the application of the third corrective stress distribution (Appendix A.2). On the other hand, in Bleich's

solution the form of the stress function necessitates that the transverse stresses vanish on the upper surface of the block. In Bleich's solution both the spalling and bursting stress zones extend to a greater depth than in Guyon's solution.

The two compression zones are more readily distinguishable in Bleich's than in Guyon's solution although a close examination of the variation of the stresses in the latter case will show that these stresses exhibit the same characteristics as in Bleich's solution. One compression zone is located beneath the spalling tension zone and to one side of the bursting tension zone. Its width and depth depend on the position of the load and the final distribution assumed for the stresses over the depth of the cross section. The second compression zone is located above the bursting tension zone and to one side (Bleich's solution) or partially beneath (Guyon's solution) the spalling tension zone. It is composed of two parts which spread out like the ribs of an arch, one either side of the load point.

The relative magnitude of the stresses in either the tension or the compression zone as opposed to the stresses in the other tension or compression zone appears to depend on the eccentricity of the applied load. For example, for $u = \frac{a}{2}$, the maximum spalling stress coefficient for Bleich's solution is 0.57 and the maximum bursting stress coefficient is 0.85. For Guyon's solution the coefficients are 1.04 and 1.09, respectively. For $u = \frac{3a}{4}$, these coefficients are 1.33 and 1.09 for Bleich's solution, and 2.18 and 2.08 for Guyon's solution. The maximum tensile stress is thus the bursting stress for an eccentricity of $\frac{a}{2}$ and the spalling stress for an eccentricity of $\frac{3a}{4}$. More important perhaps than the significance of these maximum stress values is the fact that the areas over which these higher stresses extend, follow exactly the same pattern. The values quoted above show that as the eccentricity increases, the maximum tensile stress increases. Furthermore, it appears that the maximum tensile stresses given by Guyon's solution are always greater than those given by Bleich's solution although the discrepancy in the values obviously decreases as the eccentricity decreases.

The magnitude of the finite maximum stresses in the compression zones are relatively smaller than those in the tension zones. For an eccentricity of $\frac{a}{2}$ the maximum stresses occur in the areas adjacent to the load points and for an eccentricity of $\frac{3a}{4}$ the maximum stresses occur in the area below the spalling tension zone.

(b) Shear Stresses

Figures 19 and 23 give the shear stress distributions for both Bleich's and Guyon's solutions for the loads applied with eccentricities of $u = \frac{a}{2}$ and $u = \frac{3a}{4}$, respectively. An examination of these figures shows that the shear stress distribution can be divided into approximately three zones. As in the case of the transverse stresses, these zones are more readily distinguishable in Bleich's than in Guyon's solution owing to the symmetry of the stress function.

Naturally, the division between two of the zones of shear occurs almost directly (Guyon) or exactly (Bleich) underneath the load point. The second division occurs about the center of the beam, being located somewhat closer to this line, the greater the eccentricity of the load. On either side of the load point, kidney-shaped bulbs of stress are built up, the coarseness of the mesh no doubt accounting for the fact that the second kidney-shaped bulb is not obtained in the case of Guyon's solution for $u = \frac{3a}{4}$.

Maximum shear stress coefficients for Guyon's solution (1.04 for $u = \frac{a}{2}$ and 1.01 for $u = \frac{3a}{4}$) are considerably less than those obtained by Bleich (2.43 in both cases) again due to the coarseness of the mesh. However, for points within the zones of maximum shear, the values obtained at a given point are very similar in both solutions although Bleich's solution tends to give slightly higher values. As a result, the depth to which a given level of stress extends is slightly greater in Bleich's than in Guyon's solutions. In either case, the positions of maximum shear are located at depths of about $\frac{a}{6}$ from the upper boundary. The contour for any given level of stress close to the maximum value has its greatest dimensions at a slight angle to the direction of the longitudinal axis, and has its apex close to this position of maximum stress.

It is interesting to note that there is little (Guyon) or no (Bleich) alteration in the shear stress pattern as the eccentricity of the load is altered. This can be readily seen from the expressions for the shear stress distributions in the Appendix. In Bleich's solution altering the eccentricity of the load merely shifts the stress pattern over a distance equal to the alteration in the eccentricity of the load. A similar result is obtained for Guyon's solution, although the correction for the shear stresses on the longitudinal boundaries does alter the picture slightly. Bleich's expression for the shear stresses can be exact only when the point of application of the load coincides with the axis of symmetry of the block.

(c) Longitudinal Stresses

Figures 20 and 24 give the longitudinal stress distribution for both Bleich's and Guyon's solutions for loads applied with eccentricities of $u = \frac{a}{2}$ and $u = \frac{3a}{4}$, respectively. From these figures it can be seen that the longitudinal stress distributions are similar in magnitude and extent, for points close to the actual load point. Away from the load point, differences in the distributions arise from the condition that Bleich's solution approaches a uniform compression over the section and Guyon's solution approaches the stress distribution due to pure bending.

In both solutions a bulb of pressure is built up directly under and on the axis of the load. Theoretically, this stress has a value of infinity at the actual load point, but this value has reduced to approximately 8.0 times the average compressive stress at a depth of about $\frac{a}{6}$. Around this bulb the contours of equal stress, for values less than 1.0, splay out uniformly on either side of the load point. Both solutions show that on the side of the center line away from the load point a slight tension zone exists close to the upper surface. For Guyon's solution this tension zone is connected to the tension zone caused by the stress due to pure bending at some greater depth. There is little (Guyon) or no (Bleich) variation in the magnitude of the compressive stresses as the point of application of the load is altered.

(d) Maximum Principal Stresses

Figures 21 and 25 give the maximum principal stress distributions for both Bleich's and Guyon's solutions when the load is applied with eccentricities of $u = \frac{a}{2}$ and $u = \frac{3a}{4}$, respectively. These maximum principal stresses have been computed using a Mohr's circle construction. It has already been shown that little difference is obtained by calculating the shear or longitudinal stresses in the end block up to a depth of about "a", by either Bleich's or Guyon's solutions. Any differences between the maximum principal stresses calculated in accordance with either theory, will be mainly due to differences in the transverse stresses.

The maximum principal tensile stresses are concentrated in two regions corresponding to the bursting and spalling stress zones of the transverse stress solutions. However, owing to the large shear stresses that acted over the region that separated these two zones, there is a considerable blending of the two zones, through a widening of the influence of the bursting stress zone.

In Guyon's solutions in particular these two zones almost blend into one. The depths to which these maximum principal tension zones extend only slightly exceed the depths to which the transverse tensile zones previously extended.

The largest maximum principal stress coefficients are equal to the maximum transverse stress coefficients. However the area over which a given level of stress extends is always greater for the principal tensile stresses than for the transverse tensile stresses. The major differences in the shape of the contour lines for equal stresses obtained in Bleich's solution as opposed to those obtained in Guyon's solution, are due to the existence of shear stresses on the longitudinal boundaries of the block in the former case.

4.4 Solution for a Rectangular Pretensioned Beam

Solutions are given in Figs. 26 to 33 for the transverse, shear, longitudinal, and maximum principal stress distributions in a rectangular end-block of a pretensioned beam on the basis of the hypothesis outlined in Section 4.2, Case (b). Each stress distribution is calculated first in accordance with Bleich's solution and then in accordance with Guyon's solution. The eccentricity of the prestress force was taken as equal to three-eights of the depth of the beam. The stress transfer between the steel and the concrete was assumed to be complete after a distance equal to half the depth of the beam.

In the figures, the reference system used and the dimensions of the block are the same as those outlined for the post-tensioned beams of Section 4.3, except that the grid reference lines now extend from A through to N and that the grid line A is located at a depth of $\frac{a}{12}$ instead of $\frac{a}{6}$. Any exact solution must still satisfy the same boundary conditions as were specified in Section 4.3, so that the same comments as to the shortcomings of the solutions will apply.

The stress transfer between the concrete and the steel imposes another condition. It was stated in the discussion of the assumptions in Section 4.2 that the variation of the steel stress in the end-block would be approximated algebraically by the parabola

$$y = Ax + Bx^2$$

The dependent variable y was taken as equal to total prestress force F(x) acting on any section within the anchorage zone, and the independent variable x was set equal to the distance from the free end of the beam. The constants A and B were evaluated from the following boundary conditions:

(1) at $y = 0$, $F(x) = 0$

(2) at $y = L_t$, $F(x) = P$

then

$$F(x) = P\left[\left(\frac{x}{L_t}\right) - \left(\frac{x}{L_t}\right)^2\right] \qquad 4.1$$

where P = the total prestress force.

The final solution for the pretensioned case was obtained by a summation of solutions corresponding to the application of incremental prestress forces applied at various depths within the anchorage zone. Equation (4.1) can be transformed into a more convenient form if the anchorage length L_t is divided into a finite number of equal increments, say, $k\ L_t$. If ΔP is the change in stress over the n^{th} increment, then

$$\frac{\Delta P}{P} = 2k\ (1 - 2n\ k) + k^2 \qquad 4.2$$

For the solutions given in Figs. 26-33 the anchorage length L_t was assumed as half the depth of the end-block and subdivided into six equal segments of length $\frac{a}{6}$. The incremental prestress forces to be transferred at the center of each segment (i.e. on grid lines A to F), calculated in accordance with equation 4.2, were 0.306 P; 0.250 P; 0.194 P; 0.138 P; 0.084 P, and 0.028 P respectively.

The assumption that the anchorage length is equal to a half of the depth of the beam is probably a reasonable estimate for actual beams of relatively short spans. However, the anchorage length for any given beam is not dependent on the depth of the beam. This relationship between anchorage length and depth was assumed, only because it simplified the analyses.

Evans (29) found that, in laboratory tests, the anchorage length of $\frac{5}{16}$ in. diameter strand was about 6 in. Base (17) found that in the case of plain wires, there was an increase of about eighty percent between anchorage lengths measured in the laboratory and lengths measured in the field on the same size specimens. In view of these results, a conservative estimate of the anchorage length for the 3/8-in. diameter strand to be used in typical highway bridge designs from Reference (35) would be 12 to 16 in. This anchorage length corresponds to about a half of the depth of the beam for a 35 ft. span and about a quarter of the depth of the beam for a 70 ft. span. An anchorage length of a half the depth of the beam can be said to be an upper limit to the anchorage lengths normally found in practice.

Reasonable estimates for the resultant stress distributions for anchorage lengths less than half of the depth of the beam can be made by extrapolation between the solutions for the pretensioned and post-tensioned beams.

The assumption that the prestress force has an eccentricity of three-eights of the depth of the beam may be considered as an upper limit to that found in practice. The resultant prestress force for the wires in the tension face only for the beams in Reference (35) has an eccentricity of between 0.28 and 0.31 of the depth of the beam.

In Figs. 26-33 the stresses for both Bleich's and Guyon's solutions are evaluated along the grid lines A to N, for the same horizontal increments as were used for the post-tensioned beams. In these figures, Bleich's solution for a certain type of stress is given by an even-numbered figure and Guyon's solution by an odd-numbered figure. Contour lines are drawn through positions of equal stress for coefficient increments of 0.2 except for the longitudinal stresses.

(a) Transverse Stresses

Figures 26 and 27 give the transverse stress distributions according to Bleich's and Guyon's solutions respectively. A comparison of these figures with Fig. 22 shows that there is less similarity between the stress patterns for the two solutions in the pretensioned case than there was in the post-tensioned case. The stress distribution according to Bleich's solution in the pretensioned case (Fig. 26) resembles strongly the stress distribution for Bleich's solution in the post-tensioned case (Fig. 22a). The stress distributions according to Guyon's solutions show little similarity in the two cases.

In Figs. 26 and 27 there is a discontinuity along the line of the prestress force. This discontinuity is a result of the superposition of the solutions for the post-tensioned beam to give the solution for the pretensioned beam. In both Bleich's and Guyon's solutions for the transverse stresses in a post-tensioned beam there is an infinite compression immediately under the load point. Also on the axis of loading, but at some distance below this infinite compressive stress there are high tensile stresses. The superposition of the post-tensioned cases causes the infinite compressive stresses to cancel out these high tensile stresses in the two-dimensional solution.

However an actual beam is three-dimensional and even if the wire distribution is such that the loading can be reasonably well approximated by a line load, infinite compressions cannot exist between wires. Instead tensions will occur between wires and it is reasonable to assume that these tensions will be given by the superposition of the tensions occurring along the axis of loading in the post-tensioned beam. The discontinuity thus shows that the two-dimensional transverse stress distribution approaches two solutions. The solution with infinite compressions along the axis of loading corresponds to the two-dimensional stress distribution on a vertical plane through the axis of the wire. The solution with tensile stresses along the axis of loading corresponds to the stress distribution on a vertical plane intermediate between successive wires in a horizontal direction.

In Bleich's solution the build-up in stresses in the direction of the longitudinal axis is relatively slow. For the given grid pattern, the maximum spalling stress coefficient of 0.44 occurs on line C (distance $\frac{5a}{12}$) at a depth of $\frac{a}{3}$. The maximum bursting stress coefficient of 0.50 occurs on line D (distance $\frac{7a}{12}$) on the axis of loading. A more important feature is the variation in the magnitude of the bursting and spalling stresses over the depth and length of the anchorage zone. The contours show that the stresses build up more rapidly immediately within the boundaries of the spalling stress zone than of the bursting stress zone. As a result a plateau of stress occurs in the former case and a peak of stress in the latter case. The compressive stresses are small and relatively unimportant.

In Guyon's transverse stress distribution, the end of the beam is subject to tensile stresses over its full depth; the bursting and spalling stress zones are blended into one. The resultant tension zone extends into the anchorage zone for a distance equal to about half the depth of the beam. On the upper surface however, where tensile bending stresses occur, this tension zone extends the full length of the anchorage zone.

In Guyon's solution the build-up in stresses in the direction of the longitudinal axis is relatively fast. For the given grid pattern, the maximum spalling stress coefficient of 0.67 occurs on line A at a depth of $\frac{a}{2}$ (distance $\frac{a}{12}$) on the axis of the load. The maximum bursting stress coefficient of 0.98 occurs on line C (distance $\frac{5a}{12}$) on the axis of the load. There is no sharp break between the bursting and spalling stress zones. The two zones can be distinguished by the peak nature of the stresses in the bursting zone and the more gradual stress gradient in the spalling stress zone.

A comparison of Bleich's and Guyon's solutions show that tensile stresses can be expected over a length of the anchorage zone equal to about half the depth of the beam. Compressive stresses are small and relatively unimportant. The bursting stresses are larger than the spalling stresses but a high stress level is maintained over a small area only. On the other hand a high spalling stress level is maintained over a much larger area. Apart from these similarities there is little agreement between the positions and magnitudes of the maximum stresses determined by the two different methods. The maximum bursting stress according to Guyon's solution is about twice that determined by Bleich's solution and occurs somewhat closer to the end of the beam. The maximum spalling stress by Guyon's solution is approximately half as large again as that by Bleich's solution. Moreover in the former case this maximum stress occurs near the end beam and close to this axis of loading. In the latter case the maximum spalling stress occurs some distance within the anchorage zone and just above the neutral axis.

The differences in the two solutions are due to the high spalling stresses calculated by Guyon on the free surface. Their effect on the pretensioned case may not be as drastic as that predicted since the principle of superposition used to obtain a solution hypothesizes that there is no material behind the assumed free surface. The presence of such a material would affect most strongly these surface stresses.

(b) Shear Stresses

Figures 28 and 29 give the shear stress distributions for both Bleich's and Guyon's solutions. The stress distributions are very similar to those found for the post-tensioned beam in Fig. 23. As in the latter case the shear stress distribution can be divided into approximately three zones. One dividing line lies along the axis of loading and the second line lies approximately along the center line of the beam.

In Bleich's solution kidney-shaped bulbs of stress are built up on either side of the axis of loading. A partial bulb is built up near the remote longitudinal boundary. Two symmetrical points of maximum shear stress occur. The stress coefficients at these points are 0.88 and they lie on line C (distance $\frac{7a}{12}$) at $\frac{a}{6}$ on either side of the axis of loading. The stress gradient at these points of maximum shear stress is low. About the same general stress level is maintained for some distance in both directions.

By comparison, the points of maximum shear stress in the post-tensioned case, occur closer to the axis of loading and to the end of the beam. Also, the stress gradient at the points of maximum shear stress in the post-tensioned case is much higher. However, at lower levels of stress, equal levels of shear stress cover larger areas in the pretensioned than in the post-tensioned case.

In any interpretation of Guyon's solution, the effect of the coarseness of the grid pattern must be considered. In the post-tensioned case this coarseness was the reason for the absence of the second stress bulb on the outside of the axis of loading. In the pretensioned case, it contributes to a further distortion of the existing bulb of stress. As in the post-tensioned case, the maximum shear stress coefficient obtained in Guyon's solution (0.6 on line D at depth $\frac{a}{2}$) agrees fairly well with the stress coefficient at the same point calculated by Bleich's solution. However, in Bleich's solution the use of a finer grid establishes a higher maximum closer to the axis of loading at a point not covered by the coarser grid used in Guyon's solution.

(c) Longitudinal Stresses

Figures 30 and 31 give the longitudinal stress distributions for Bleich's and Guyon's solutions respectively. The stress patterns are very similar to those obtained in the post-tensioned cases. As a result the comments made on the distribution of stresses in these cases (p.48) are still valid.

The build up in stresses is of necessity slower than in the post-tensioned case. In the pretensioned case however a greater discrepancy arises between stresses calculated by Bleich's method and stresses calculated by Guyon's method. This discrepancy becomes more noticeable with distance along the longitudinal axis. It is due to the difference in boundary conditions imposed at the end of the anchorage zones in the original solutions. The superposition of solutions for concentrated loads to yield the solutions for the pretensioned beam introduces this difference in boundary conditions at a relatively faster rate.

(d) Maximum Principal Stresses

Figures 32 and 33 give the maximum principal stresses according to Bleich's and Guyon's solutions respectively. The discontinuity along the axis of loading has been ignored and the stresses plotted as if finite stresses only existed at these points. The stress patterns are very similar to those obtained in the pretensioned case. The major difference is that the magnitudes of the maximum tensile stresses are much smaller and that these maxima no longer occur on or adjacent to the end of the beam, but at some finite distance within the beam.

For the same reasons as in the post-tensioned case, any differences in the maximum principal stress patterns of either Bleich's or Guyon's solutions are mainly due to differences in the transverse stresses. Moreover these differences have been minimized by superposition.

The maximum principal tensile stresses are concentrated in two regions corresponding to the bursting and spalling stress zones of the transverse stress solutions. The bursting stress zone is a region of high stress gradients, small in area and located on the axis of loading. The spalling stress zone is a region of comparatively uniform stresses, larger in area, and located closer to the end and center of the beam.

4.5 Summary and Discussion

In this chapter both Bleich's and Guyon's two-dimensional analyses have been used to study the anchorage zone stresses in prestressed concrete beams. Initially, it was hypothesized that the anchorage zone stresses in a post-tensioned beam would be given by the stress distribution due to the application of a single concentrated line load on the upper surface of a block of elastic material and that the anchorage zone stresses in a pretensioned beam could be obtained by the superpositions of the above solutions for a series of individual loads distributed over some finite distance within the block. The assumptions inherent in these hypotheses were outlined and their possible effects discussed.

Solutions were obtained for the transverse, shear, longitudinal, and maximum principal stress distributions in the anchorage zone of a post-tensioned beam with the prestressing force applied at eccentricities of a quarter and three-eighths of the depth of the beam. The transverse tensile stresses were termed bursting and spalling stresses according to their location. The bursting stress zone was located at some depth on the axis of loading, and the spalling stress zone was located close to the end of the beam, but away from the axis of loading. It was found that as the eccentricity increased the maximum tensile stresses increased. For low values of eccentricity, maximum tensile stresses occurred in the bursting stress zone and for higher values of eccentricity maximum tensile stresses occurred in the spalling stress zone. Maximum principal tensile stresses were not significantly greater than the transverse tensile stresses, and their distributions were essentially similar. The analyses showed that stresses up to fifty percent greater than those listed in Guyon's tables (9) could be obtained at positions intermediate between those listed in the tables.

In general, for the longitudinal and shear stresses, Bleich's and Guyon's solutions were comparable. For the transverse and maximum principal stresses, Guyon's solutions gave higher values than Bleich's solutions.

Solutions were obtained for the transverse, shear, longitudinal, and maximum principal stress distributions in the anchorage zone of a pretensioned beam with the prestressing force applied at an eccentricity of three-eights of the depth of the beam. The anchorage length of the reinforcement was assumed to be half the depth of the beam. The transfer of force from the reinforcement to the concrete was assumed to vary as a parabola over this length. Agreement between the two solutions was not as good as for the post-tensioned cases. Transverse tensile stresses extended over about half the length of the anchorage zone. Bursting stresses were considerably larger than spalling stresses but were much more localized. The distributions of the longitudinal and shear stresses were similar to those for the post-tensioned case. The maximum principal stresses were not significantly different from the transverse stresses except in the spalling stress zone where an appreciable increase in the value of the stresses was obtained.

The following table gives the position and magnitude of the maximum transverse tensile stress coefficients for each of the types of loading investigated. Positions are defined in accordance with the notation shown on Fig. 17. Coefficients are multiples of the average compressive stress.

Transverse Tensile Stress Coefficients

Type of Loading	Method	Max. Spalling Stresses		Max. Bursting Stresses	
		Magnitude	Position	Magnitude	Position
$u = \frac{a}{2}$	Bleich	0.57	$\frac{-a}{2}, \frac{a}{12}$	0.85	$\frac{a}{2}, \frac{a}{3}$
Post-Tensioned	Guyon	1.26	$\frac{3a}{4}, 0$	1.09	$\frac{a}{2}, 0+$
$u = \frac{3a}{4}$	Bleich	1.33	$\frac{-a}{4}, \frac{a}{6}$	1.09	$\frac{3a}{4}, \frac{a}{12}$
Post-Tensioned	Guyon	2.18	$\frac{a}{2}, 0$	2.08	$\frac{3a}{4}, 0+$
$u = \frac{3a}{4}$	Bleich	0.44	$\frac{-a}{4}, \frac{5a}{12}$	0.50	$\frac{3a}{4}, \frac{7a}{12}$
Pretensioned	Guyon	0.67	$\frac{a}{2}, \frac{a}{12}$	0.98	$\frac{3a}{4}, \frac{5a}{12}$

The above table shows that the tensile stresses in pretensioned beams (and the maximum principal stresses) are significantly lower than the same stresses in post-tensioned beams. In the pretensioned beam, the maximum bursting stresses were only about a half and the maximum spalling stresses only about a third of those in the post-tensioned beam.

If the analysis is to take into account the shape of the cross section, an approximation for the transformation of the two-dimensional solution would be to assume that the stresses at any level act over a width equal to the width of the beam at that level. For an I-beam without an end-block as opposed to a beam with an end-block, the stresses in the web would be increased in the ratio of the width of the flange to the width of the web. An average value of this ratio is about three. In this case, the spalling stresses in a pretensioned beam without an end-block could be a great as in a post-tensioned beam with an end-block. For example, from the previous table the maximum spalling stress coefficients in a pretensioned I-beam would by 1.32 and 2.01 by Bleich's and Guyon's solutions, and in a post-tensioned rectangular beam they would be 1.33 and 2.18 respectively.

The spalling stresses plotted in Figs. 26 and 27 show that there is little variation in these stresses over approximately the middle half of the depth of the beam if the prestressing reinforcement is concentrated in one flange. It follows that, for the same total prestressing force, redistribution of reinforcement from one flange to the other should not relieve the spalling stresses in the web. On the other hand, a uniform "fanning out" of the reinforcement over the depth of the beam might eliminate the possibility of longitudinal cracking.

The assumption that the anchorage length of the reinforcement is equal to half of the depth of the beam represents for strand reinforcement a reasonable upper limit to the anchorage length that should occur in practice, although there is no logical relationship between the anchorage length and the depth of the beam. Test results indicate that shorter anchorage lengths may be common, in which case the stress coefficients should be intermediate between those given in the previous table for the solutions for pretensioned and post-tensioned cases. If an end-block is not present, spalling stresses even greater than those predicted for the post-tensioned rectangular beam could occur in the pretensioned beam.

5. PROPOSED EXPLORATORY INVESTIGATION

5.1 Object and Scope

The ultimate object of the proposed experimental investigation is the development of a rational method for the design of transverse reinforcement in the anchorage zones of pretensioned beams. Although this is a practical goal, certain basic phenomena have to be studied in detail before results of practical significance can be obtained.

The investigation can be divided into two more or less distinct phases. The first phase is the investigation of conditions that lead to the formation of a longitudinal crack in the anchorage zone. It will involve the comparison of measured strains with strains computed on the assumption that concrete is a linearly elastic material. This phase should perforce result in modifications of the theoretical approach to reconcile it with observed phenomena. The second phase of the investigation is a study of the action of the transverse reinforcement in the anchorage zone, with emphasis on its behavior after longitudinal cracking has occurred. In short, the exploratory investigation is planned to answer the questions "What starts a crack?" and "What stops a crack?" under relatively simple laboratory conditions.

The major variables involved in the problem may be divided into two general groups: (a) variables related to the effect of the prestressing force, and (b) variables affecting the resistance of the anchorage zone.

In the first group are the magnitude of the prestressing force, the distribution of the reinforcement over the cross-section, the inclination of the reinforcement to the longitudinal axis of the beam, and the rate of transfer of the force from the reinforcement to the concrete. In the second group are the shape and size of the beam section, and the quality of the concrete. The rate of transfer of the force from the reinforcement to the concrete is affected by many variables such as time dependent effects, manner of release of the reinforcement, the surface condition of the reinforcement, the depth of concrete below the reinforcement, and also the concrete strength. Naturally, it is not practical to study experimentally the effects of all the variables. Especially in this exploratory series of tests, it is very desirable that the variables be limited so that the results can be compared with the available knowledge and with each other in as simple and direct a manner as possible.

Although the investigation is planned to study anchorage zone stresses in pretensioned beams, the information obtained will be useful also for the design of post-tensioned beams.

5.2 Test Program

(a) Test Specimens, Instrumentation and Test Procedure

The test specimens will be plain or reinforced concrete "blocks" as shown in Fig. 34. The cross section will be rectangular (Fig. 34c) or I-shaped (Fig. 34d). The specimens will be cast in pairs monolithically. The vertical broken lines in Fig. 34a and b represent the "end" of each specimen. The overall height, h, and the web thickness, b', will be varied. The flange thickness will be 6-in. for all the specimens.

The plain specimens (Fig. 34a) will be loaded eccentrically through a stiff plate extending across the width of the section. The load will be increased to failure in several increments.

The strand reinforcement in the reinforced specimens (Fig. 34b) will be pretensioned to approximately 200,000 psi in the early series of tests. During the test, the force will be transferred to the concrete in several increments.

The measurements will include the total load on the concrete, the overall deformation of the concrete, and the slip of the strand, if any. A detailed picture of the deformation of the specimen will be obtained by measuring strains in two orthogonal directions on all surfaces of the specimens. The strains will be measured mechanically over gage lengths of 2-in. as indicated in Fig. 34e. The development of cracks will be recorded.

Control specimens will comprise standard cylinders to be used in compression and splitting tests, plain concrete beams for modulus of rupture tests, and specimens for pull-out tests on the strand.

The maximum size of the gravel to be used is 3/8-in. The cement will be Type III. The prestressing reinforcement may vary from 1/4 to 3/8-in. diameter strand. In specimens with loads applied at large eccentricities intermediate grade reinforcement may be used.

(b) Outline of Tests

The proposed experimental program is divided into six series, each series consisting of three pairs of specimens. The variables in each series are indicated in Table I.

The target concrete strength will be 5000 psi for all the specimens. The eccentricity of the prestressing force on the applied load will be kept constant at 3/8 of the over-all depth.

The major variable in the first two series of tests is the depth of the section. The amount of longitudinal reinforcement is to be varied in Series 2 in order to maintain a constant reinforcement ratio. The primary object of these two series is to determine the smallest depth of specimen on which reliable strain measurements can be made using a gage length of 2 in. Critical information should also be obtained about the differences between the strain conditions in the anchorage zones of post-tensioned (Series 1) and pretensioned (Series 2) beams.

The major variable in series 3 and 4 is the shape of the cross section. In both series the specimens will be I-shaped, and the web thickness will be varied.

In Series 5 the major variable is the amount of longitudinal reinforcement. On the basis of information to be obtained from Series 1 through 4, the specimens of Series 5 will be designed to develop serious longitudinal cracking.

The type of specimen which exhibited the most severe cracking in Series 5 will be used in Series 6 with various amounts of transverse reinforcement in order to study the effect of transverse reinforcement on longitudinal cracking.

At the conclusion of Series 6, it is planned that the results of the investigation will be evaluated as a whole to determine if further experimental work is required.

6. SUMMARY

The object of this report is to review and discuss available information useful for the determination of anchorage zone stresses in pretensioned prestressed concrete beams. Research on anchorage zone stresses in both post- and pre-tensioned beams and on the rate of stress transfer in the anchorage zone of a pretensioned beams is reviewed. Two theoretical analyses are used to determine possible anchorage zone stress distributions and to provide a basis for the determination of the critical factors. On the basis of this information, a proposed test series aimed at developing a rational method for the design of transverse reinforcement in the anchorage zones of pretensioned beams is outlined.

Reviews are made of 13 investigations concerned with anchorage zone stresses in prestressed concrete beams. Eleven of the investigations were for post-tensioned and two for pretensioned beams. Eleven of the investigations were theoretical and only two experimental. For theoretical analyses, the theory of elasticity was used in six investigations, photoelasticity in three, and the lattice analogy in two. Eight of these investigations were basically two-dimensional and three were three-dimensional. Three of the theoretical investigations included limited experimental work. It is concluded that, for post-tensioned beams, the available experimental data are not adequate to justify the acceptance any one particular analysis and that almost no information is available about the behavior or the mode of failure of end-blocks in pretensioned beams.

Reviews are made of eight studies concerned with the determination of the bond characteristics of prestressing reinforcement. The variables in these studies were the effects of alterations in the type and surface condition of the reinforcement, concrete strength, wire diameter, manner of release, depth of concrete under the reinforcement, and time-dependent effects. Interpretations of the results were not always in agreement. It is concluded that these investigations are not conclusive. The rate of stress transfer cannot be predicted with any degree of precision, even for a given wire under a given set of conditions.

Two theoretical analyses, one due to Bleich and one due to Guyon, are used to study possible transverse, shear, longitudinal and maximum principal stress distributions in end-blocks. For a post-tensioned beam these distributions are determined for a single concentrated line load with eccentricities of a

half and three-eights of the depth of the beam. For a pretensioned beam, these distributions are determined for a single line load with an eccentricity of three-eights of the depth of the beam and an anchorage length of half the depth of the beam. Under these loading conditions, maximum principal tensile stresses are not significantly greater than transverse tensile stresses and their distributions are essentially similar. Two regions of high tensile stresses exist. One region, termed the bursting stress zone, lies at some depth on the axis of loading, and the other region, termed the spalling stress zone, lies near the end of the beam and away from the axis of loading. Maximum tensile stresses increase as the eccentricity of the applied load increases. For pretensioned beams, the spalling stresses were only about a third and the bursting stresses only about a half of those for post-tensioned beams.

For pretensioned I-beams without end-blocks, it appears that concentration of the prestressing reinforcement in flanges gives spalling stresses in the web greater than the bursting stress along the wires and that these spalling stresses are comparable or even higher than the predicted spalling stresses in post-tensioned beams. Under these circumstances, failure is likely to occur by longitudinal splitting of the web.

The immediate object of the proposed exploratory tests is to investigate the applicability of the theoretical solutions to actual cases. The major variables in the six series of tests, each comprising three specimens, are listed in Table 1.

LIST OF REFERENCES

1. Ribière, M. C., "Sur divers Cas de la Flexion des Prismes rectangles," Bordeaux 1889.
2. Bleich, F., "Der gerade Stab mit Rechteckquerschnitt als ebenes Problem", Der Bauingenieur, No. 9 pp. 255-259 and No. 10 pp. 304-307, 1923.
3. Sievers, H., "Uber den Spannungszustand im Bereich der Ankerplatten von Spanngliedern vorgespannter Stahlbeton-konstruktionen," Der Bauingenieur, Vol. 31, No. 4 April 1956, pp. 134-1356.
4. Morsch, E., "Uber die Berechnung der Gelenkquader", Beton und Eisen, No. 12 1923, pp. 156-161.
5. Magnel, G., "Design of the Ends of Prestressed Concrete Beams", Concrete and Constructional Engineering, Vol. 44 No. 5 May 1949, pp. 141-148.
6. Chaikes, S., "Calcul des Abouts des Poutres en Beton precontraint", International Congress of Prestressed Concrete, Communication B. 41 A.I.G., Ghent, 1951, pp. 565-591.
7. Bruggeling, A. S. G., (in Dutch). De Ingenieur, No. 27 1950.
8. Guyon, Y., "Contraintes dans les Pieces prismatiques soumises à des Forces appliquees sur leurs Bases, au Voisinage de ces Bases," International Association for Bridge and Structural Engineering, Publications, Vol. 11 1951, pp. 165-226.
9. Guyon, Y., Prestressed Concrete, 1st Edition, J. Wiley and Sons, Inc. New York, 1953.
10. Christodoulides, S. P., "A two-dimensional Investigation of the End Anchorages of Post-Tensioned Concrete Beams", The Structural Engineer Vol. 33 No. 4 April 1955, pp. 120-133.
11. Christodoulides, S. P., "The Distribution of Stresses around the End Anchorages of Prestressed Concrete Beams", International Association for Bridge and Structural Engineering. Publications, Vol. 16 1956, pp. 55-70.
12. Ban, S., H. Muguruma, and Z. Ogaki, "Anchorage Zone Stress Distributions in Post-Tensioned Concrete Members", Proceedings, World Conference on Prestressed Concrete, San Francisco, July 1957, pp. 16.1-16.14.
13. Ramaswamy, G. S. and H. Goel, "Stresses in End Blocks of Prestressed Beams by Lattice Analogy", Proceedings, World Conference on Prestressed Concrete, San Francisco, July 1957, pp. 23.1-23.4.
14. Mahajan, K. D., "Analysis of Stresses in a Prestressed Beam Using Araldite Models", Indian Construction News August 1958, pp. 112-117.

15. Douglas, D. J. and N. S. Trahair, "An Examination of the Stresses in the Anchorage Zone of a Post-Tensioned Prestressed Concrete Beam", Magazine of Concrete Research, Vol. 12, No. 34 March 1960, pp. 9-18.

16. Ross, A. D., "Some Problems in Concrete Construction", Magazine of Concrete Research, Vol. 12, No. 34 March 1960, pp. 27-28.

17. Base, G. D., "An Investigation of the Transmission Length in Pretensioned Concrete", Third Congress of the Federation Internationale de la Precontrainte, Berlin, 1958, Session III, Paper No. 9.

18. Marshall, W. T., "Laboratory Investigation of Horizontal End-Zone Cracking in Pretensioned Prestressed Concrete", 6th Annual Prestressed Concrete Institute Convention, New York, September 1960.

19. Hoyer, E. and E. Friedrich, "Beitrag zur Frage der Haftspannung in Eisenbetonbauteilen", Beton und Eisen (Berlin), 1939 Vol. 38, No. 6 pp. 107-110.

20. Marshall, G., "End Anchorage and Bond Stress in Prestressed Concrete", Magazine of Concrete Research Vol. 1, pp. 123-127, December 1949.

21. Janney, J. R., "Nature of Bond in Pretensioned Prestressed Concrete Journal A. C. I. May 1954, Proceedings, Vol. 50 pp. 717-736.

22. Linzell, S. O., "Design Studies and Loading Tests of Prestressed Concrete Beams", State of Ohio, Department of Highways Research Report 4:65-68 1954.

23. Lin, T. Y., Design of Prestressed Concrete Structures, J. Wiley and Sons, Inc., New York 1955.

24. Ozell, A. M. and W. D. Givens, "Curing Methods and Duration Studies of Pretensioned Units", Florida Engineering and Industrial Experiment Station Bulletin 82, 1956.

25. Ruble, E. I., Panel Discussion, Journal of Prestressed Concrete Institute, Vol. 1 No. 2, pp. 10-22 1956.

26. Monson, E. M., "Stress Distribution in the Anchorage Zone of a Prestressed Concrete I-Beam, Unpublished M.S. Thesis, Iowa State University, Ames, Iowa 1957.

27. Ratz, E. H., M. M. Holmjanski, and V. M. Kolner, "The Transmission of Prestress to Concrete by Bond", Third Congress of the Federation, Internationale de la Precontrainte (Berlin) 1958, Session III, paper no. 10.

28. G. A. Dinsmore, P. L. Deutsch and J. L. Montemayor, "Anchorage and Bond in Pretensioned Prestressed Concrete Members" Fritz Laboratory Report 223-19. Lehigh University, Dec. 1958.

29. Evans, R. H., "Transmission Length and Bond Stress in Pretensioned Prestressed Concrete", Indian Construction News, Vol. 7 No. 8 August 1958, pp. 69-76.

30. Evans, R. H., "Research and Developments in Prestressing", Journal Inst. Civ. Engrs. Vol. 35 p. 231, February 1951.

31. Hawkes, J. M. and R. H. Evans, "Bond Stresses in Reinforced Concrete Columns and Beams. The Structural Engineer Vol. 29, No. 12, Dec. 1951.

32. Evans, R. H. and A. Williams, "The Use of X-Rays in Measuring Bond Stresses in Prestressed Concrete" World Conference on Prestressed Concrete, San Franscisco, July-August 1957.

33. Faulkes, K. A., Unpublished M. S. Thesis, University of New South Wales, Sydney, Australia, 1958.

34. Goodier, J. N., "Compression of Rectangular Blocks and the Bending of Beams by Non-Linear Distribution of Forces", Transactions of American Society of Mechanical Engineers", 1932.

35. "Standard Plans for Highway Bridge Superstructures", U. S. Department of Commerce, Bureau of Public Roads, U. S. Government Printing Office, Washington, D. C., 1956.

TABLE 1

OUTLINE OF PROPOSED EXPLORATORY INVESTIGATION

Series	Depth	Longitudinal Reinforcement	Ratio of Web to Flange Width	Transverse Reinforcement
1	Variable	None	--	None
2	Variable	Variable	--	None
3	Constant	None	Variable	None
4	Constant	Constant	Variable	None
5	Constant	Variable	Constant	None
6	Constant	Constant	Constant	Variable

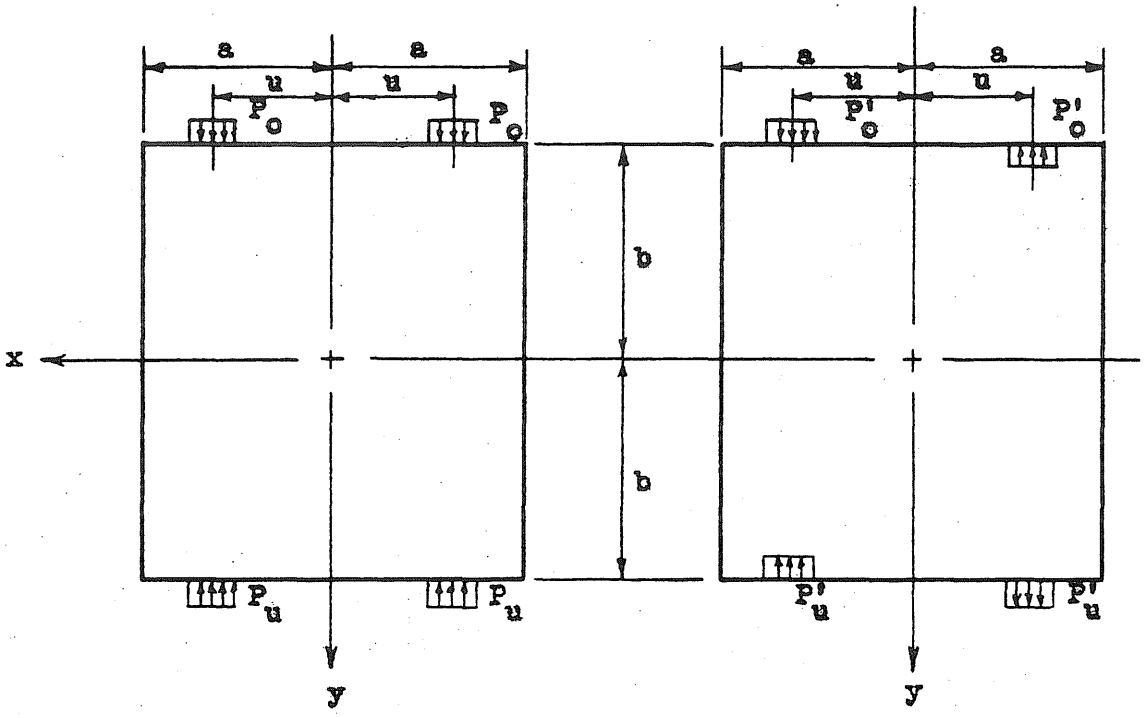

(a) Symmetrical Loading (b) Anti-Symmetrical Loading

FIG. 1 LOADING ARRANGEMENT - BLEICH

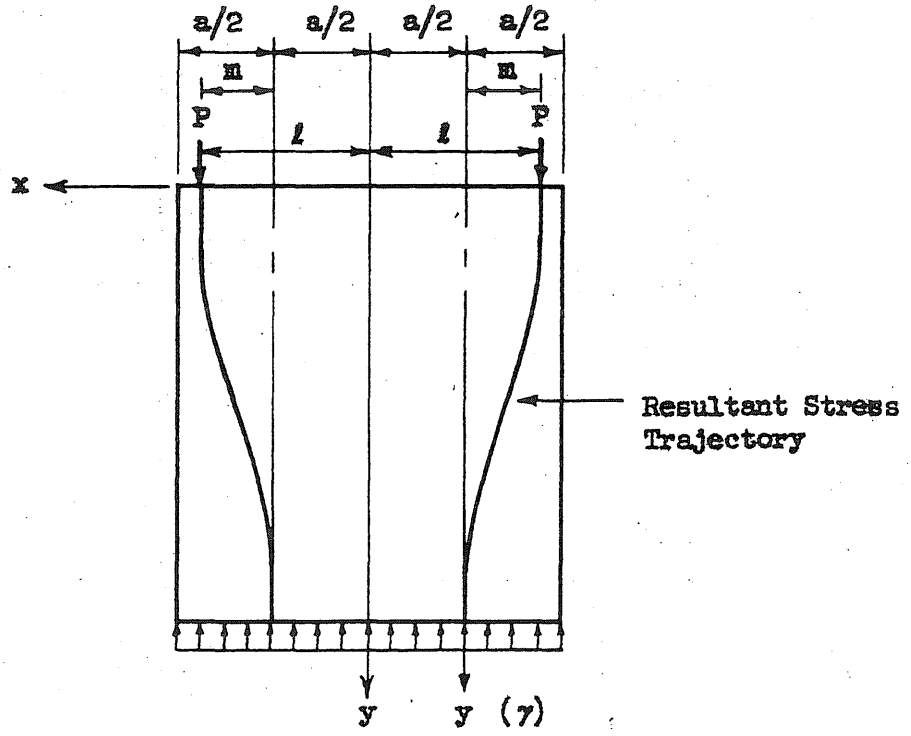

FIG. 2 LOADING ARRANGEMENT - SIEVERS

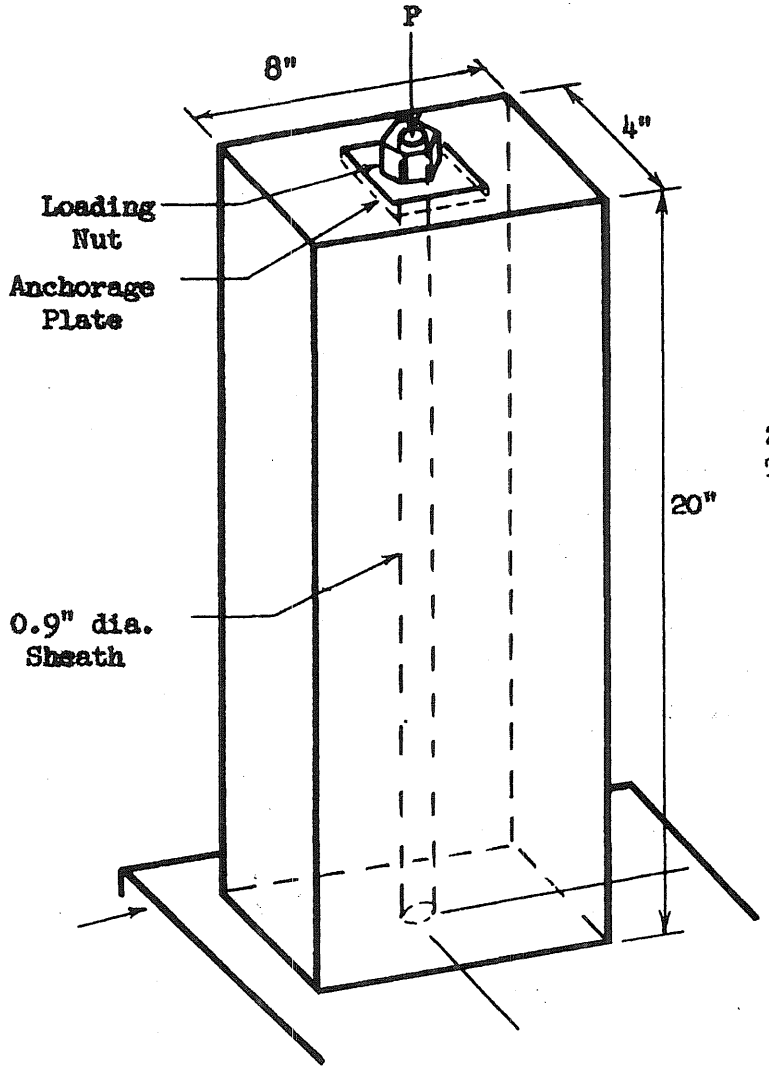

FIG. 3 DIMENSIONS OF TEST SPECIMENS AND LOADING ARRANGEMENT BAN

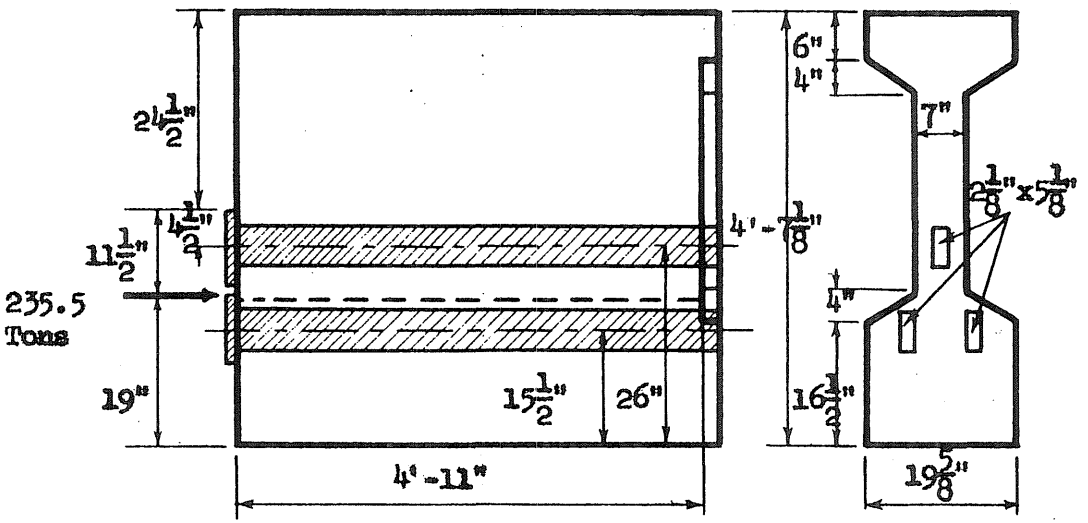

FIG. 4 DIMENSIONS OF END BLOCK TESTED BY MAGNEL

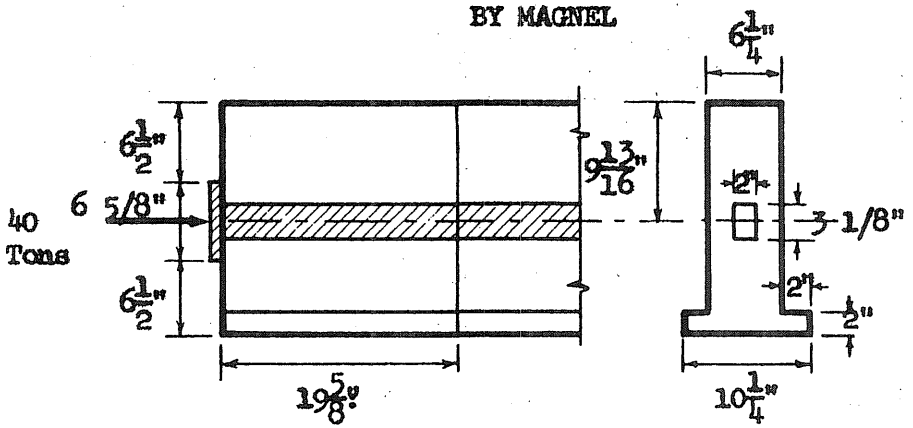

FIG. 5 DIMENSIONS OF END-BLOCK IN POST-TENSIONED BEAM REPORTED BY MAGNEL

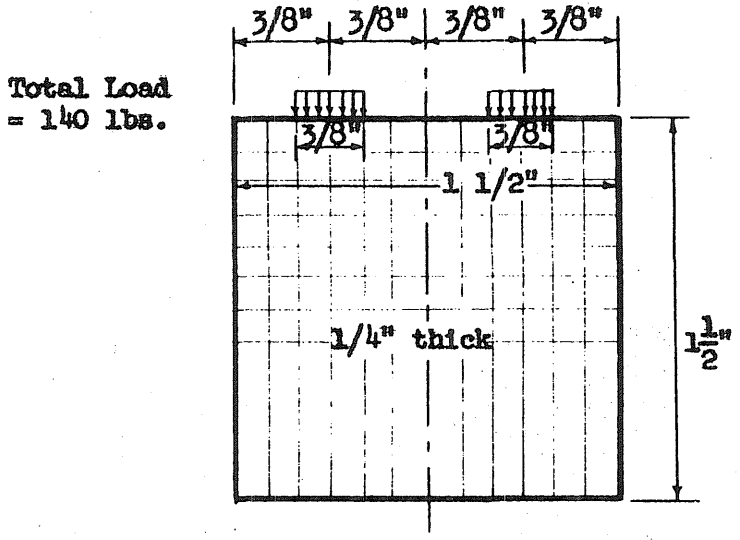

FIG. 6 LOADING ARRANGEMENT - CHRISTODOULIDES

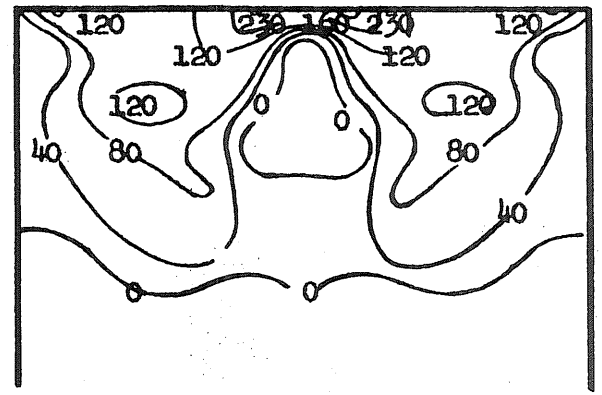

FIG. 7 PRINCIPAL TENSILE STRESSES (psi) CHRISTODOULIDES

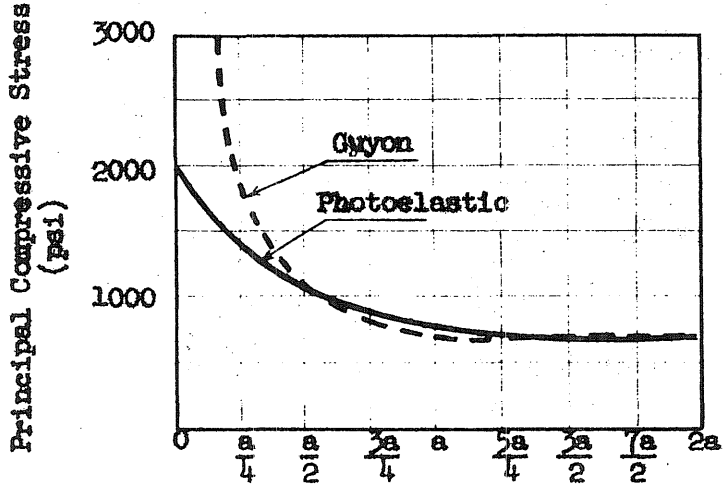

(a)

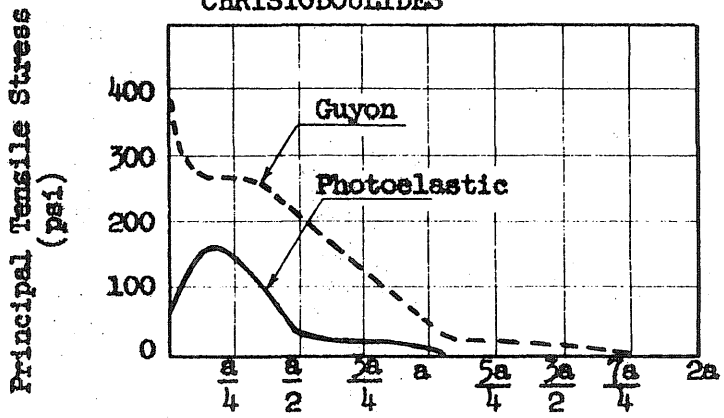

(b)

FIG. 8 COMPARISON OF PRINCIPAL STRESSES - MAHAJAN

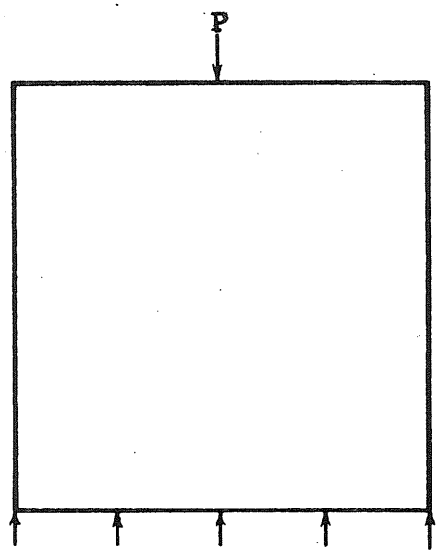

(a) Loading Arrangement

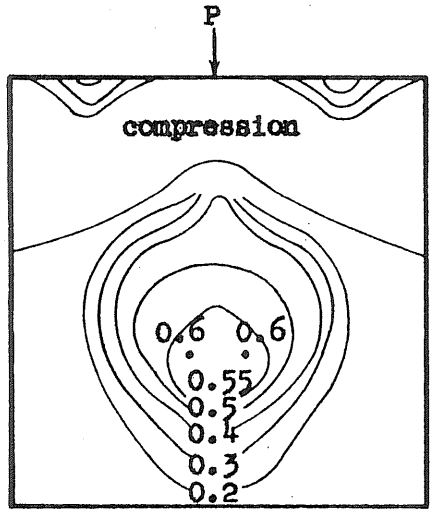

(b) Transverse Stress Distribution

FIG. 9 LATTICE ANALOGY SOLUTION - RAMASWAMY AND GOEL

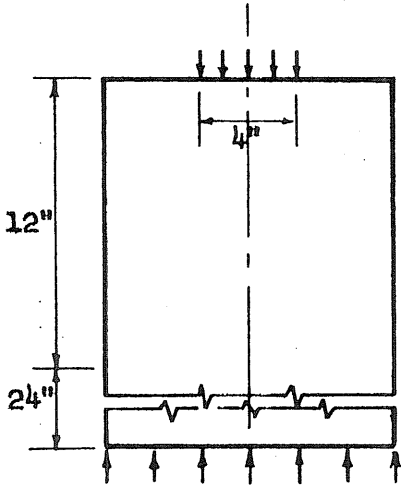

(a) Loading Arrangement

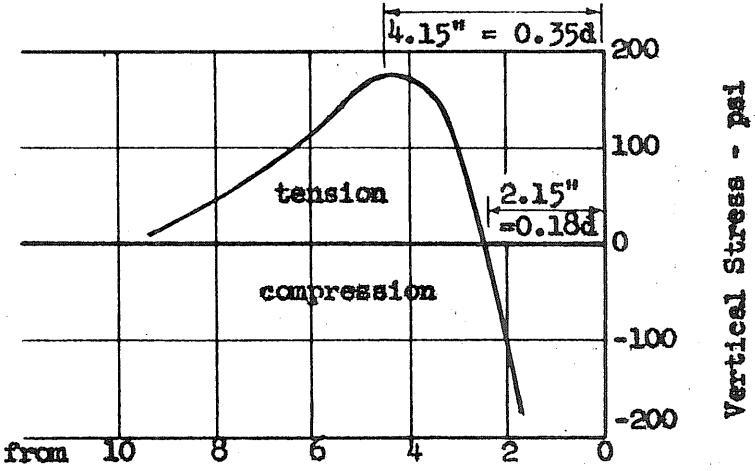

(b) Transverse Stresses along Horizontal Axis

FIG. 10 LATTICE ANALOGY SOLUTION - ROSS

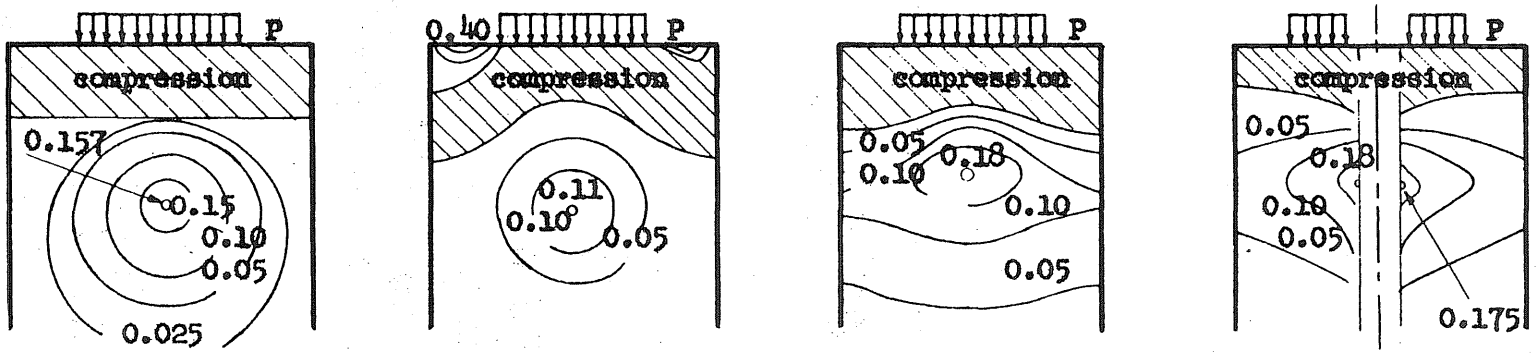

FIG. 11 COMPARISON OF TRANSVERSE STRESS DISTRIBUTIONS
Douglas and Trahair

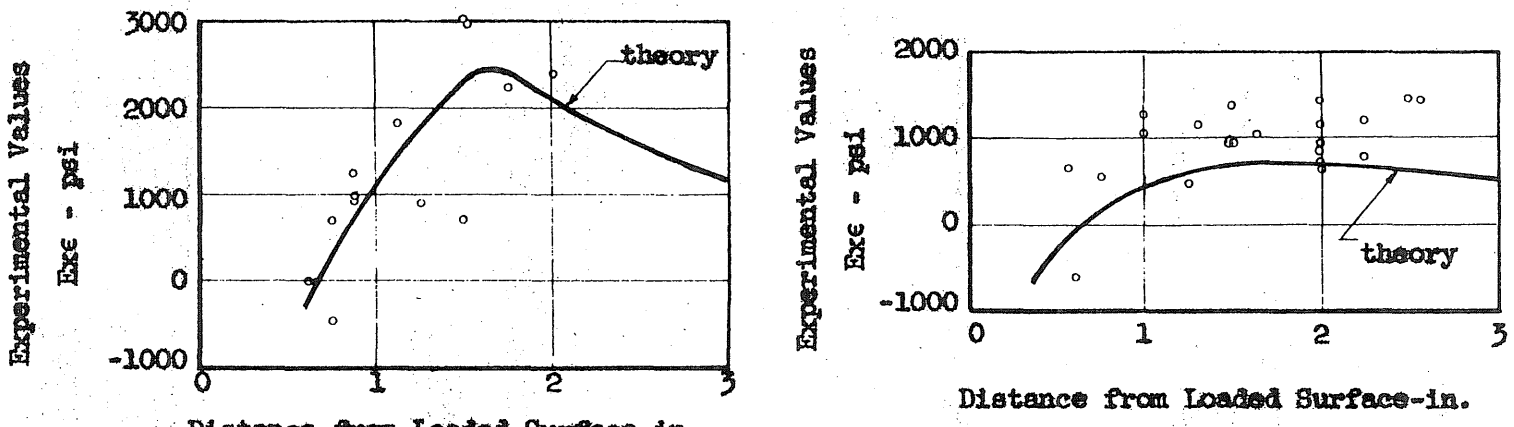

FIG. 12 COMPARISON OF MEASURED AND THEORETICAL HOOP STRESSES
DOUGLAS AND TRAHAIR

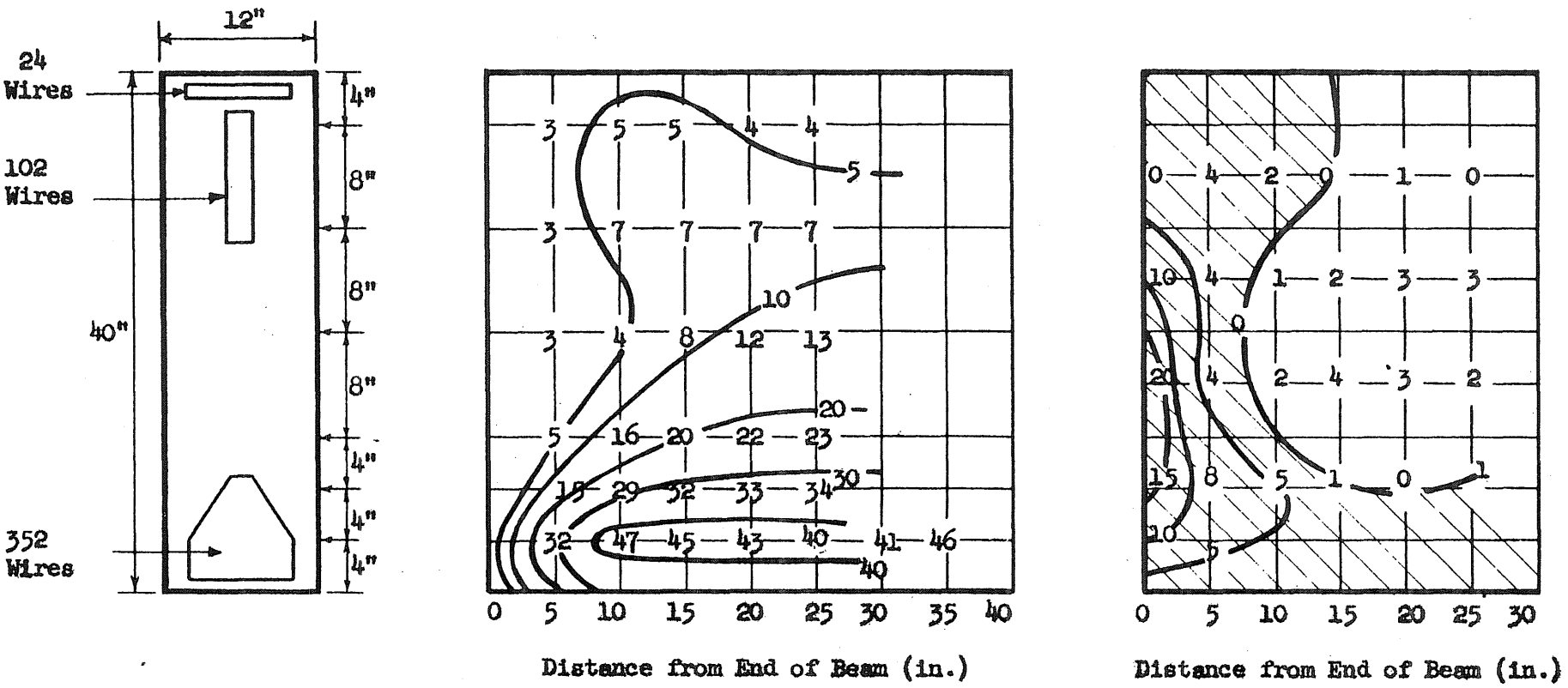

(a) Detail of Wire Positions and Beam Dimensions

(b) Longitudinal Strain Distribution

(c) Vertical Strain Distribution

FIG. 13 STRAIN MEASUREMENTS IN THE ANCHORAGE ZONE OF A PRETENSIONED RECTANGULAR BEAM - BASE

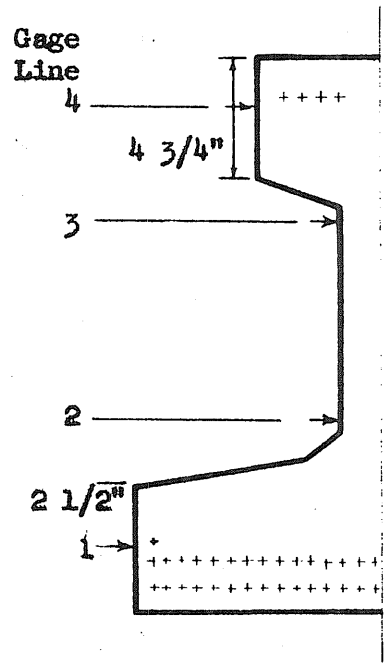

(a) Detail of Wire positions and Beam Dimensions

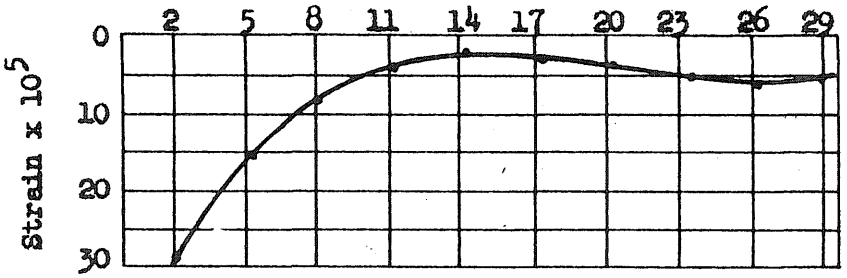

(b) Transverse Tensile Strains in Web

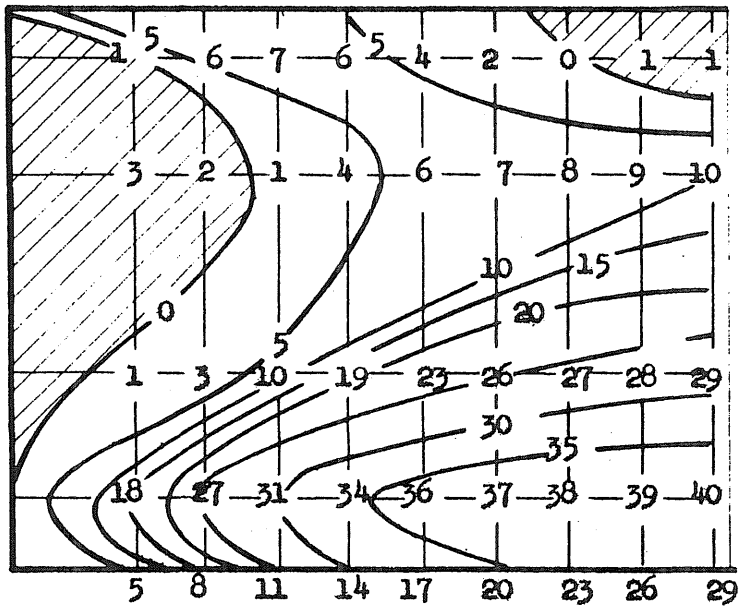

(c) Longitudinal Strain Distribution - Strain x 10^5

FIG. 14 STRAIN MEASUREMENTS IN THE ANCHORAGE ZONE OF AN INVERTED PRETENSIONED T-BEAM - BASE

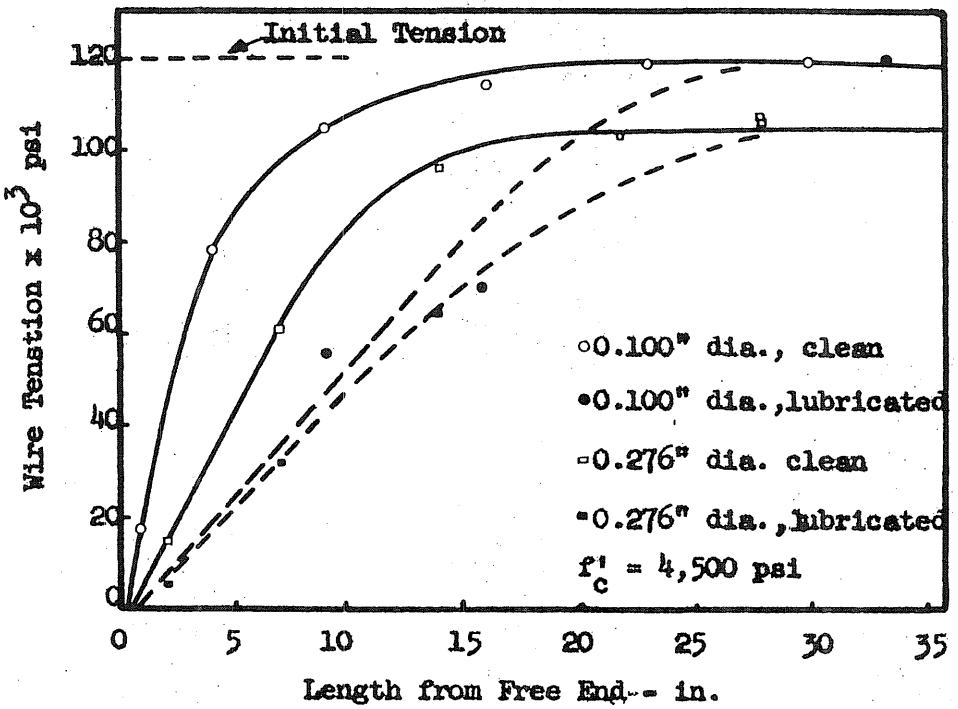

FIG. 15 STRESS TRANSFER DISTRIBUTIONS

JANNEY

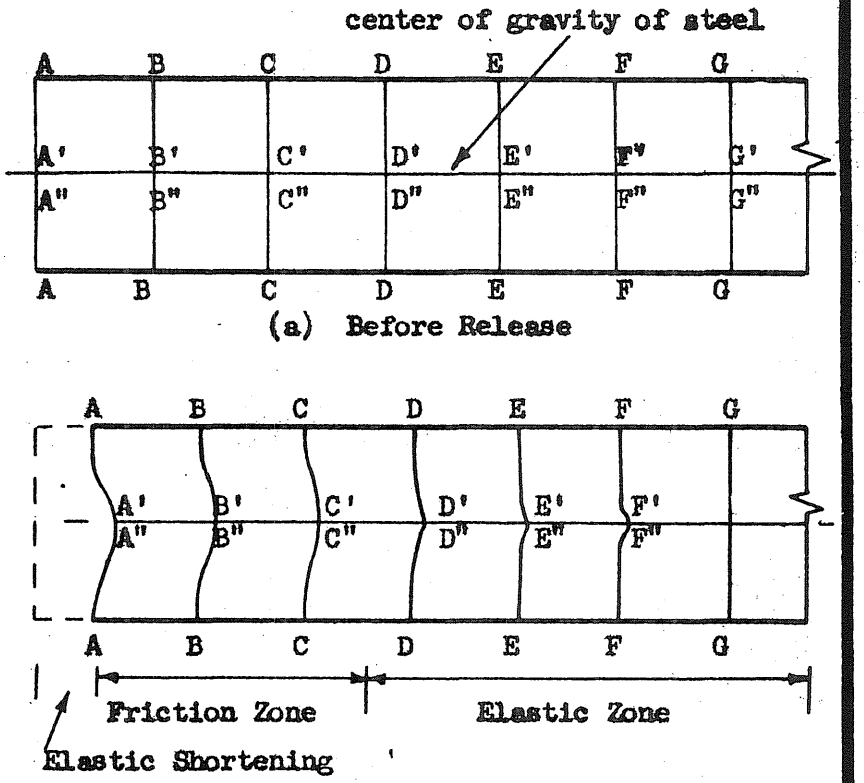

FIG. 16 ANCHORAGE ZONE DEFORMATIONS

DINSMORE

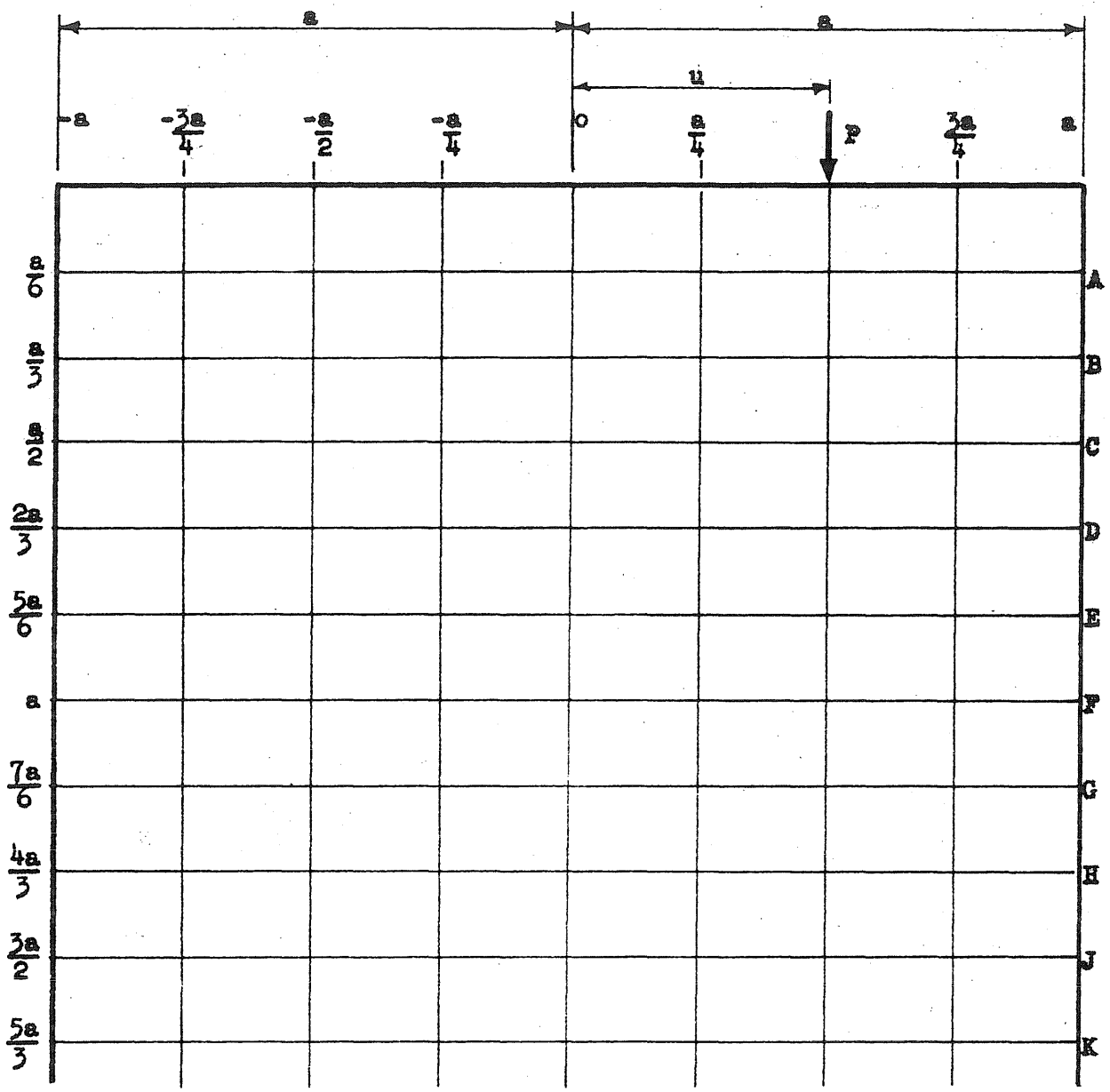

FIG. 17 LOADING ARRANGEMENT AND REFERENCE SYSTEM - POST-TENSIONED

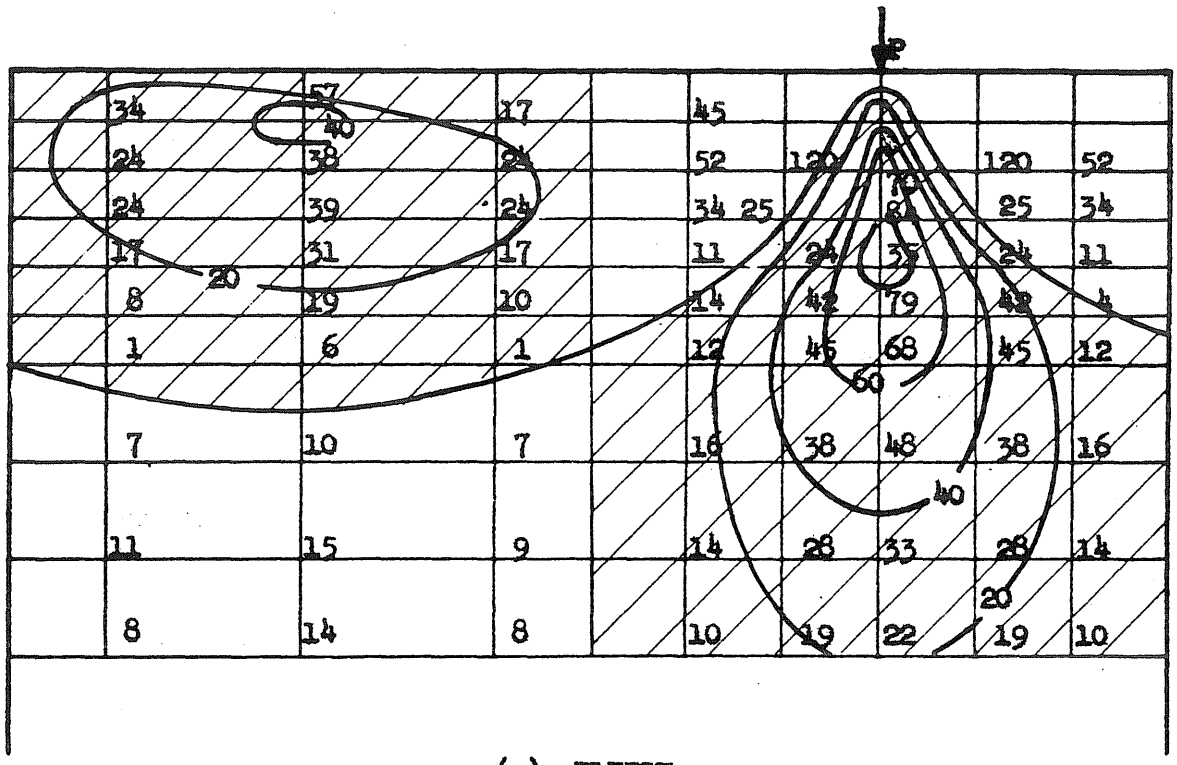

(a) BLEICH

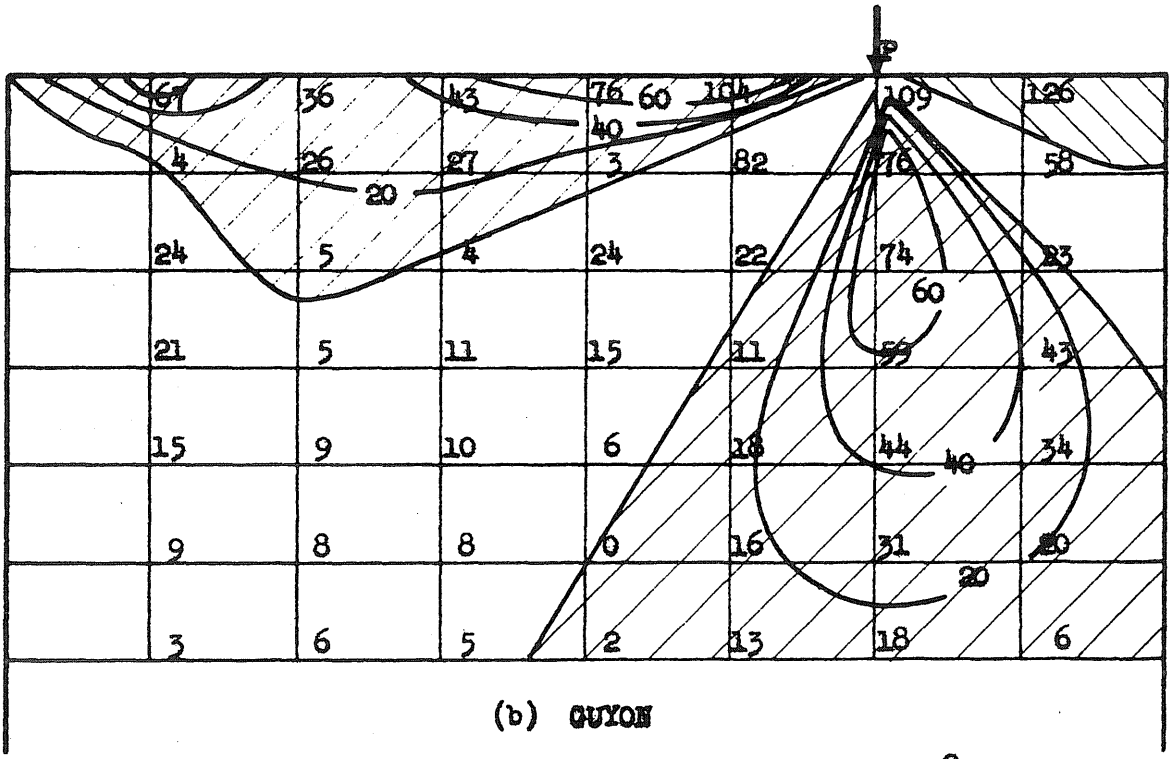

(b) GUYON

Coefficients of Average Compressive Stress x 10^2

FIG. 18 TRANSVERSE STRESS COEFFICIENTS - POST-TENSIONED

$u = \frac{a}{2}$

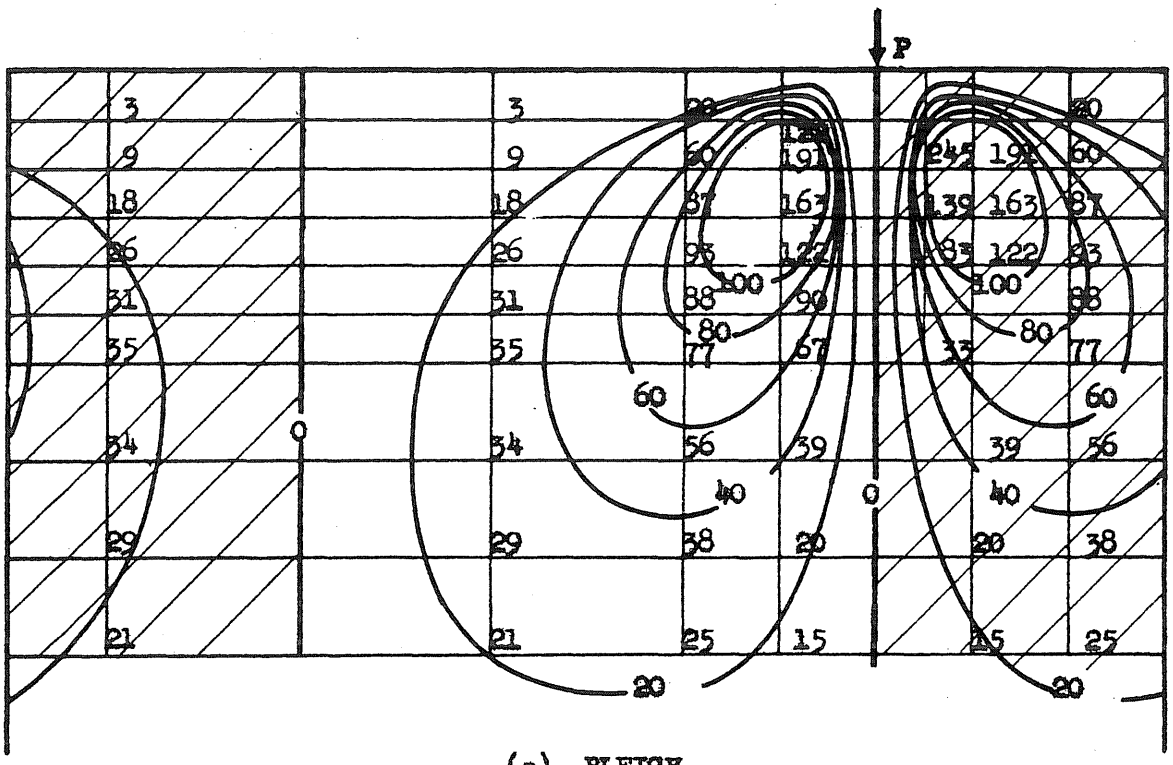

(a) BLEICH

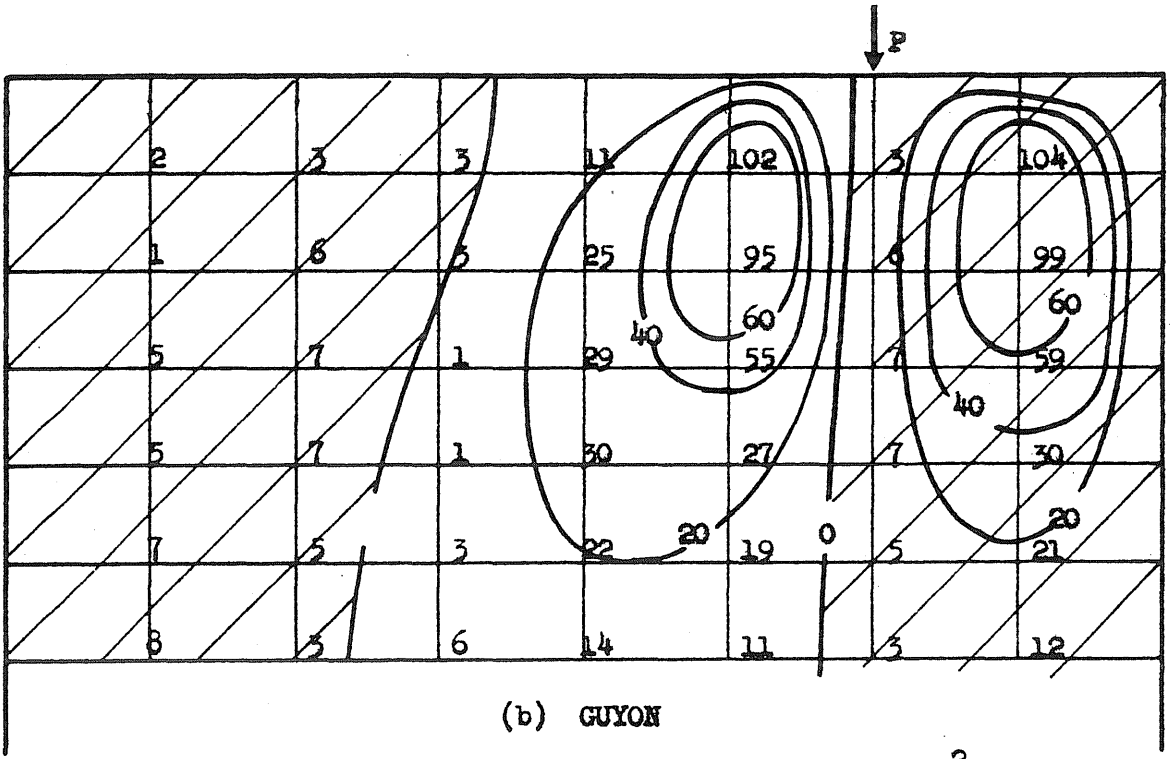

(b) GUYON

Coefficients of Average Compressive Stress x 10^2

FIG. 19 SHEAR STRESS COEFFICIENTS - POST-TENSIONED

$u = \frac{a}{2}$

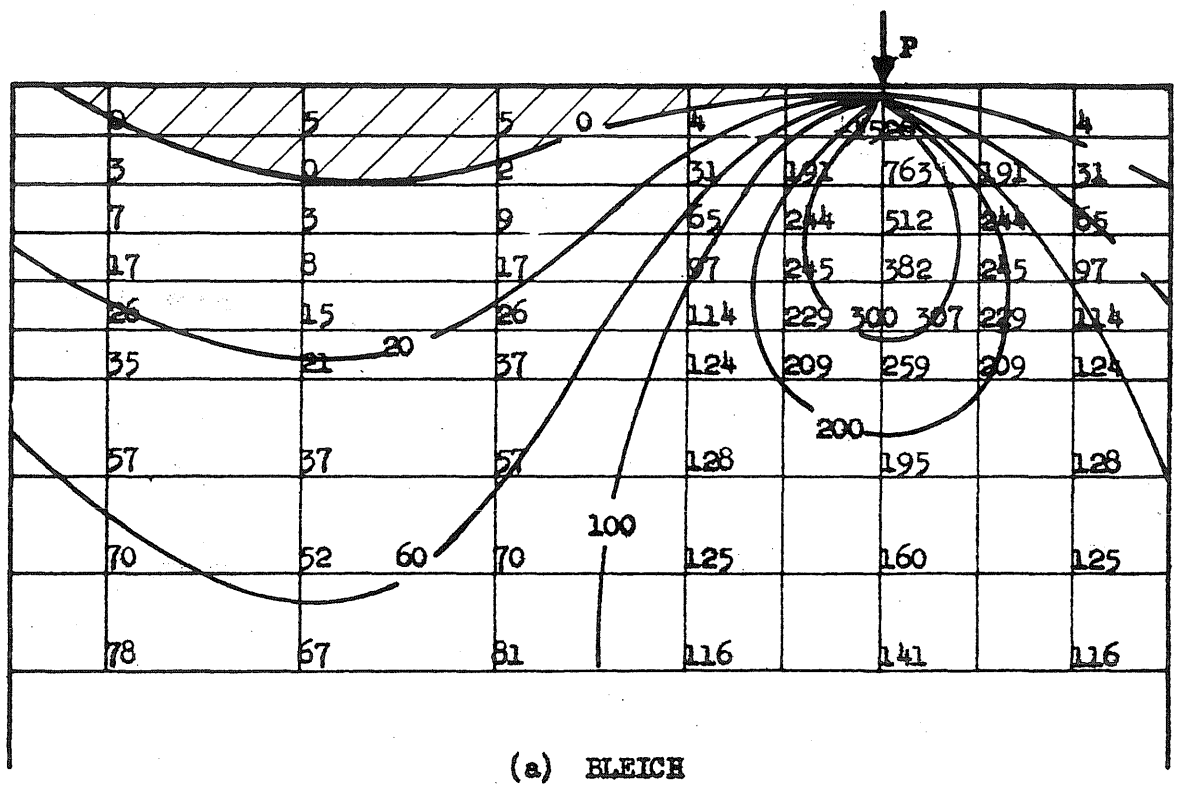

(a) BLEICH

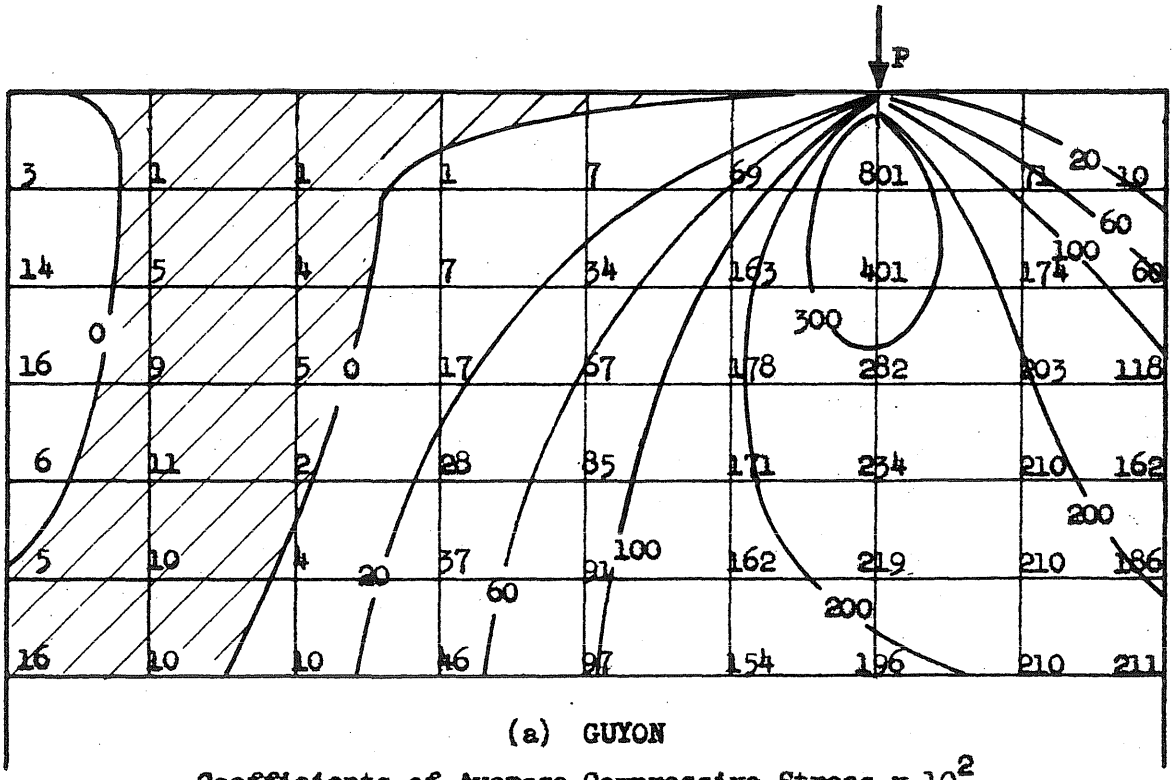

(a) GUYON

Coefficients of Average Compressive Stress x 10^2

FIG. 2C LONGITUDINAL STRESS COEFFICIENTS - POST-TENSIONED

GUYON, $u = \frac{a}{2}$

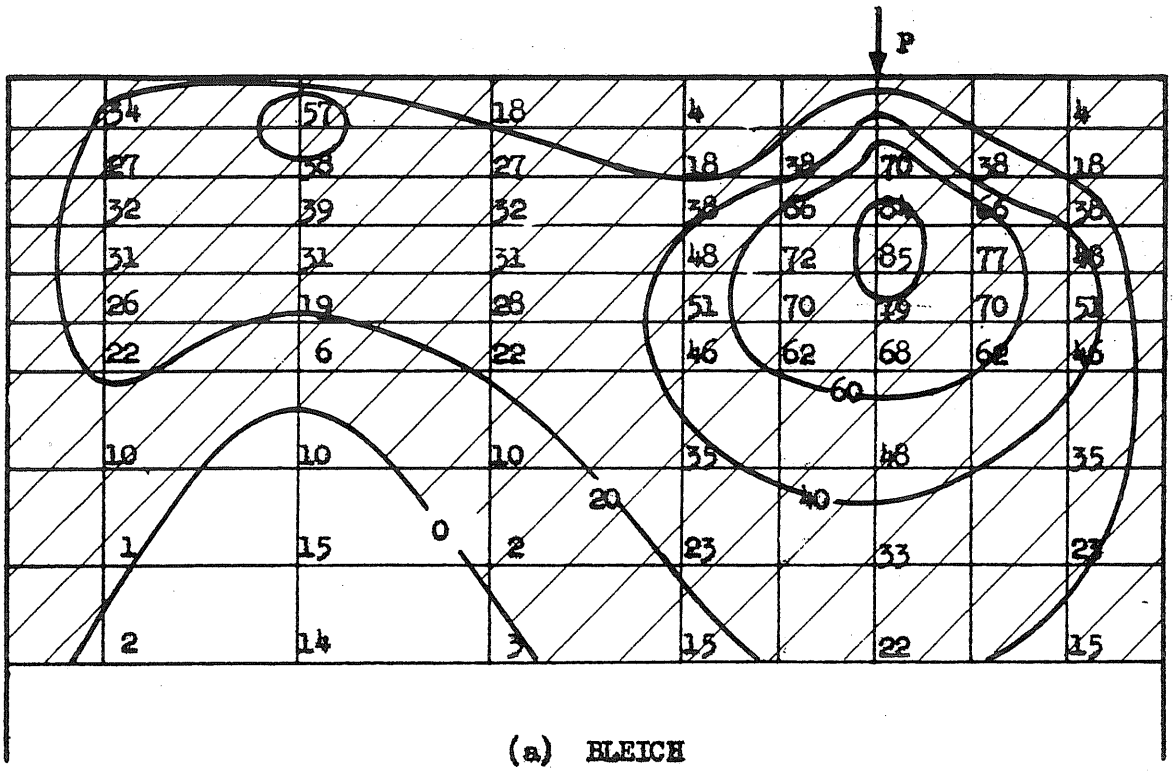

(a) BLEICH

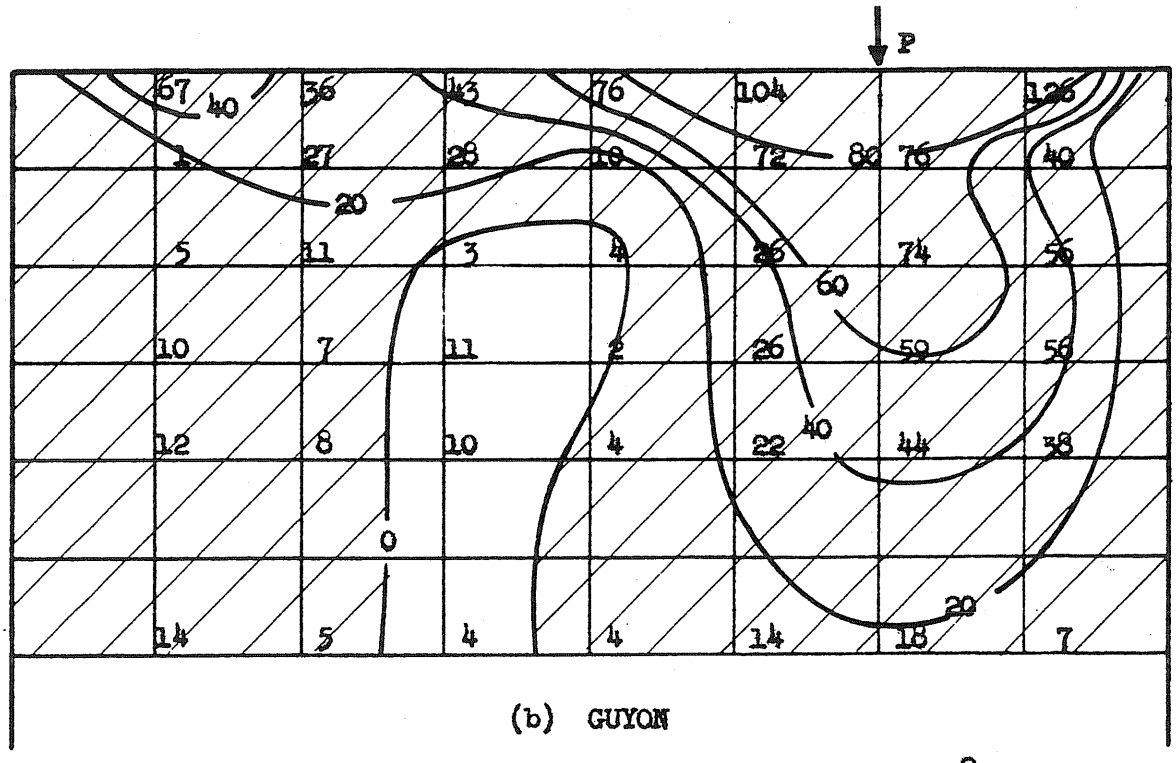

(b) GUYON

Coefficients of Average Compressive Stress x 10^2

FIG. 21 MAXIMUM PRINCIPAL STRESS COEFFICIENTS - POST-TENSIONED

$u = \frac{a}{2}$

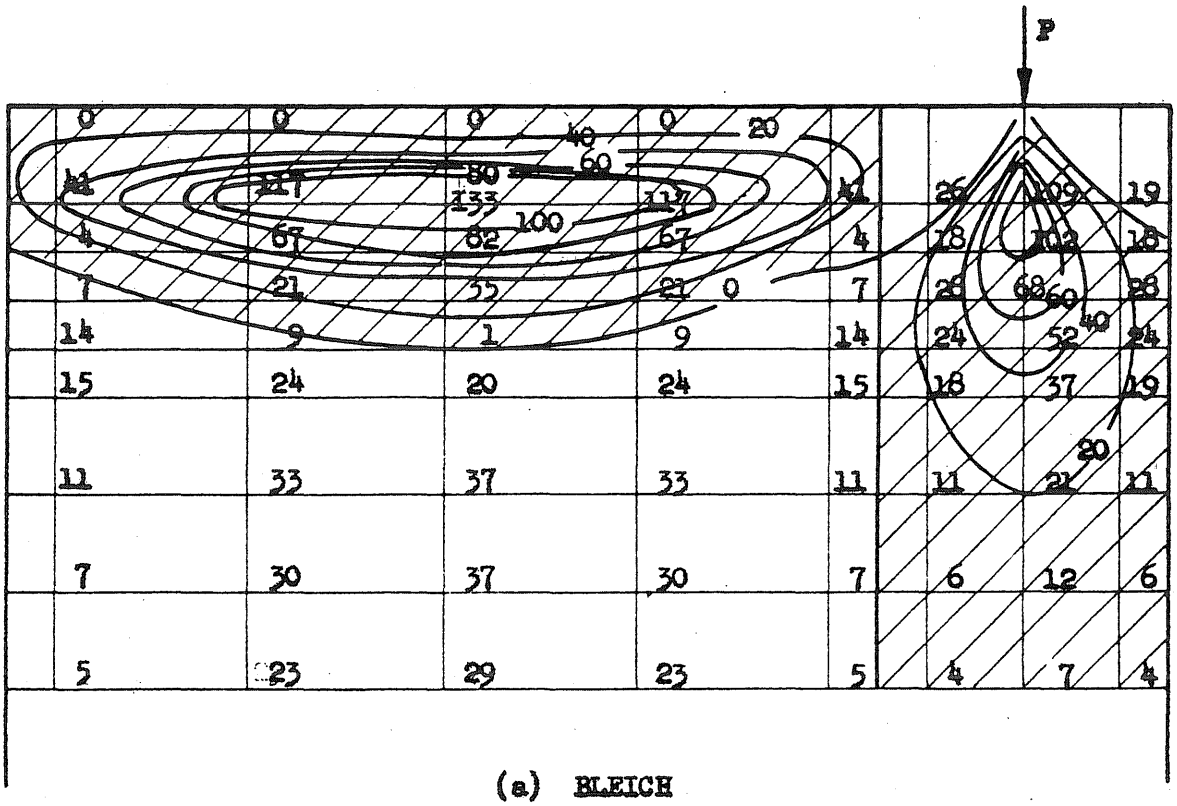

(a) BLEICH

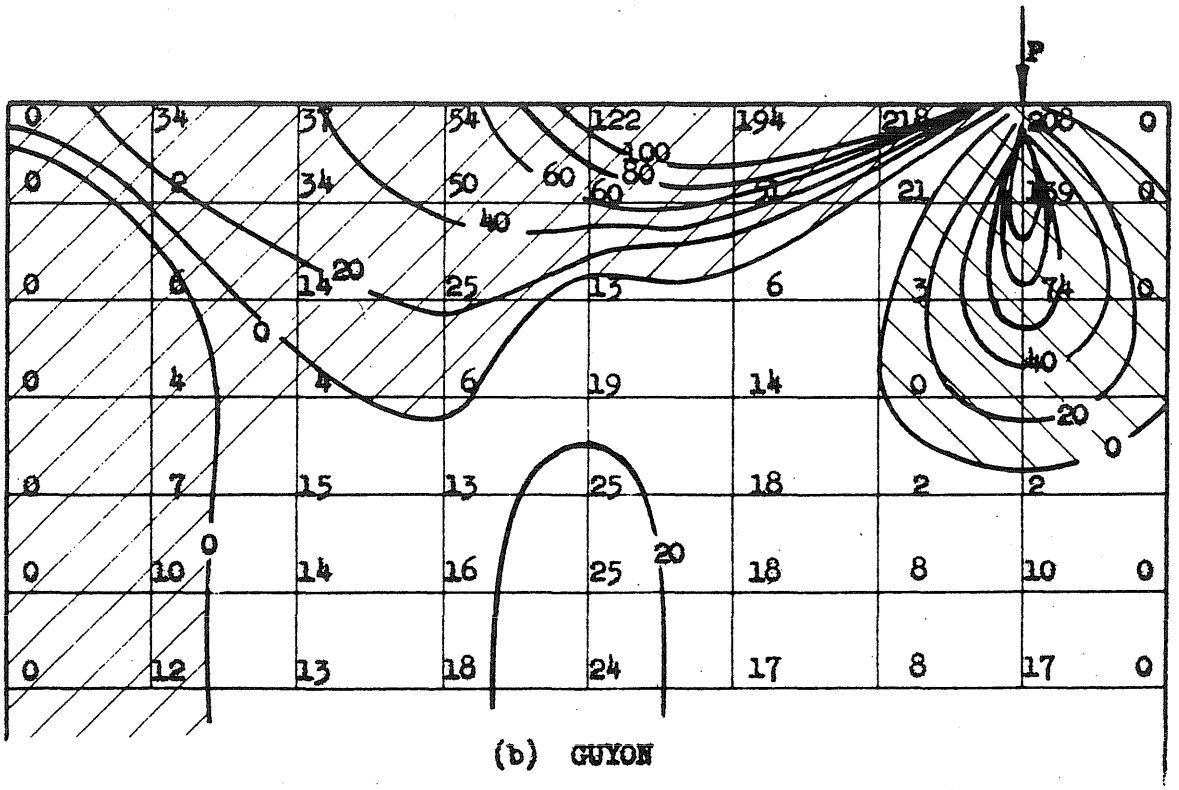

(b) GUYON

Coefficients of Average Compressive Stress x 10^2

FIG. 22 TRANSVERSE STRESS COEFFICIENTS - POST-TENSIONED

$u = \frac{3a}{4}$

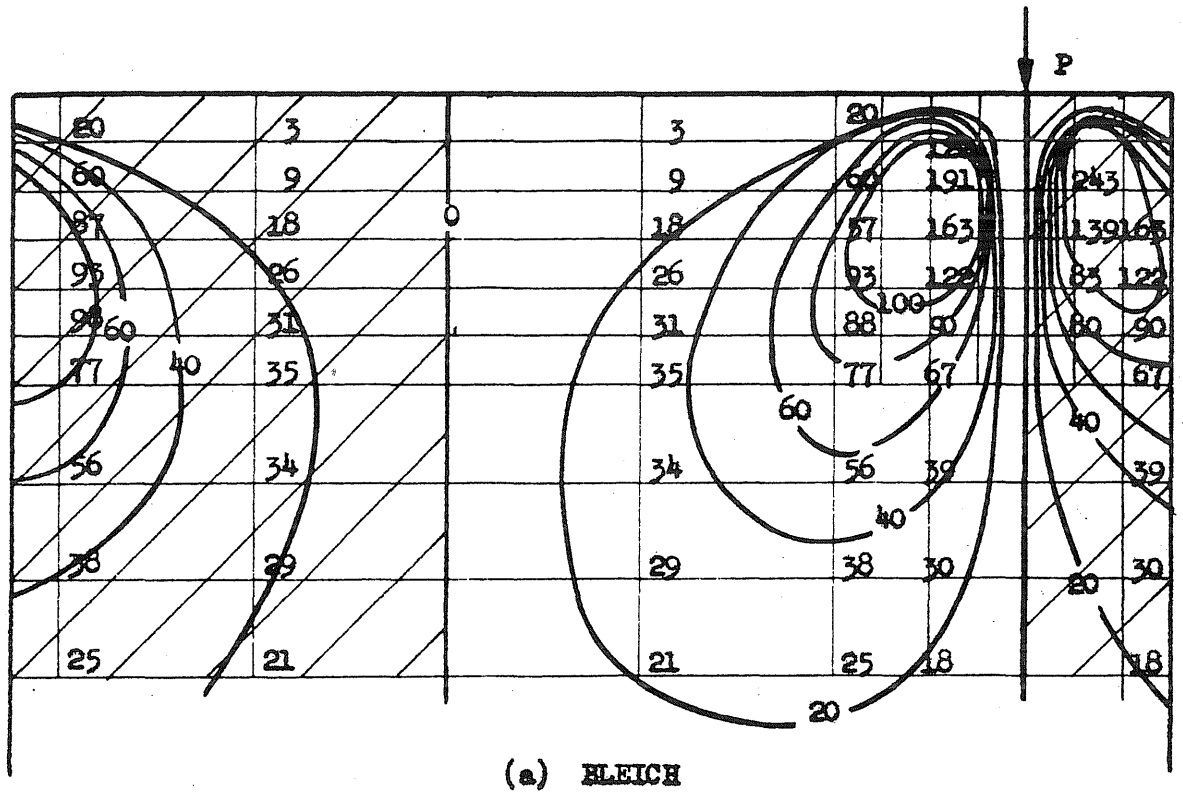

(a) BLEICH

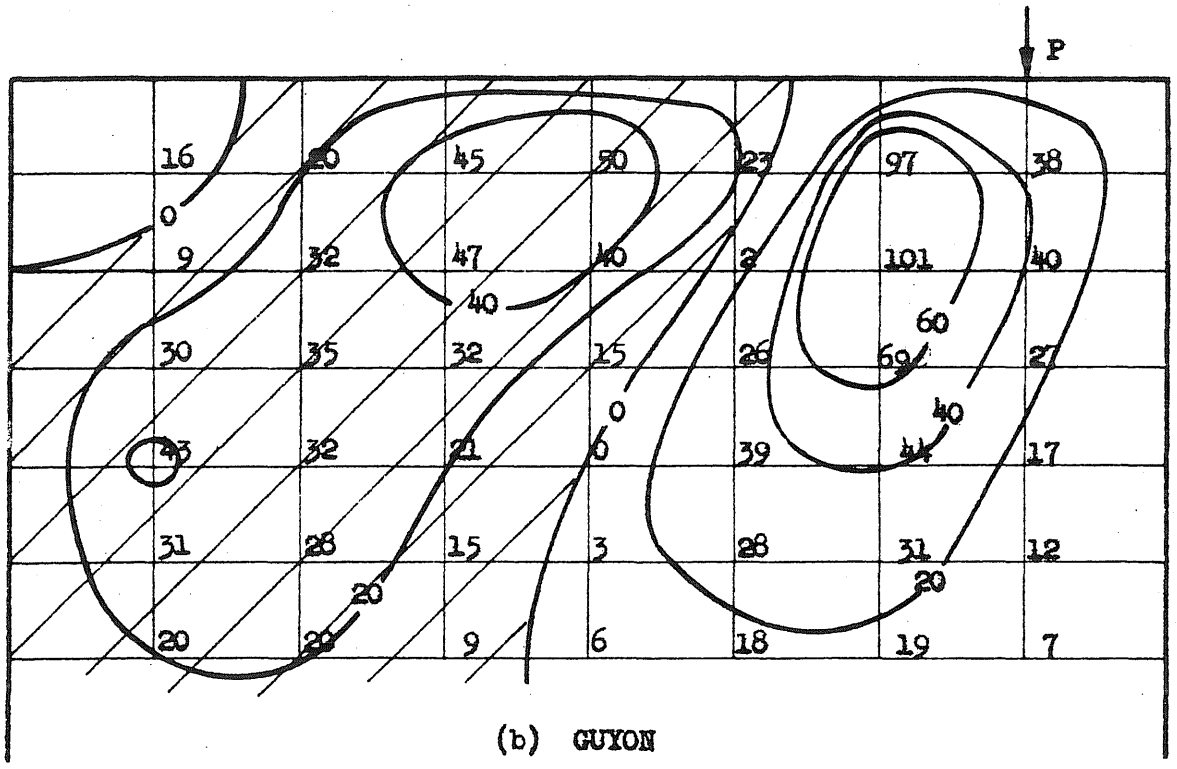

(b) GUYON

Coefficients of Average Compressive Stress x 10^2

FIG. 23 SHEAR STRESS COEFFICIENTS - POST-TENSIONED

$u = \frac{3a}{4}$

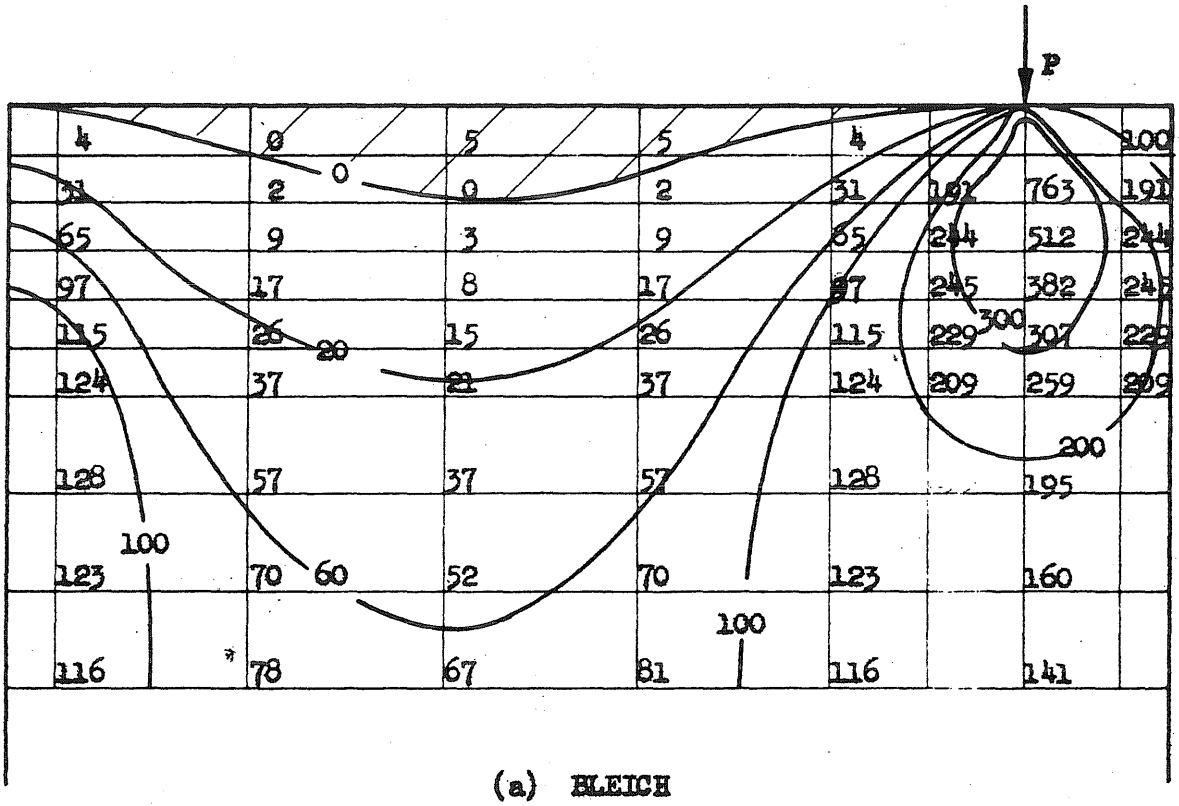

(a) BLEICH

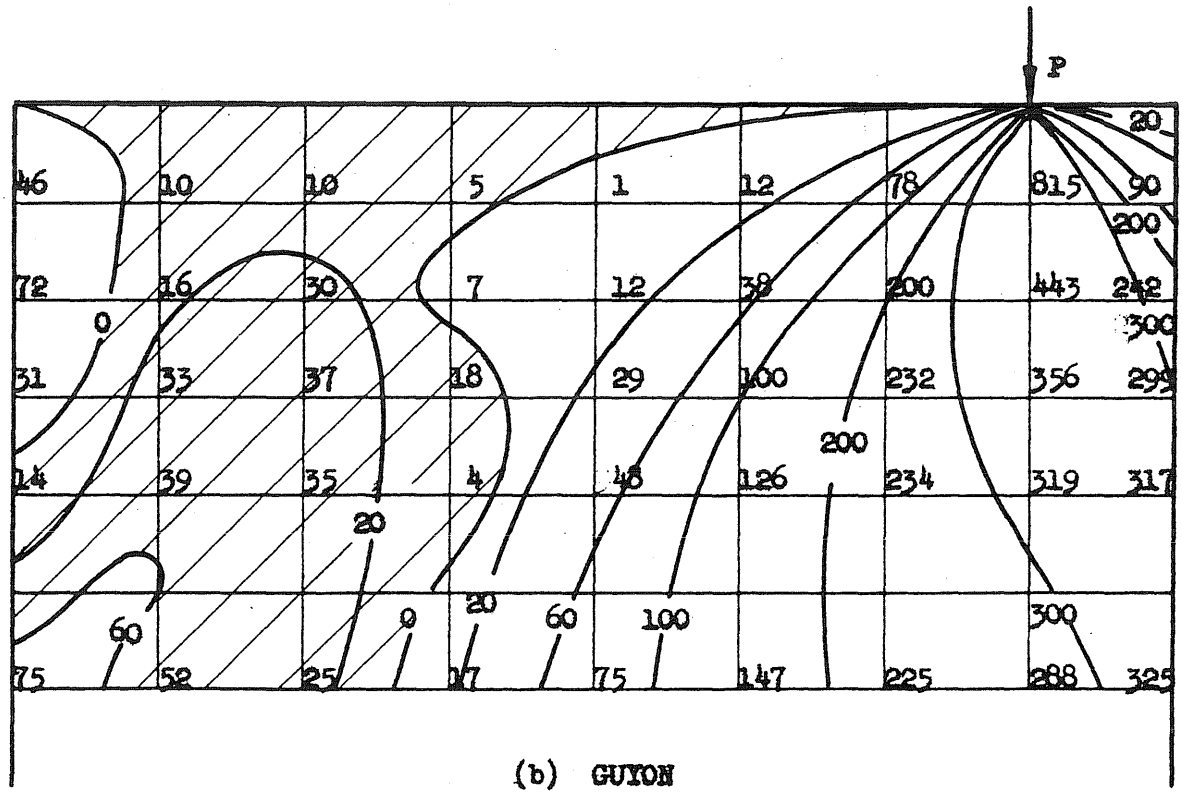

(b) GUYON

Coefficients of Average Compressive Stress x 10^2

FIG. 24 LONGITUDINAL STRESS COEFFICIENTS - POST-TENSIONED

$u = \frac{3a}{4}$

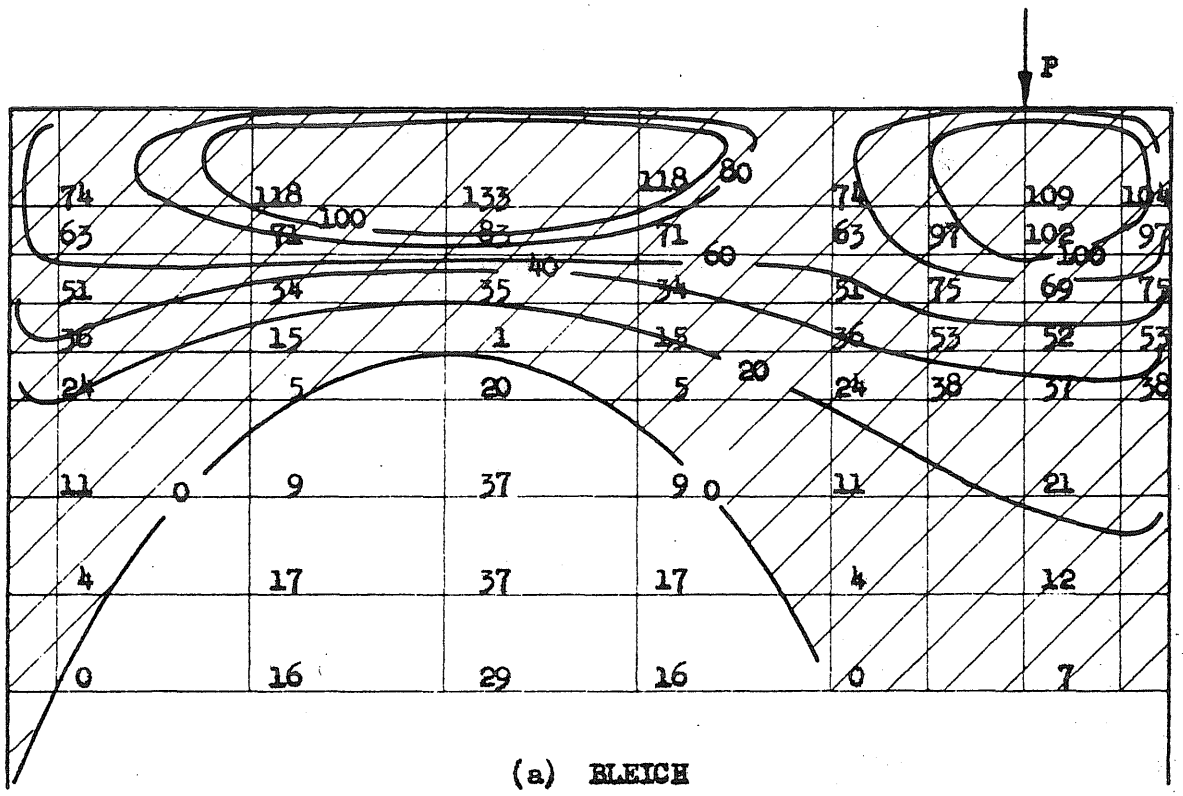

(a) BLEICH

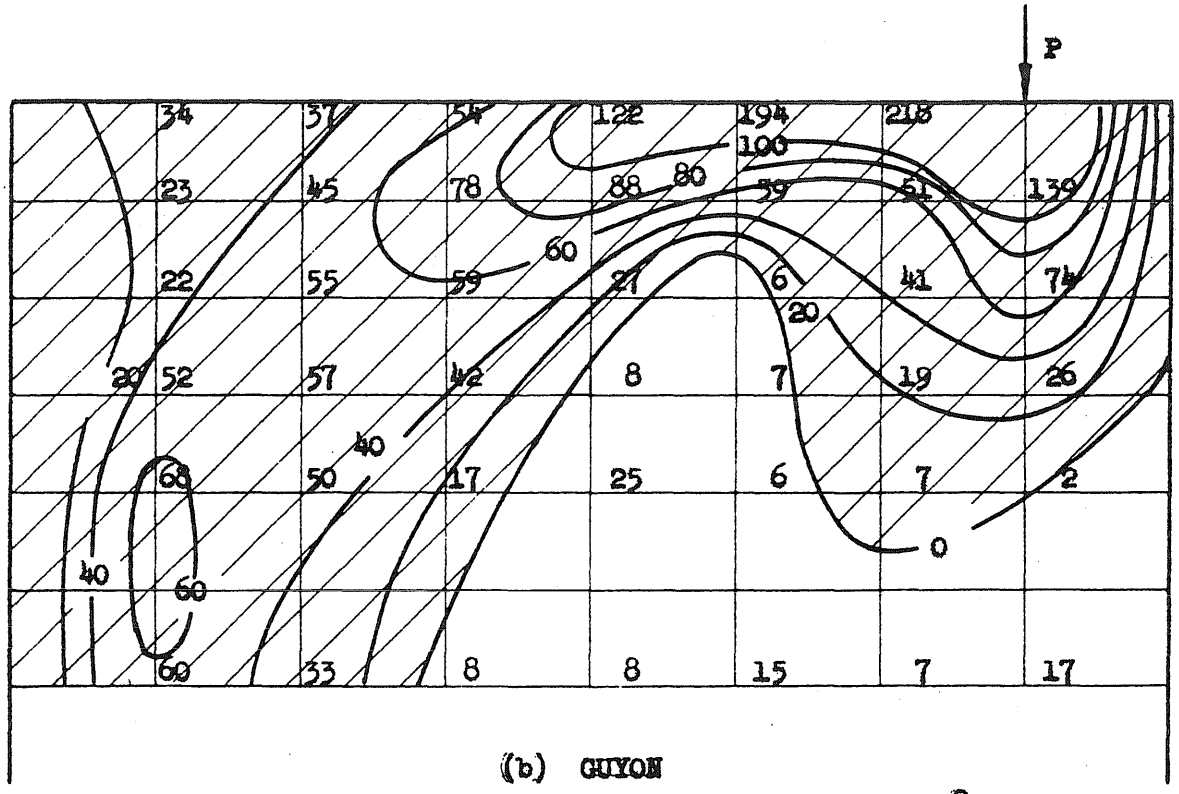

(b) GUYON

Coefficients of Average Compressive Stress x 10^2

FIG. 25 MAXIMUM PRINCIPAL STRESS COEFFICIENTS - POST-TENSIONED

$u = \frac{3a}{4}$

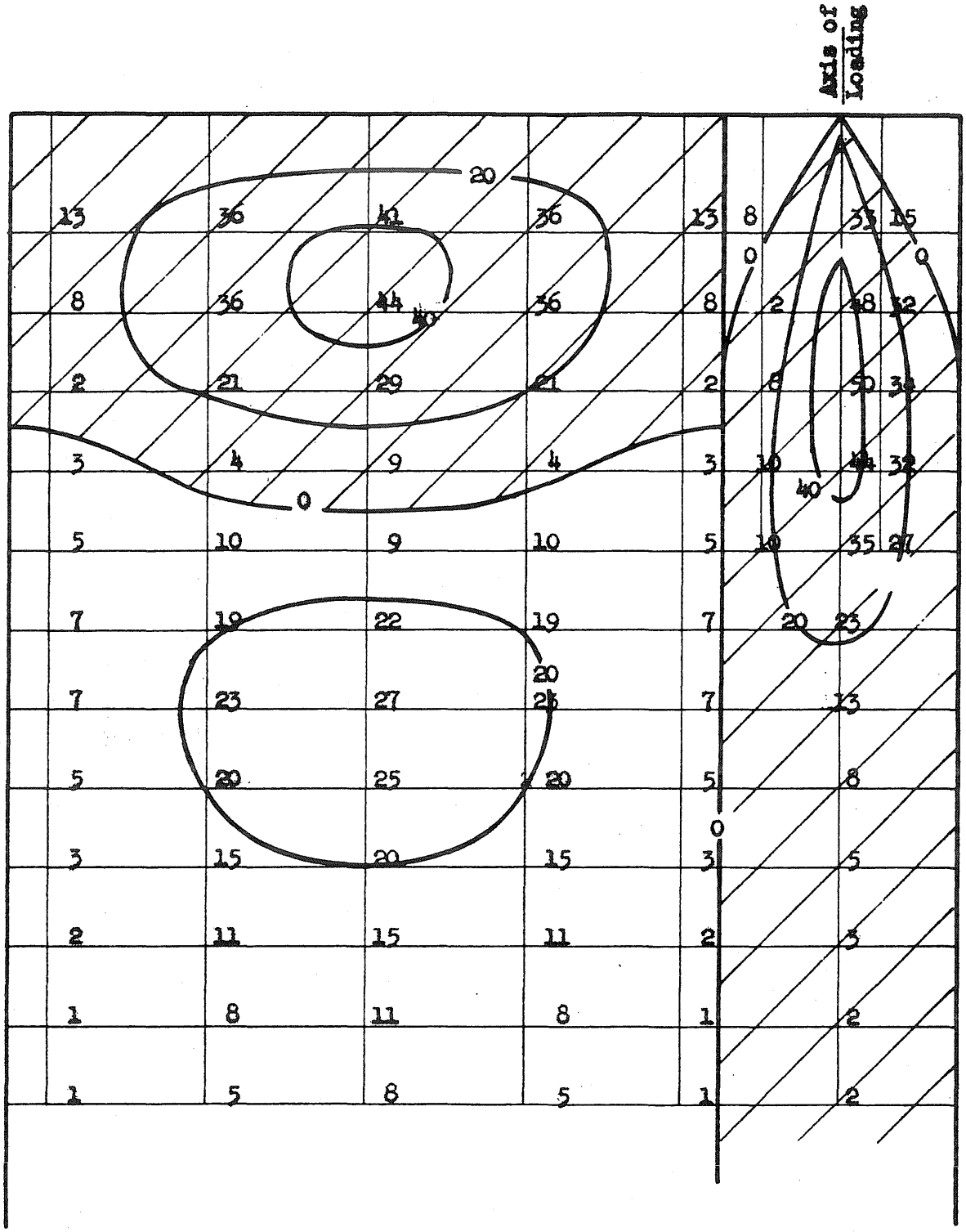

Coefficients of Average Compressive Stress x 10^2

FIG. 26 TRANSVERSE STRESS COEFFICIENTS - PRETENSIONED BLEICH, $u = \frac{3a}{4}$

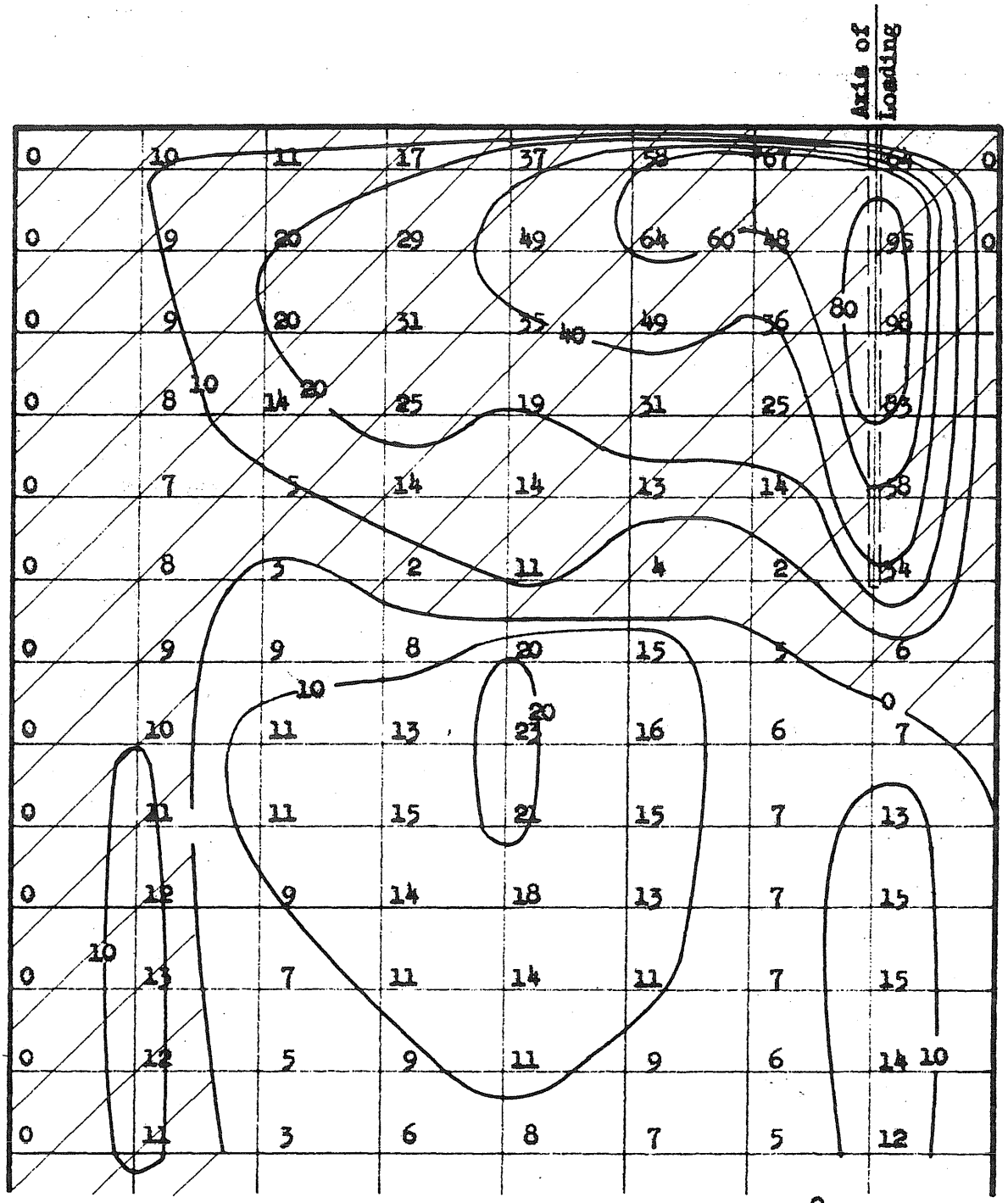

FIG. 27 TRANSVERSE STRESS COEFFICIENTS - PRETENSIONED

GUYON, $u = \frac{3a}{4}$

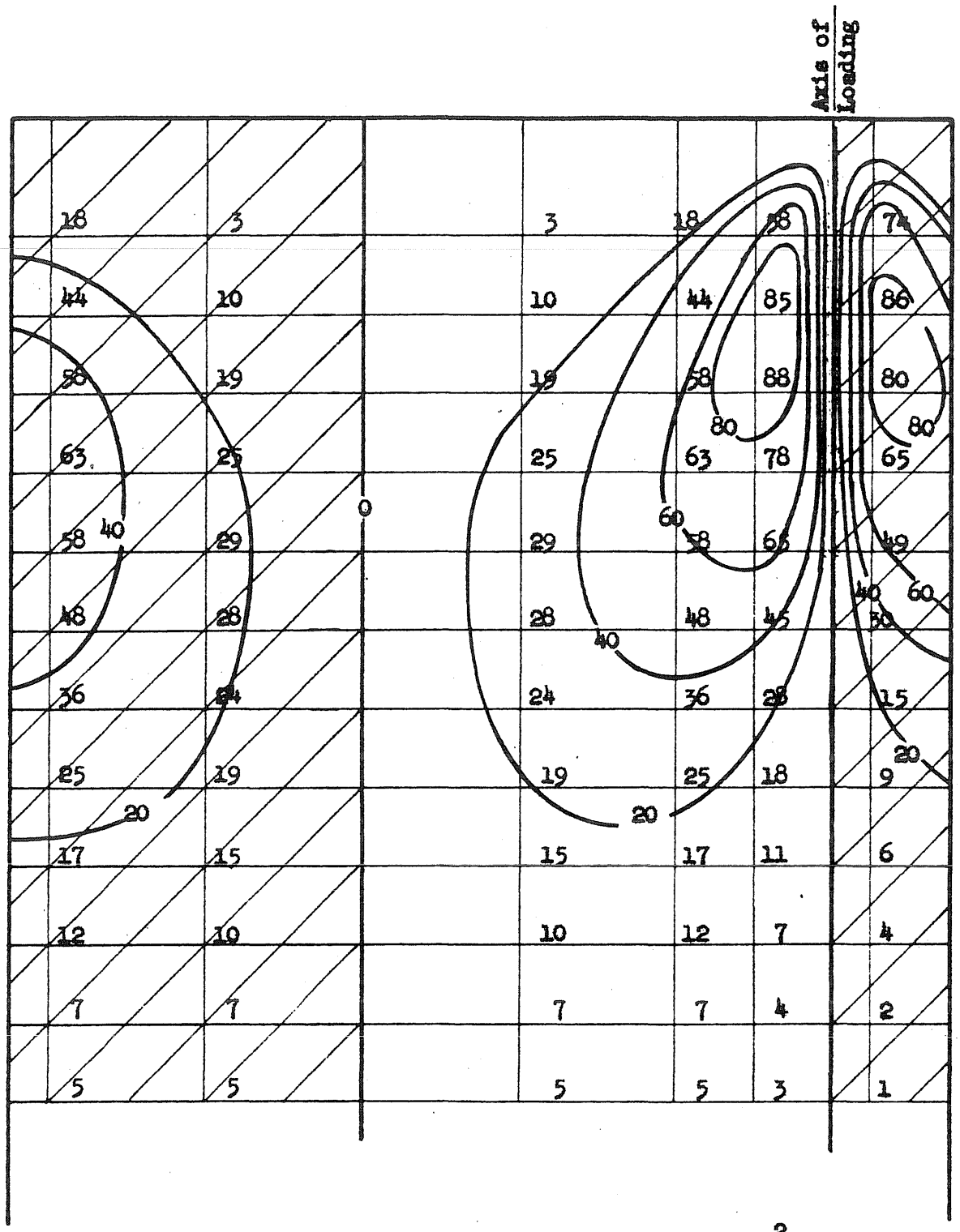

Coefficients of Average Compressive Stress x 10^2

FIG. 28 SHEAR STRESS COEFFICIENTS - PRETENSIONED

BLEICH, $u = \frac{3a}{4}$

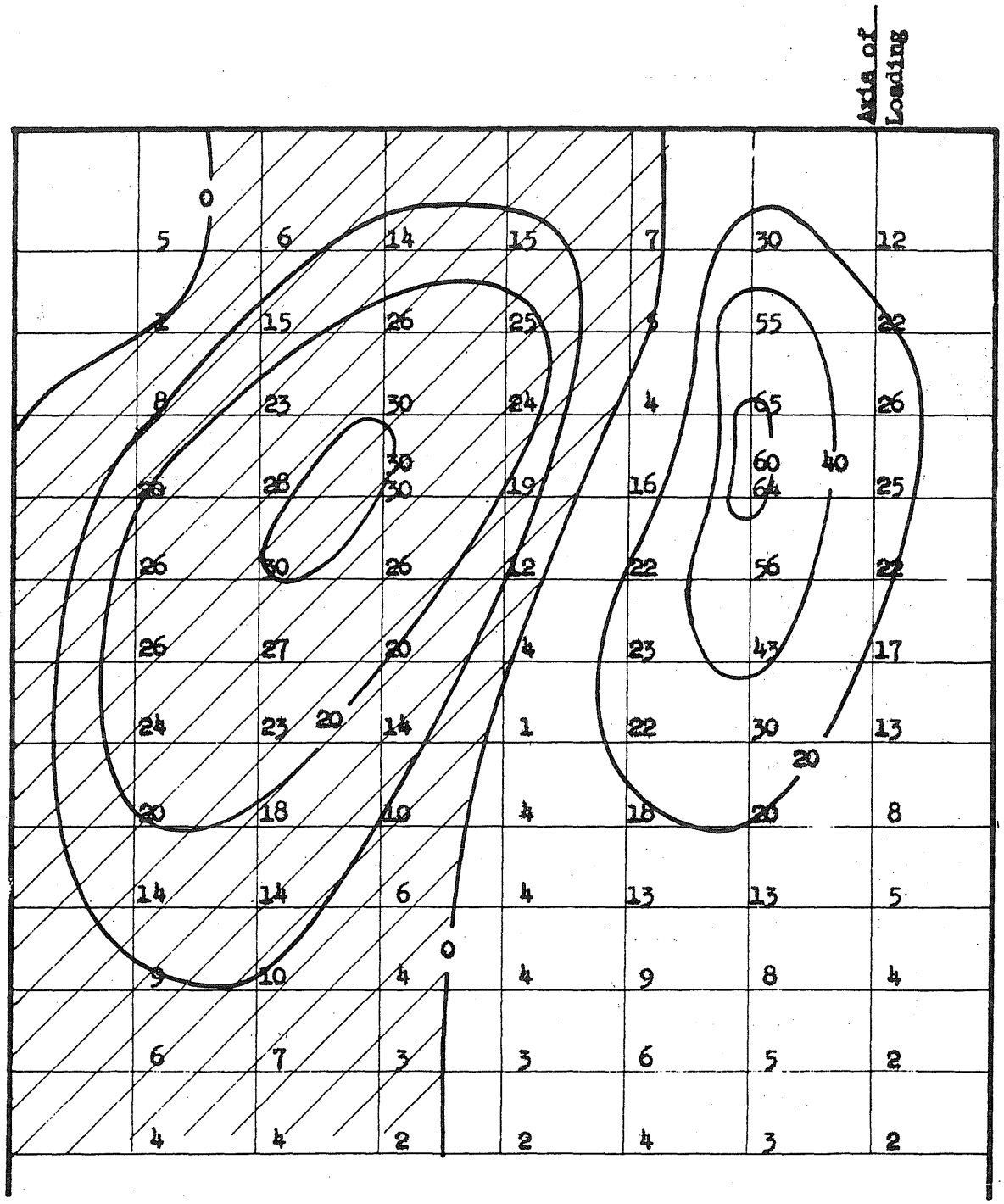

Coefficients of Average Compressive Stress x 10^2

FIG. 29 SHEAR STRESS COEFFICIENTS - PRETENSIONED

GUYON, $u = \frac{3a}{4}$

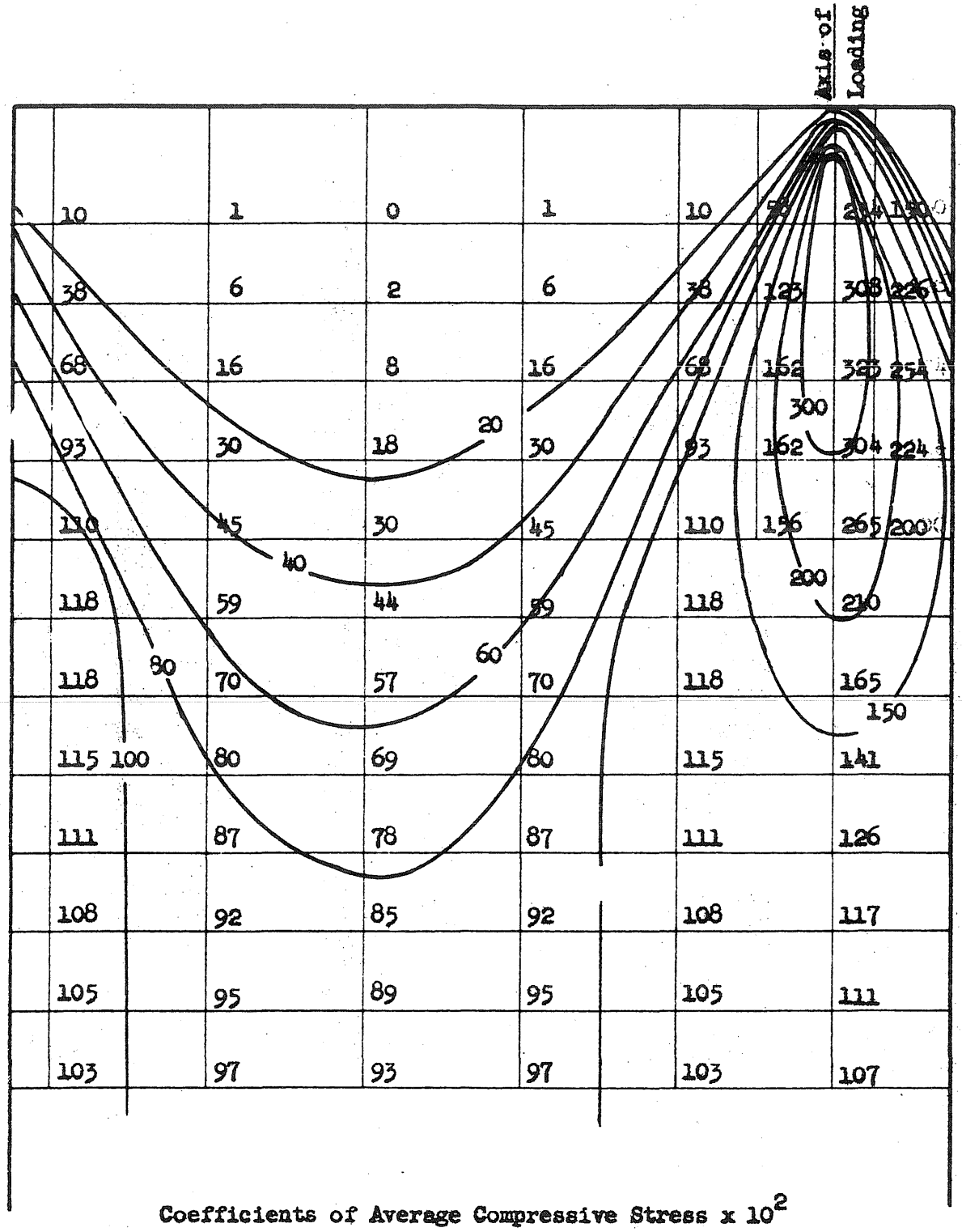

Coefficients of Average Compressive Stress x 10^2

FIG. 30 LONGITUDINAL STRESS COEFFICIENTS - PRETENSIONED

BEAM, $a = \frac{3\varepsilon}{4}$

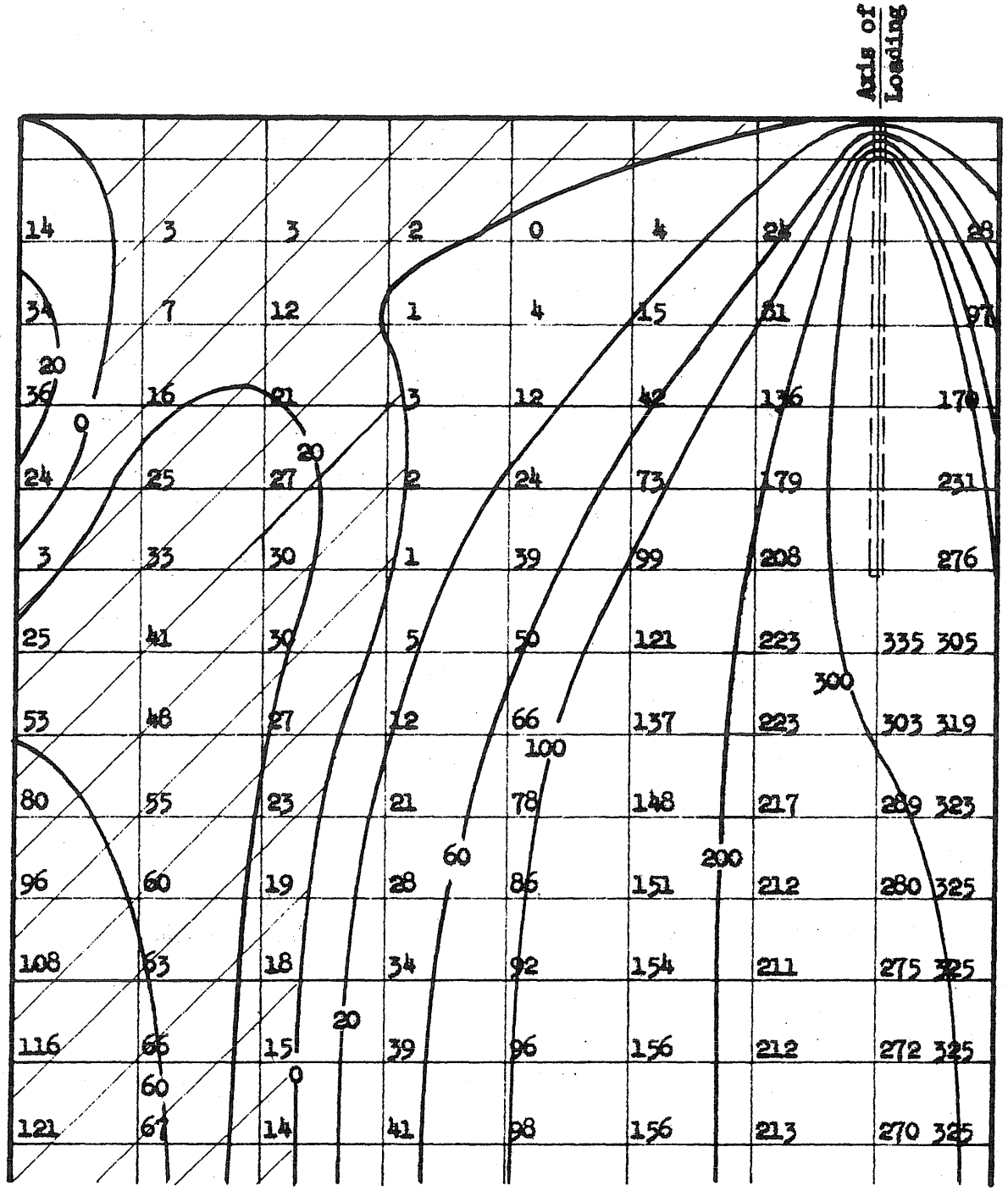

Coefficients of Average Compressive Stress x 10^2

FIG. 31 LONGITUDINAL STRESS COEFFICIENTS - PRETENSIONED

GUYON, $u = \frac{3a}{4}$

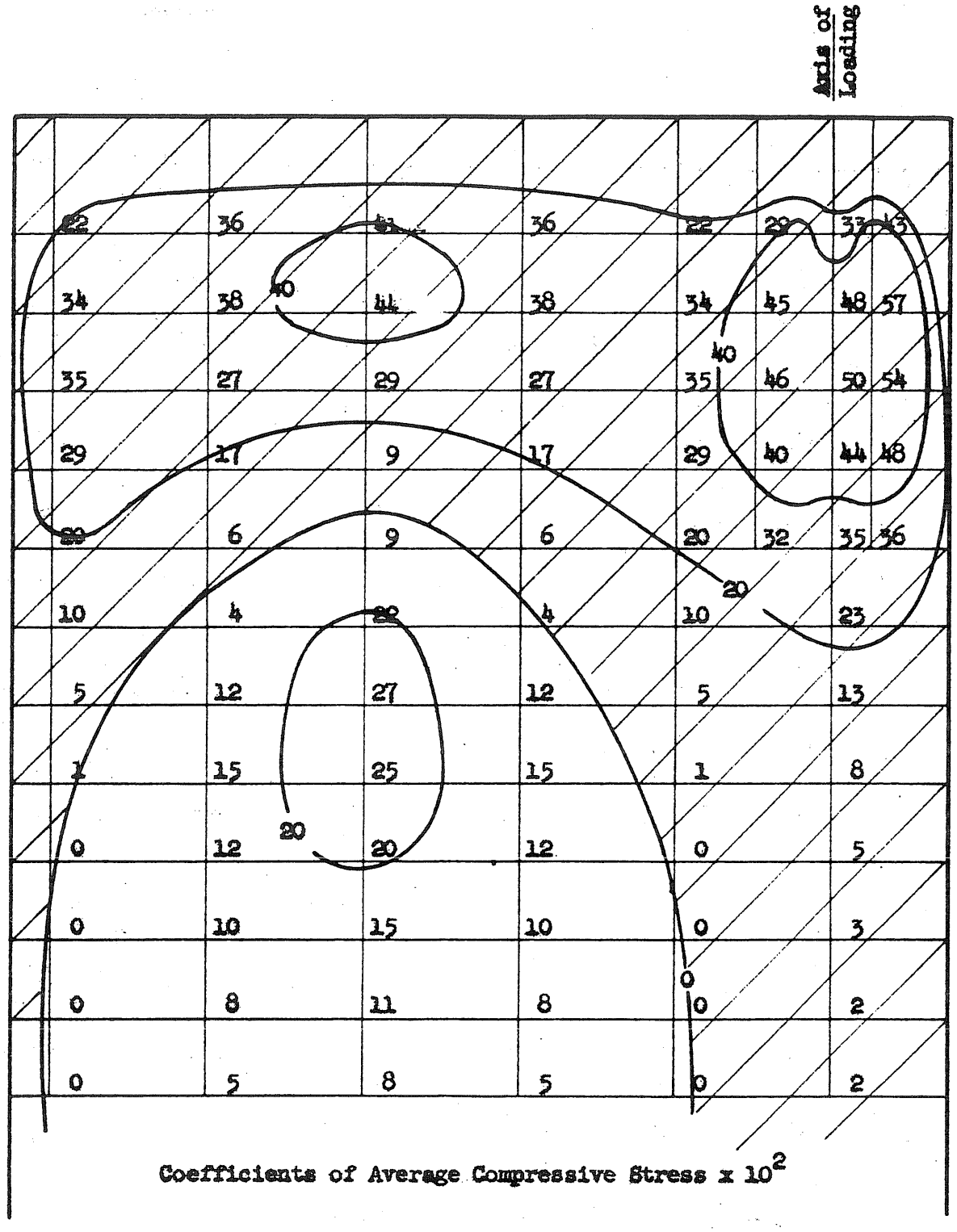

FIG. 32 MAXIMUM PRINCIPAL STRESS COEFFICIENTS - PRETENSIONED

ELEICH, $u = \frac{3a}{4}$

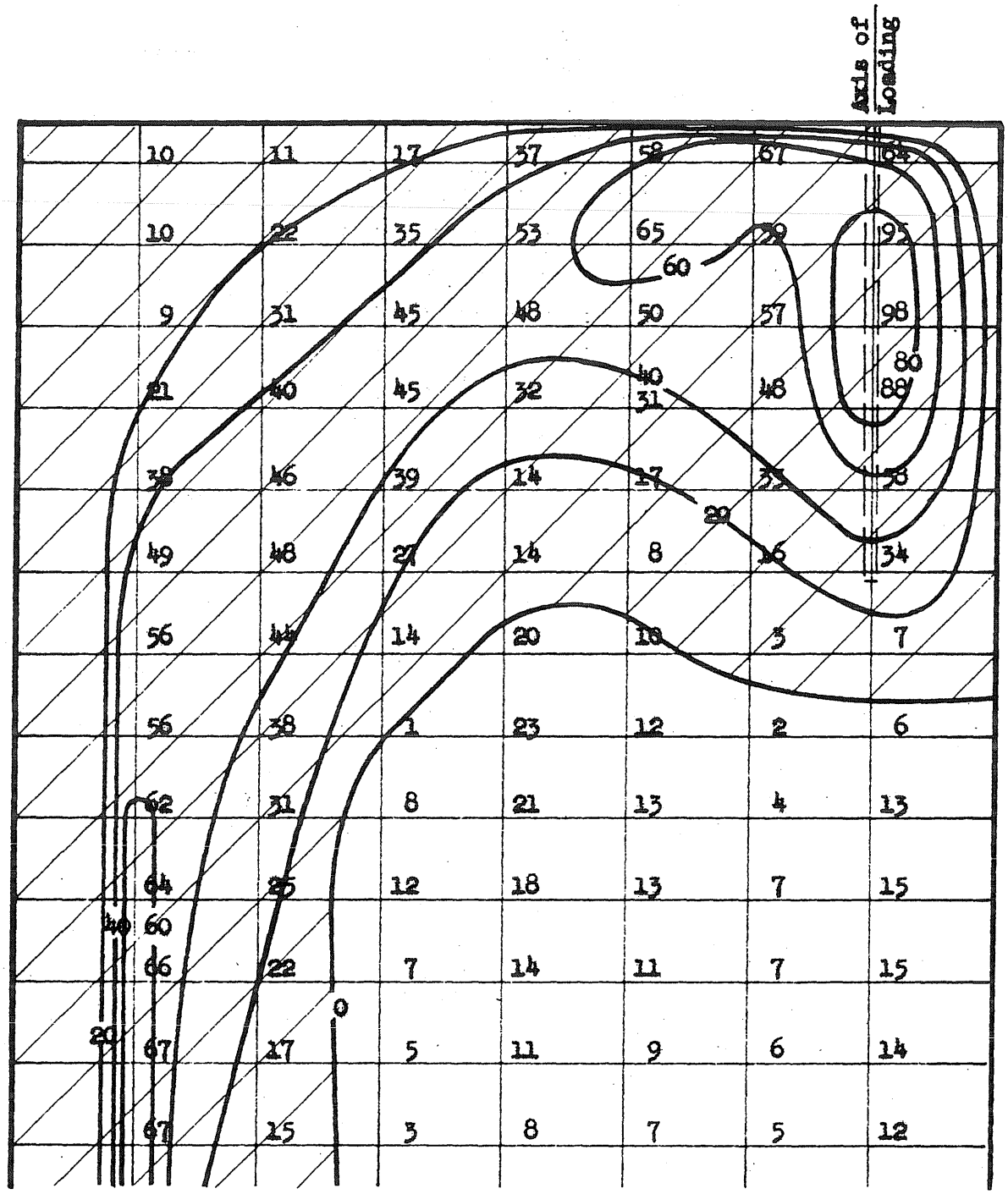

Coefficients of Average Compressive Stress

FIG. 33 MAXIMUM PRINCIPAL STRESS COEFFICIENTS - PRETENSIONED

GUYON, $u = \frac{3a}{4}$

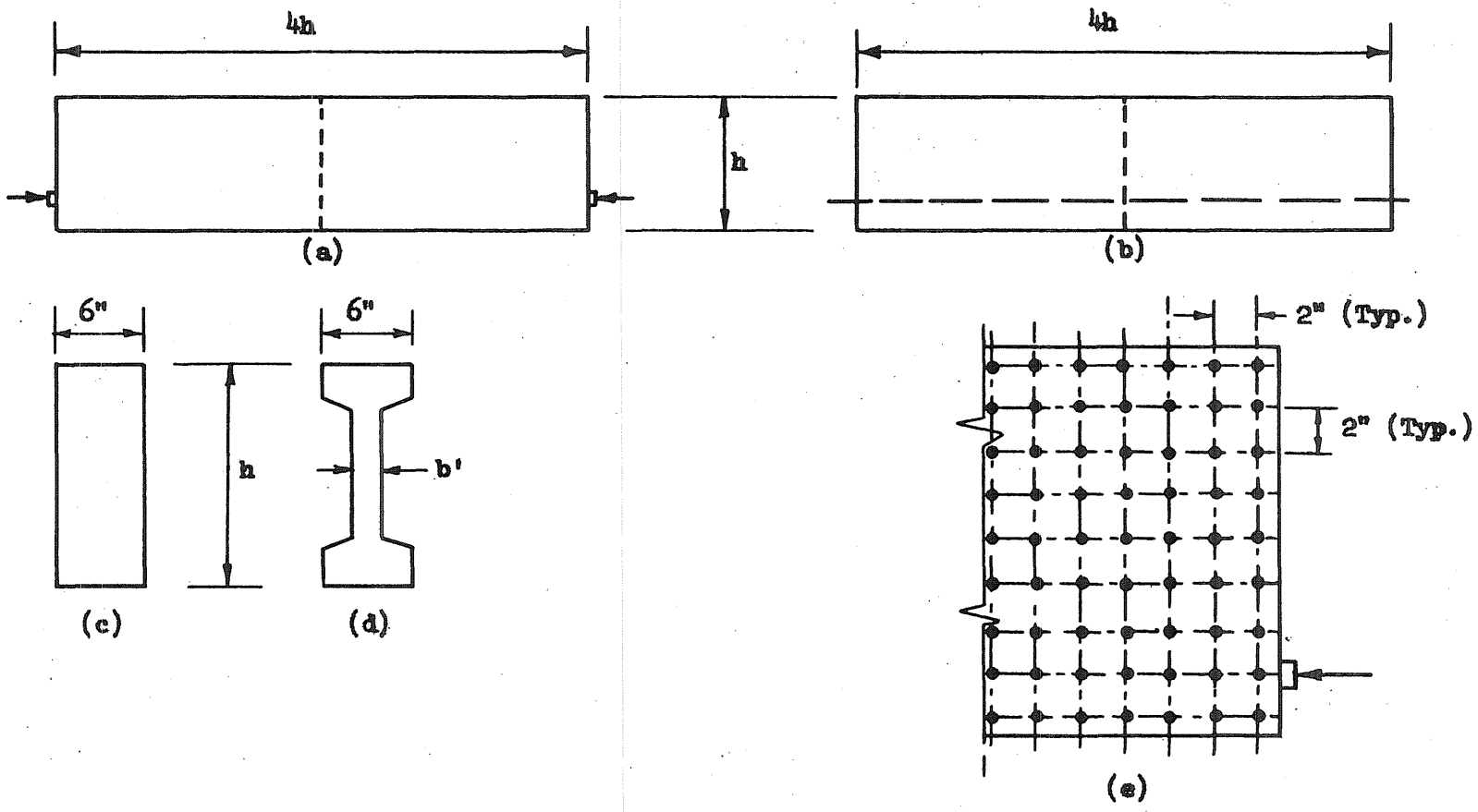

FIG. 34 TEST SPECIMENS

APPENDIX A

A.1 Analysis by F. Bleich

A.2 Analysis by Y. Guyon

A.1 ANALYSIS BY F. BLEICH

Consider a straight beam with a rectangular cross section of depth 2a and length 2b. The coordinate system is as shown in Fig. 1.

Suppose the beam is subjected to loads of the form

$$P_o(x) = \frac{A_o}{2} + \Sigma A_N \cos \frac{n\pi x}{a} + \Sigma A'_N \cos \frac{n\pi x}{a} \text{ on the upper surface}$$

and

$$P_u(x) = \frac{B_o}{2} + \Sigma B_N \cos \frac{n\pi x}{a} + \Sigma B'_N \cos \frac{n\pi x}{a} \text{ on the lower surface}$$

where

$$A_N = \frac{1}{a}\int_{a}^{+a} P_o(\lambda) \cos \frac{n\pi\lambda}{a} \text{ and } B_n = \frac{1}{a}\int_{-a}^{+a} P_u(\lambda) \cos \frac{n\pi\lambda}{a}\, d\lambda$$

According to the theory of elasticity, if φ is a stress function that satisfies Airy's equation

$$\frac{\partial^4\varphi}{\partial x^4} + \frac{2\partial^4\varphi}{\partial x^2\partial y^2} + \frac{\partial^4\varphi}{\partial y^4} = 0 \qquad (1)$$

then the stresses at any point within the beam are given by the following expressions;

$$\sigma_x = \frac{\partial^2\varphi}{\partial y^2} = \text{transverse stress} \qquad (2)$$

$$\sigma_y = \frac{\partial^2\varphi}{\partial x^2} = \text{longitudinal stress} \qquad (3)$$

$$\tau = \frac{-\partial^2\varphi}{\partial x\partial y} = \text{shear stress} \qquad (4)$$

Any loading can be broken down into a combination of symmetrical and anti-symmetrical loadings. Each of these is analysed separately.

Case (a) Symmetrical Loads.

A solution of the form $\varphi_n = Z \cos n\frac{\pi x}{a}$ will satisfy equation (1) if

$$\frac{\partial^4 Z}{\partial y^4} - \frac{2n^2\pi^2}{a^2}\frac{d^2Z}{dy^2} + \frac{n^4\pi^4 Z}{a^4} = 0$$

The general solution of this equation is

$$Z = A \cosh np + B \sinh np + Cy \cosh np + Dy \sinh np \qquad (5)$$

where $p = \frac{\pi y}{a}$

The boundary conditions require

for $y = +b$	$\sigma_y = P_o(x)$	Condition I
	$\tau = 0$	Condition II
for $y = -b$	$\sigma_y = P_u(x)$	Condition III
	$\tau = 0$	Condition IV

Conditions II and IV give

$$C = \frac{-B \frac{n\pi}{a} \cosh \frac{n\pi b}{a}}{\frac{n\pi b}{a} \sinh \frac{n\pi b}{a} + \cosh \frac{n\pi b}{a}} \qquad D = \frac{-A \frac{n\pi}{a} \sinh \frac{n\pi b}{a}}{\frac{n\pi b}{a} \cosh \frac{n\pi b}{a} + \sinh \frac{n\pi b}{a}}$$

Conditions I and III

$$A = \frac{-A_n + B_n}{\frac{n^2\pi^2}{a^2}} \cdot \frac{\frac{n\pi b}{a} \cosh \frac{n\pi b}{a} + \sinh \frac{n\pi b}{a}}{\sinh \frac{2n\pi b}{a} + \frac{2n\pi b}{a}}$$

$$B = \frac{-A_n - B_n}{\frac{n^2\pi^2}{a^2}} \cdot \frac{\frac{n\pi b}{a} \sinh \frac{n\pi b}{a} + \cosh \frac{n\pi b}{a}}{\sinh \frac{2n\pi b}{a} - \frac{2n\pi b}{a}}$$

Substitution of these constants, into equation (5) yields the expression for Z. The stresses can the be evaluated in accordance with equations (2), (3), and (4).

$$\sigma_x = \sum_{n=1}^{\infty} (A_N + B_N) \frac{(\sinh \frac{n\pi b}{a} - \frac{n\pi b}{a} \cosh \frac{n\pi b}{a}) \cosh np + np \sinh \frac{n\pi b}{a} \sinh np}{\sinh \frac{2n\pi b}{a} + \frac{2n\pi b}{a}} \cos \frac{n\pi x}{a}$$

$$+ \sum_{n=1}^{\infty} (A_N - B_N) \frac{(\cosh \frac{n\pi b}{a} - \frac{n\pi b}{a} \sinh \frac{n\pi b}{a}) \sinh np + np \cosh \frac{n\pi b}{a} \cosh np}{\sinh \frac{2n\pi b}{a} - \frac{2n\pi b}{a}} \cos \frac{n\pi x}{a}$$

$$\sigma_y = \frac{A_o}{2} + \sum_{n=1}^{\infty} (A_N + B_N) \frac{(\sinh \frac{n\pi b}{a} + \frac{n\pi b}{a} \cosh \frac{n\pi b}{a}) \cosh np - np \sinh \frac{n\pi b}{a} \sinh np}{\sinh \frac{2n\pi b}{a} + \frac{2n\pi b}{a}} \cos \frac{n\pi x}{a}$$

$$+ \sum_{n=1}^{\infty} (A_N - B_N) \frac{(\cosh \frac{n\pi b}{a} + \frac{n\pi b}{a} \sinh \frac{n\pi b}{a}) \sinh np - np \cosh \frac{n\pi b}{a} \cosh np}{\sinh \frac{2n\pi b}{a} - \frac{2n\pi b}{a}} \cos \frac{n\pi x}{a}$$

$$\tau = \sum_{n=1}^{\infty} (A_N + B_N) \frac{np \sinh \frac{n\pi b}{a} \cosh np - \frac{n\pi b}{a} \cosh \frac{n\pi b}{a} \sinh \frac{n\pi y}{a}}{\sinh \frac{2n\pi b}{a} + \frac{2n\pi b}{a}} \cdot \sin \frac{n\pi x}{a}$$

$$+ \sum_{n=1}^{\infty} (A_N - B_N) \frac{np \cosh \frac{n\pi b}{a} \sinh np - \frac{n\pi b}{a} \sinh \frac{n\pi b}{a} \cosh np}{\sinh \frac{2n\pi b}{a} - \frac{2n\pi b}{a}} \cdot \sin \frac{n\pi x}{a}$$

Case (b) Anti-Symmetrical Loads

A similar method can be used to solve the stresses for anti-symmetrical loads. These stresses are σ_x', σ_y' and τ' and are of the same form as σ_x, σ_y and τ. For example:

$$\sigma_x' = \sum_{n=1}^{\infty} (A_N' + B_N') \frac{(\sinh \frac{n\pi b}{a} - \frac{n\pi b}{a} \cosh \frac{n\pi b}{a}) \cosh np + np \sinh \frac{n\pi b}{a} \sinh np}{\sinh \frac{2n\pi b}{a} + \frac{2n\pi b}{a}} \cdot \sin \frac{n\pi x}{a}$$

$$+ \sum_{n=1}^{\infty} (A_N' - B_N') \frac{(\cosh \frac{n\pi b}{a} - \frac{n\pi b}{a} \sinh \frac{n\pi b}{a}) \sinh np + np \cosh \frac{n\pi b}{a} \cosh np}{\sinh \frac{2n\pi b}{a} - \frac{2n\pi b}{a}} \cdot \sin \frac{n\pi x}{a}$$

Longitudinal Boundary Conditions

for $x = \pm a$ $\quad \sigma_x = 0$ - Condition V

$\tau = 0$ - Condition VI

The symmetrical loading satisfies conditions VI but not condition V. The anti-symmetrical loading satisfies condition V but not condition VI.

For plates in which $b \gg a$. Bleich suggests (i) that condition V be satisfied by applying equal and opposite transverse stresses at the longitudinal boundaries (ii) that condition VI need not be satisfied since for this shape of plate the shear stresses will not be important.

Case (c) Single Eccentric Load

Combination of the stresses for the two types of loading will give the solution for a single concentrated eccentric load on both the upper and lower surfaces.

Suppose the load is applied with an eccentricity u

Then $\frac{A_o}{2} = \frac{B_o}{2} = \frac{-P}{2a}$ and $A_N = B_N = \frac{-P}{a} \cos \frac{n\pi u}{a}$

$$A'_N = B'_N = \frac{-P}{a} \sin \frac{n\pi u}{a}$$

$$A_N - B_N = 0 \quad \text{and} \quad A'_N - B'_N = 0$$

Further if $b \gg a$ $\sinh np \approx \cosh np \approx \frac{e^{np}}{2}$

and $\sinh \frac{2n\pi b}{a} + \frac{2n\pi b}{a} \approx \sinh \frac{2n\pi b}{a} \approx \frac{e}{2} \frac{2n\pi b}{a}$

Bleich does not develop this solution any further. The following analysis is that of the writer.

If the origin is moved from the center of the plate to the junction of the upper surface and the axis of symmetry, then,

$$\sigma_x = \frac{-P}{a} \sum_{n=1}^{\infty} [1-np]e^{-np} \left[\cos \frac{n\pi u}{a} \cos \frac{n\pi x}{a} - \cos \frac{n\pi u}{a} \cos n\pi + \sin \frac{n\pi u}{a} \sin \frac{n\pi x}{a}\right]$$

$$\sigma_y = \frac{-P}{2a} \frac{-P}{a} \sum_{n=1}^{\infty} [1+np]e^{-np} \left[\cos \frac{n\pi u}{a} \cos \frac{n\pi x}{a} + \sin \frac{n\pi u}{a} \sin \frac{n\pi x}{a}\right]$$

$$\tau = \frac{P}{a} \sum_{n=1}^{\infty} np\, e^{-np} \left[\cos \frac{n\pi u}{a} \sin \frac{n\pi u}{a} - \sin \frac{n\pi u}{a} \cos \frac{n\pi x}{a}\right]$$

If, the origin is shifted to the point of application of the load and if $x = u + x'$; $\frac{\pi x'}{a} = \beta$; $\frac{\pi u}{a} = \alpha$;

$$\sigma_x = \frac{-P}{a} \sum_{n=1}^{\infty} [1-np]e^{-np} [\cos n\beta - \cos n\alpha \cos n\pi]$$

Then

$$\sigma_y = \frac{-P}{2a} \frac{-P}{a} \sum_{n=1}^{\infty} [1+np]e^{-np} [\cos n\beta]$$

$$\tau = \frac{-P}{a} \sum_{n=1}^{\infty} [-np]e^{-np} [\sin n\beta]$$

A.2 ANALYSIS BY Y. GUYON

1. Approximate Solution

Consider a rectangular prism, width 2b, depth 2a and length 2h. Let the origin of the coordinate system lie on one end of the axis of the prism. Assume that the loadings on the surfaces y = 0 and y = 2h are the same and are independent of the width.

Any loading can be developed from a superposition of a symmetrical and an anti-symmetrical loading. From the theory of elasticity, if any stress function φ satisfies Airy's equation

$$\frac{\partial^4 \varphi}{\partial x^4} + \frac{2\partial^4 \varphi}{\partial x^2 \partial y^2} + \frac{\partial^4 \varphi}{\partial y^4} = 0 \qquad (1)$$

the stress are given by

$$\sigma_y = \frac{\partial^2 \varphi}{\partial x^2} \qquad \text{- longitudinal stress} \qquad (2)$$

$$\sigma_x = \frac{\partial^2 \varphi}{\partial y^2} \qquad \text{- transverse stress} \qquad (3)$$

$$\tau = \frac{\partial^2 \varphi}{\partial x \partial y} \qquad \text{- shear stress} \qquad (4)$$

Case (a) Symmetrical Loads.

Any set of symmetrical loads can be represented by the function

$$\bar{\omega} = A_o + \Sigma A_n \cos n\alpha \text{ where } \alpha = \frac{\pi x}{a}$$

and

$$A_o = \frac{1}{\pi}\int_o^\pi \bar{\omega}(\alpha)\, d\alpha$$

$$A_n = \frac{2}{\pi}\int_o^\pi \bar{\omega}(\alpha) \cos n\alpha \, d\alpha$$

A solution of the form $\varphi_n = Z \cos n\alpha$ will satisfy equation (1) if

$$\frac{d^4 Z}{dy^4} - \frac{2n^2\pi^2}{a^2}\frac{d^2 Z}{dy^2} + \frac{n^4\pi^4 Z}{a^4} = 0$$

Solving

$$Z = \left(A + B\frac{n\pi y}{a}\right)\cosh\frac{n\pi y}{a} + \left(C + D\frac{n\pi y}{a}\right)\sinh\frac{n\pi y}{a} \qquad - (5)$$

The boundary conditions at y = 0 and y = 2h require that

$$\sigma_y = \bar{\omega} \text{ and } \tau = 0$$

Substituting in equation (5)

$$A = -A_n \frac{a^2}{n^2\pi^2}; \quad B = -C = -A_n \frac{a^2}{n^2\pi^2} \frac{\cosh q - 1}{\sinh q + q}; \quad D = \frac{A_n a^2}{n^2\pi^2} \frac{\sinh q}{\sinh q + 1}$$

where $q = n\pi \frac{2h}{a}$

If $2h > 4a$ then $q > 4\pi$ and $\sinh q \approx \cosh q$

In general q and 1 are negligible in comparison to sinh q or cosh q;

$$\text{then } A = B = -C = -D = -A_n \frac{a^2}{n^2\pi^2}$$

$$\text{and } Z = -A_n \frac{a^2}{n^2\pi^2} (np + 1)e^{-np} \qquad (6)$$

$$\text{where } p = \frac{\pi y}{a}$$

The substitution os this expression for Z in the stress function φ_n yields transverse stresses that does not satisfy the condition $\sigma_x = 0$ at the boundaries $x = \pm a$.

Suppose a stress system II is imposed on this existing stress system I such that equal and opposite transverse forces are applied along these boundaries. The addition of stress systems I and II yield final stresses of the form

$$\sigma_x = -\Sigma A_n (np-1)e^{-np} \left[\cos n\alpha + (-1)^{n+1}\right]$$

$$\sigma_y = A_o + \Sigma A_n (np+1)e^{-np} \cos n\alpha \qquad \text{(A)}$$

$$\tau = \Sigma A_n np e^{-np} \sin n\alpha$$

Case (b) Anti-Symmetrical Loads.

The loading system can be written as

$$\bar{\omega}' = \Sigma A_n' \sin n\alpha$$

and a set of stress corresponding to those developed for system I case (a) can be derived but these stresses will not satisfy the conditions that $\tau = 0$ at $x = \pm a$.

If a second stress system is applied as before composed of equal and opposite tractions at these boundaries then the addition of the two systems will yield stresses

$$\sigma_x' = -\Sigma A_n' (np-1) \left[\sin n\alpha - \alpha\frac{(\pi^2-\alpha^2)}{2\pi^2} n(-1)^{n+1}\right]$$

$$\sigma_y' = \frac{3}{2} M \frac{x}{a^3} + \Sigma A_n' (np+1)e^{-np} \left[\sin n\alpha - \frac{3\alpha}{\pi^2} \frac{(-1)^{n+1}}{n}\right] \qquad (B)$$

$$\tau = -\Sigma A_n' npe^{-np} \left[\cos n\alpha + (-1)^{n+1} 3 \frac{\alpha^2-\pi^2}{2\pi^2}\right]$$

where M = moment on the section.

Case (c) Single Eccentric Load.

If stress systems A and B are combined they will give the solution for an eccentric load.

Suppose the load is applied with an eccentricity u.

Let $\varphi = \frac{\pi u}{a}$ and $\alpha - \varphi = \beta$

then $$\sigma_x = \frac{P}{a} \Sigma (np-1)e^{-np} \left[\cos n\beta - \cos n(\pi-\varphi) - \alpha \frac{(\pi^2-\alpha^2)}{2\pi^2} n \sin n(\pi-\varphi)\right.$$

$$\sigma_y = \frac{-P}{2a}\left(1+\frac{3ux}{a^2}\right) \frac{-P}{a} \Sigma (np+1)e^{-np} \left[\cos n\beta - \frac{3\alpha}{\pi^2} \sin \frac{n(\pi-\varphi)}{n}\right] \qquad (C)$$

$$\tau = \frac{-P}{a} \Sigma npe^{-np} \left[\sin n\beta - \frac{3\alpha^2-\pi^2}{2\pi^2} \sin n(\pi-\varphi)\right]$$

The σ_y and τ stresses according to this system C are those used in the tables given by Guyon in Reference (9). The transverse stresses σ_x are derived by the following analysis.

2. Exact Solution.

Symmetrical Loading - Transverse Stresses Only

Consider the n^{th} term of the loading function

$$\bar{\omega}_n = A_n \cos n\alpha$$

The stresses corresponding to this n^{th} term will be proportional to A_n and can be written as

$$\sigma_{nx} = A_n \nu_{nx}$$

If the different coefficients ν_{nx} are known for the stress σ_{nx} then the total stress σ_x at any point is given by

$$\sigma_x = \Sigma A_n \nu_n (xy)$$

For equation A system I

$$\nu_n^1 = -(np-1)e^{-np} \cos n\alpha$$

Corrective forces have now to be applied for the tractions at the longitudinal boundaries. The function that yields these corrective forces can be written as

$$-r_1 = (-1)^{n+1} \left(-1 + \Sigma\, b_m \sin \frac{m\pi y}{2h}\right)$$

$$\text{if } k = \frac{a}{2h} \text{ then } -r_1 = (-1)^{n+1} \left(-1 + \Sigma\, b_m \sin mkp\right)$$

These tractions set up forces at y = 0 composed of;

(i) a stress ν_x $\quad \nu_n^2 = -(-1)^{n+1} \left[-1 + \Sigma\, b_n f_n(\alpha) \sin mk\right]$

(ii) parasitical reactions $\quad \tau_n^2 = -(-1)^{n+1} \Sigma\, b_n g_n(\alpha)$

It is still necessary however to again annul the tangential stresses τ_n^2 that have been set up. At this stage the stress desired ν_n, can be written as

$$\nu_n = \nu_n^1 + \nu_n^2 + \text{effect of } (-\tau_n^2)$$

$$= -(np-1)e^{-np} \cos n\alpha + (-1)^{n+1} -(-1)^{n+1} \Sigma\, b_n f_n(\alpha) \sin \frac{np}{6}$$

$$+ \text{effect of } (-\tau_n^2)$$

The cycle could be continued but parasitical reactions would again be created. Suppose however that the tangential reactions $(-\tau_n^2)$ introduced to eliminate the parasitical stresses of the previous system, have an essentially linear law, say $(-\tau_n^2) = K_n \alpha$. The stresses created by this system would satisfy all the boundary conditions so that

$$\nu_n = \nu_n^1 + \nu_n^2 + \nu_n^3$$

Consider the effect of a linear tangential load

$$\theta = \frac{\alpha}{2} = \Sigma\, (-1)^{n+1} \sin \frac{m\alpha}{m}$$

The calculation can be broken up as follows:

System	Applied Load	Development	Stress (σ_x)	Parasitical Stresses
a	θ, tangential on y=0	$\Sigma(-1)^{m+1} \sin \frac{m\alpha}{m}$	$\nu_a(\alpha)$	$\nu_a(\pi)$ normal on faces $x = \pm a$
b	$-\nu_a(\pi)$ normal on $x = \pm a$	$\Sigma\, d_p \sin \frac{p\pi y}{2h}$	$\nu_b(\alpha)$	τ, tangential on face y = 0
c	$-\tau$ tangential			

To a first approximation the tangential reactions of system C again follow a linear law. The cycle is thus complete.

Suppose now ν_x is the true stress due to θ.

Then $\nu_x = \nu_a + \nu_b + \nu_c + \nu_d + \ldots$ (7)

but $\nu_c + \nu_d + \ldots$ is the true stress ν_x created by $-\tau$.
This stress is thus proportional to the stress ν_x created by θ.
Suppose $-\tau = -C\alpha$ where C = constant
then ν_x (due to $-\tau$) = ν_x (due to θ). $\frac{-\tau}{\theta} = \nu_x$ (due to θ). $\frac{-C\alpha}{\frac{\alpha}{2}} = -2C\nu_x$ (θ)

Rewriting equation (7) gives $\nu_x = \frac{\nu_a + \nu_b}{1+2C}$ (8)

ν_x then satisfies all the boundary conditions. However it has been stated that the completion of the cycles is an approximation only and a correction must be introduced. In order to examplify this correction suppose the plane $x = \frac{3a}{4}$ is considered.
The correction reduces to the use of $\tau_n(0) = C' \alpha$ say, not $\tau_n(0) = C\alpha$. The latter represents a certain mean law while in the former C' is still a constant but has a value such that the resultant of the tangential forces to the right of $\frac{3a}{4}$ is the same for the linear law C' as for the true law $\tau_n(0)$. This value C' is used in equation (8). At each plane x = a/2, a/4 etc there will be different values of C, say C", C'" which similar to C' vary only slightly from C.

If ν_n^3 is the stress ν_x due to $(-\tau_m^2)$

$$\nu_n^3 = \nu_x \text{ (due to } \frac{\alpha}{2}). \frac{K_n}{1/2} = 2 K_n \nu_x \text{ (due to } \frac{\alpha}{2})$$

ν_x (due to $\frac{\alpha}{2}$) is given by equation (8). Values of K_n', K_n'' etc are chosen in the same manner as C', C" etc above.
The stress ν_x under the load $\bar{w}_n$ = cos nα (the nth term of the loading function $\bar{w}$) is;

$$\nu_{nx} = \nu_n' + \nu_n^2 + \nu_n^3$$

The stress σ_x at any point is thus

$$\sigma_x = A_1 \nu_{1x} + A_2 \nu_{2x} + A_3 \nu_{3x}$$

These coefficients ν_{1x}, ν_{2x} are tabulated in reference (8) for n = 1 to n = 10.

In a similar manner anti-symmetrical stresses σ_x' can be developed.

The combination of these symmetrical and anti-symmetrical solutions are used to give the values for σ_x, the transverse stress, given in the tables of references(9).